FEDERAL UNIVERSITY OF CEARÁ

TECHNOLOGY CENTER

DEPARTMENT OF ELECTRICAL ENGINEERING

POSTGRADUATE PROGRAM IN ELECTRICAL ENGINEERING

POSTGRADUATE IN ELECTRICAL ENGINEERING

LUIS RODOLFO REBOUÇAS COUTINHO

TARIFF SPACES: A NEW CONCEPT FOR OPTIMIZING THE USE OF ELECTRICAL LOADS IN SMART HOMES

FORTALEZA

2024

LUIS RODOLFO REBOUÇAS COUTINHO

TARIFF SPACES: A NEW CONCEPT FOR OPTIMIZING THE USE OF ELECTRICAL LOADS IN SMART HOMES

Thesis presented to the Postgraduate Program in Electrical Engineering of the Technology Center from the Federal University of Ceará, as a partial requirement for attaining the degree of Doctor in Electrical Engineering. Concentration Area: Electrical Engineering - Power Systems.

Supervisor: Prof. Dr. Giovanni Cordeiro Barroso.
Co-supervisor: Prof. Dr. Bruno de Athayde Prata.

FORTALEZA

2024

Dados Internacionais de Catalogação na Publicação
Universidade Federal do Ceará
Sistema de Bibliotecas
Gerada automaticamente pelo módulo Catalog, mediante os dados fornecidos pelo(a) autor(a)

C896t Coutinho, Luis Rodolfo Rebouças.
Tariff Spaces: a new concept for optimizing the use of electrical loads in smart homes / Luis Rodolfo Rebouças Coutinho. – 2024.
94 f. : il. color.

Tese (doutorado) – Universidade Federal do Ceará, Centro de Tecnologia, Programa de Pós-Graduação em Engenharia Elétrica, Fortaleza, 2024.
Orientação: Prof. Dr. Giovanni Cordeiro Barroso.
Coorientação: Prof. Dr. Bruno de Athayde Prata.

1. Smart Home Controllers. 2. Load-side Management. 3. Smart Grids. 4. Tariff Space. 5. Load Scheduler Optimization. I. Título.

CDD 621.3

LUIS RODOLFO REBOUÇAS COUTINHO

TARIFF SPACES: A NEW CONCEPT FOR OPTIMIZING THE USE OF ELECTRICAL LOADS IN SMART HOMES

Thesis presented to the Postgraduate Program in Electrical Engineering of the Technology Center from the Federal University of Ceará, as a partial requirement for attaining the degree of Doctor in Electrical Engineering. Concentration Area: Electrical Engineering - Power Systems.

Approved on: 02/07/2024.

EXAMINING COMMITTEE

Prof. Dr. Giovanni Cordeiro Barroso (Supervisor)
Federal University of Ceará (UFC)

Prof. Dr. Bruno de Athayde Prata (Co-supervisor)
Federal University of Ceará (UFC)

Prof. Dr. Fabrício Gonzales Nogueira
Federal University of Ceará (UFC)

Prof. Dr. Manoel Bezerra Campelo Neto
Federal University of Ceará (UFC)

Prof. Dr. José Renato de Brito Sousa
Federal Institute of Education, Science and Technology of Ceará (IFCE)

To my dear wife, Helen, son Heitor, and beloved mother, Liduina, your unwavering support and love have been the foundation of my journey in pursuit of knowledge.

ACKNOWLEDGEMENTS

I extend my deepest gratitude to my Supervisor and Co-supervisor for their invaluable guidance, unwavering support, and profound expertise throughout the journey of this thesis. Their mentorship has been instrumental in shaping my research and fostering my academic growth.

I would like to express my sincere appreciation to all the professors and colleagues from graduation and post-graduation program who have contributed to my intellectual development and enriched my academic experience. Special thanks are due to Tiago Sandino, Jonatha Costa and Stephanie Santos for their exceptional collaboration and insightful discussions. Your encouragement and camaraderie have made this journey all the more rewarding.

I am also indebted to the Julia Language Forum for their invaluable assistance and support in navigating the intricacies of programming. Their collective wisdom and willingness to help have been indispensable in overcoming challenges and achieving success in my research endeavors.

Lastly, to all those whose names may not be mentioned but whose support has been felt throughout this endeavor, I offer my heartfelt appreciation. Your encouragement, understanding, and belief in my abilities have been a source of inspiration and motivation. This thesis stands as a testament to the collective effort and collaboration that have made it possible.

"... Without innocence the cross is only iron,
Hope is only an illusion ..." (Tuomas
Holopainen, 2002)

RESUMO

O contexto deste trabalho está relacionado ao agendamento de eletrodomésticos, levando em consideração as variações nos custos de energia durante o dia, devido às tarifas domésticas brasileiras oficiais: constante e branca. A tarifa branca pode atingir um preço médio cerca de 17% mais baixo do que a constante, mas cobra o dobro de seu valor durante as horas de pico. Propomos uma metodologia para, além de diminuir o custo, reduzir o desconforto do usuário devido ao deslocamento temporal de dispositivos controláveis, apresentando uma solução equilibrada por meio da análise analítica de um novo método aqui denominado *Espaço Tarifário*, derivado dos postos tarifários de tarifa branca. Para alcançar esse objetivo, exploramos as propriedades geométricas do movimento dos dispositivos através do *Espaço Tarifário* (*locus* geométrico da carga), sobre o qual podemos definir uma região limitada na qual o custo de uma carga sob a tarifa branca será igual ou menor do que o custo sob a tarifa constante. Como teste para a eficiência desta nova metodologia, coletamos alguns benchmarks (como tempo de execução e uso de memória) em relação a um algoritmo multi-objetivo clássico (Hierarchical) disponível no portfólio de linguagens no qual o projeto foi executado (linguagem Julia). Como resultado, ambas as metodologias alcançam resultados similares, mas aquela apresentada nesta tese mostra uma redução significativa no tempo de processamento e no uso de memória, o que poderia levar à implementação futura da solução em um sistema embarcado simples e de baixo custo, como um ARM Cortex M. Além de agendar eletrodomésticos com base em variações nos custos de energia, esta pesquisa aborda a adaptação em tempo real às mudanças nos preços de energia, preferências do usuário e condições ambientais em residências. A metodologia proposta alcança eficiência computacional e responsividade em tempo real significativas em comparação com algoritmos multiobjetivo tradicionais. Sem restrições de resposta à demanda, a solução principal é aproximadamente 10000 vezes mais rápida que o algoritmo multiobjetivo clássico. Com restrições de resposta à demanda, foi proposta uma metodologia híbrida que reduz o tempo de processamento geral em 50% em comparação com o algoritmo clássico sob as mesmas restrições. Esse destaque para a adaptação em tempo real aprimora a aplicabilidade e a eficácia de nossa abordagem de agendamento em ambientes residenciais dinâmicos.

Palavras-chave: Controladores Para Casas Inteligentes; Gerenciamento Pelo Lado Da Demanda; Smart Grids; Wspaço Tarifário; Optimização De Um Escalonador De Cargas.

ABSTRACT

The background of this work is related to the scheduling of household appliances, taking into account variations in energy costs during the day, due to official Brazilian domestic tariffs: constant and white. The white tariff can reach an average price which is around 17% lower than the constant price, but charges twice its value at peak hours. In addition to cost reduction, we propose a methodology to reduce user discomfort due to time shifting of controllable devices, presenting a balanced solution through the analytical analysis of a new method here called *Tariff Space*, derived from white tariff posts. To achieve this goal, we explore the geometric properties of the movement of devices through the *Tariff Space* (geometric locus of the load), over which we can define a limited region in which the cost of a load under the white tariff will be equal to or less than the constant tariff. As a trial for the efficiency of this new methodology, we collected some benchmarks (such as execution time and memory usage) against a classic multi-objective algorithm (Hierarchical) available in the language portfolio in which the project has been executed (Julia language). As a result, both methodologies achieve similar results, but the one presented in this thesis shows a significant reduction in processing time and memory usage, which could lead to the future implementation of the solution in a simple, low-cost embedded system like an ARM cortex M. In addition to scheduling household appliances based on energy cost variations, this research addresses real-time adaptation to changing energy prices, user preferences, and environmental conditions in residential settings. The proposed methodology achieves significant computational efficiency and real-time responsiveness compared to traditional multi-objective algorithms. Without demand response constraints, the main solution is approximately 10000 times faster than the classic multi-objective algorithm. With demand response constraints, an hybrid methodology that reduces overall processing time by 50% compared to the classic algorithm under the same constraints has been proposed. This emphasis on real-time adaptation enhances the practical applicability and effectiveness of our scheduling approach in dynamic residential environments.

Keywords: Smart Home Controllers ; Load-side Management; Smart Grids; Tariff Space; Load Scheduler Optimization.

LIST OF FIGURES

LIST OF TABLES

LIST OF ALGORITHMS

LIST OF ABBREVIATIONS AND ACRONYMS

T_c	conventional tariff
T_f	off-peak post tariff
T_i	intermediate post tariff
T_p	peak post tariff
AI	artificial intelligence
ANEEL	National Electric Power Agency
BAS	building automation systems
CL	controllable load
CPP	critical peak pricing
DL	detectable load
DR	demand response
DSM	demand-side management
EV	electric vehicle
FP	fixed plan
GAs	genetic algorithm
HEMS	home energy management system
HVAC	heating, ventilation, and air conditioning
IEMS	intelligent energy management systems
IoT	internet of things
JuMP	Julia Modeling Language for mathematical optimization
LP	linear programming
MIP	mixed integer programming
PSO	particle swarm optimization
PV	photovoltaic
QoE	consumer quality of experience
RTP	real-time price
SG	smart grid
SH	smart home
SHC	smart home controller
SHRS	Smart Home Reasoning System

SLR	systematic literature review
SM	smart meter
ToU	time-of-use

LIST OF SYMBOLS

T_c	Conventional tariff
T_i	Intermediate post tariff
T_p	Peak post tariff
T_f	Off-peak post tariff
$L_i.W$	Width of the i^{th} load, usually measured in minutes
$L_i.W\Delta$	Discrete load width
$L_i.r$	Release time of the i^{th} load
$L_i.e$	Expected on time of the i^{th} load by user
$L_i.d$	Deadline instant of the i^{th} load
$L_i.s$	Range with all possible start times of the i^{th} load, $L_i.s \geq L_i.r$
$L_i.f$	Finishing time of the i^{th} load, $L_i.f = L_i.s + L_i.W \leq L_i.d$
Δt	Discrete step in which a load could move through time, common to all loads in set
$L_i.P(t)$	Behavior of the i^{th} load through time
$L_i.\bar{P}_i$	Average power of the i^{th} load
$L_i.\hat{P}_i$	Peak power of the i^{th} load
$L_i.\mu$	Relevance of the i^{th} load, $\in [0,1]$
k	Proportion of discrete time related to 1 hour, $k = \left(\frac{60}{\Delta t}\right)$

CONTENTS

1 INTRODUCTION

In 1989, Sanghvi (1989) already pointed to the increasing trend in electric loads quantity and so in the power demand. Their work discussed many solutions, like the use of dynamic pricing and time-of-use (ToU) tariff, which became a reality in the years to follow. About 20 years later, (Ipakchi e Albuyeh, 2009) listed the same power demand concerns, adding to it a new player: the electric vehicle (EV). The impact of EV on the energy grid was also the main problem for Clement-Nyns *et al.* (2009), Sortomme e El-Sharkawi (2010). Their research includes scenarios with the coordination of smart chargers. In the same paper, (Ipakchi e Albuyeh, 2009) points to a lack of reliability of the traditional energy grid due to the prospection of renewable energy sources and increased costs to maintain the transmission and distribution networks. Electric energy should be generated closer to its final consumer, and a better communication framework needed to be built, as claimed in (UNITED STATES. Congress., 2007) when the term smart grid (SG) was used for the first time. Nowadays, the transport sector is a major source of gas emissions. There are many challenges related to modernizing and increasing the use of public transportation and transitioning from internal combustion to electric vehicles, which cannot be considered gas emission-free if the electric matrix behind it is still based on natural gas or coal (Bleviss, 2021).

In the context of SG, its evolution is fairly elucidated through the concepts of demand response (DR) and demand-side management (DSM) Gellings e Samotyj (2013). The latter reaches out to the end-users through tariff signals offered by the local energy market, often referred to as critical peak pricing (CPP), real-time price (RTP), and ToU (Byrne, 2015). During identified demand peaks, the corresponding hours incur higher charges, thus encouraging users to reschedule their appliance usage to reduce their bills. Legal deals with energy suppliers and smart home controller (SHC) have been important instruments through which customers can optimize their energy consumption behaviors and achieve efficient management of the entire electrical network (Albuquerque, 2018). A system grid view of the DR problem and their issues related to industrial scenarios can be seen in the reviews by Perera e Kamalaruban (2011), Santos J M Soares e Prata (2023) respectively.

The Brazilian National Electric Power Agency (ANEEL) classifies electric energy users into two groups: A, which is connected to the grid with voltages higher than 2.3 kV; and B, for voltages below 2.3 kV. Included here are the residential consumers, classified as B1 (ANEEL: Brazil, 2021). For the B1 group, two options of energy tariff are available: conventional tariff

(T_c), which is constant over time, and white tariff, which is subdivided into three hourly constant posts: peak post tariff (T_p), intermediate post tariff (T_i) and off-peak post tariff (T_f). Because Brazil spans a continental size, its energy market is divided into several regional segments, each of which could define their tariff values and post hours in accordance with the previous definitions. (ANEEL: Brazil, 2023). Table 1 summarizes the costs of both tariffs in the official Brazilian currency for the local energy market closest to the author of this thesis (ENEL (Ceará), 2023). Figure 1 illustrate the values of white tariff and the constant one. Note that there is no billing related to demand response or demand peaks covered by Brazilian official resolution (ANEEL: Brazil, 2021) for the B1 group, but this work will consider it due to its relevance for the global scenario.

Table 1 – Comparison between conventional tariff and white tariff over time.

Period	Tariff Post	T_c (R$/kWh)	White Tariff (R$/kWh)
00:00 to 16:30	Off-peak	0.74373	0.62124
16:30 to 17:30	Intermediate	0.74373	1.03901
17:30 to 20:30	Peak	0.74373	1.63527
20:30 to 21:30	Intermediate	0.74373	1.03901
21:30 to 00:00	Off-peak	0.74373	0.62124

Source: Prepared by the author.

Figure 1 – Comparison between conventional tariff and white tariff over time

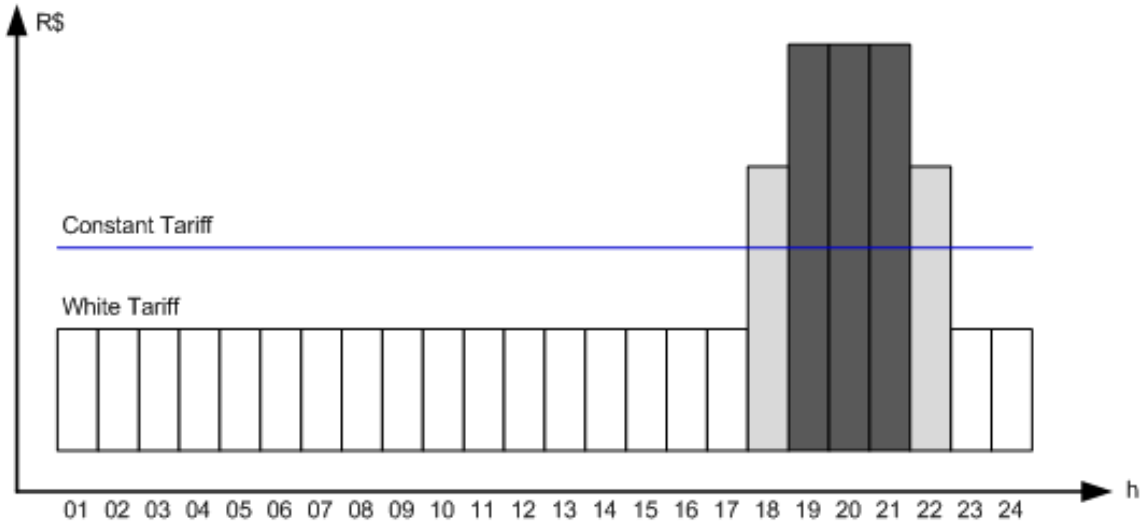

Source: Prepared by the author.

This study presents an innovative approach to scheduling household appliances. Its goal is to reduce energy costs and enhance user comfort by optimizing the timing of appliance operation according to users' typical preferences.We examined aspects of the energy pricing structure in Brazil and broke down time into a geometric framework, allowing us to track when

appliances are in use. Through detailed analysis, we identified a point in this framework that minimizes cost and the need for shifting loads. Our benchmark tests demonstrate that our method is significantly faster and more memory-efficient compared to traditional algorithms for similar optimization tasks. This efficiency could pave the way for its integration into small, embedded systems in the future.

To address a specific constraint related to managing demand response peaks that the geometric framework alone could not handle, a hybrid methodology was developed. This hybrid approach enhances the robustness and versatility of the overall methodology, ensuring that it can effectively manage the limitations encountered during the scheduling process.

As specific objectives we can list:

1. **Develop a New Methodology:** Create a novel approach for scheduling household appliances using a geometric time framework.
2. **Optimize Timing for Cost and Comfort:** Optimize the timing of household appliance operations to reduce energy costs and enhance user comfort.
3. **Benchmark Performance:** Conduct benchmark tests to compare the new geometric time framework methodology with traditional algorithms in terms of speed and memory efficiency.
4. **Compare with Linear Programming:** Evaluate the proposed geometric time framework methodology against a linear programming algorithm to highlight differences in performance and effectiveness.
5. **Develop Hybrid Methodology:** Propose and implement a hybrid methodology to address specific constraints that the geometric framework alone cannot handle.
6. **Detailed Code Implementation:** Provide the details and implementation of the methodology in the Julia programming language, including all relevant algorithms and procedures.

The remainder of this thesis is divided as follows: Chapter 2 presents the literature review. Chapter 3 discusses load modeling and defines study case scenarios. Chapter 4 states the SHC mathematical model equations and constraints. Chapter 5 introduces the concept of tariff spaces and sets its properties regarding geometric *locus* and also explains how the proposed methodology works. In Chapter 6, the simulation results are shown and discussed. Chapter 7 condenses the contributions of this work and points out some future assignments to improve it.

2 LITERATURE REVIEW

Currently, many studies have proposed solutions for energy efficiency in the domestic environment due to the constant increase in both energy consumption and electricity tariffs. In a smart home (SH) scenario, home energy management system (HEMS) controllers are installed to schedule loads at times when the tariff is lower off-peak post (Albuquerque, 2018). This scheduling typically takes into account the user's preferences and habits, which can lead to a confrontation with the maximization of the savings.

Considering the scenario with (un)interruptible loads under dynamic pricing, Kim e Poor (2011) studied the scheduling problem using Markov decision process as a possible solver. To provide a strategy for efficient management of electric energy and peak control in a domestic environment, (Giorgio e Pimpinella, 2012) proposes the design of a SHC using binary linear programming. To deal with uncertainties in appliance use habits and renewable energy generation, Chen *et al.* (2013) propose a home appliance scheduler combining linear and stochastic programming. Concerned about peak load demand, Venkatesh (2015) modeled the appliances considering the worst-case scenario and photovoltaic (PV) as negative load into CPLEX solver, modeling the scheduling problem as mixed integer programming (MIP). Considering the Day-ahead load scenario, a model of a household with PV system and including thermally controlled loads was proposed by Wang *et al.* (2015), which used quadratic programming to minimize the user cost.

Most renewable systems use batteries as energy storage unity, which usage should be modeled and constrained (Huang *et al.*, 2016). The same author used two point estimation and gradient-based particle swarm optimization (PSO) to minimize cost and improve demand response in a HEMS. Diesel generators are also a common power source, as considered in Rahmani-Andebili (2017) which used genetic algorithm (GAs) and linear programming (LP) to model the trade between SHC and local distribution company. Both authors used stochastic models to model dynamic parameters.

The behavior of home appliances is a recurrent concern in this topic due to its unique and intricate characteristics. Subdividing a multiple-stage load into a combination of virtual loads estimated by their peak energy consumption seems to be a reasonable way to handle this problem (Farrokhifar *et al.*, 2018). Additionally, defining policies based on weather (Lu *et al.*, 2020) or user life habits (Luo *et al.*, 2020) are also valid methods to optimize a HEMS.

However, load reallocation can cause discomfort in the user's habits and trigger

physical and psychological issues (Costa *et al.*, 2023). Over time, many authors have proposed methodologies to balance the cost *versus* comfort problem using different techniques like fuzzy logic (Mohsenzadeh *et al.*, 2013; Chekired *et al.*, 2017; Costa *et al.*, 2023) integer programming (Bezerra Filho *et al.*, 2015; Albuquerque *et al.*, 2018), convex optimization (Ma *et al.*, 2016), GAs (Ogunjuyigbe *et al.*, 2017; Albuquerque, 2018; Manzoor *et al.*, 2017; Chen *et al.*, 2022), PSO (Lin e Hu, 2018; Santos, 2019) and stochastic programming (Gazafroudi *et al.*, 2019; Akbari-Dibavar *et al.*, 2020; Zeynali *et al.*, 2020), to name a few relevant works.

The authors in Ali (2022) propose an optimization-based DSM scheduler and energy controller for a smart home considering renewable energy generation and battery storage systems to achieve a reduction in energy cost and peak-to-average ratio in demand, and to improve user comfort in terms of thermal, illumination, and appliance usage preference. Their Mathematical models are executed in many optimization algorithms.

The scheduling of appliances, considering user habits, can also improve the comfort issue. A Context-Aware Framework, stated on a wireless sensor network to identify behavioral patterns and habits, can generate recommendations that allow energy savings at homes (García *et al.*, 2017). By monitoring rooms occupancy, a Multi-Agent System can analyze the household data and improve the energy consumption of heating, ventilation, and air conditioning (HVAC) systems (González-Briones *et al.*, 2018). By analyzing patterns from user habits and PV generation a HEMS can avoid power peak consumption penalties (Luo *et al.*, 2020). Noninvasive load monitoring approaches and a taxonomy of methodologies to optimize energy consumption have been reviewed by Schirmer e Mporas (2023).

The studies can be extended to smart builds or even to smart districts by using a two-level approach. The first level is described as the base unit of energy consumption, such as a SH with PV for example. The second level is composed of an array of base units, in addition to shared co-generation and energy storage. For example, in one residential building, each apartment has a solar panel on some windows and share also energy from a PV and/or wind turbine systems on the roof (Rajasekhar *et al.*, 2019; Çimen *et al.*, 2022; Chen *et al.*, 2022; Mansouri *et al.*, 2022).

In preparation for this work, some relevant review articles related to the topic were also found.

The authors in O'Grady *et al.* (2021) conducted a systematic literature review (SLR) and meta-analysis, adhering to PRISMA guidelines. Their study focuses on building automation

systems (BAS), which are increasingly being integrated into modern buildings to enhance energy efficiency and occupant comfort. The review included studies from databases such as Scopus, Web of Science, and IEEE Xplore, and selected them based on specific criteria focusing on the implementation, performance, and outcomes of BAS.

The review identified several key themes in BAS research:

- Energy Efficiency: Many studies highlighted the role of BAS in reducing energy consumption through optimized control of HVAC systems (ASHRAE, 2017), lighting, and other building services.
- Occupant Comfort: BAS implementations were found to improve indoor environmental quality, including air quality, temperature, and lighting, thereby enhancing occupant comfort and productivity.
- Technology Trends: Recent advancements include the integration of internet of things (IoT), artificial intelligence (AI), and machine learning to enhance BAS functionality. These technologies enable predictive maintenance, real-time monitoring, and adaptive control strategies.
- Challenges and Barriers: Common challenges in BAS adoption include high upfront costs, technical complexity, and the need for skilled personnel to manage and maintain these systems.

The meta-analysis indicates that while BAS offer substantial benefits, their effectiveness is highly dependent on proper design, implementation, and ongoing management. The findings suggest a need for standardized protocols and best practices to ensure optimal performance. Furthermore, future research should focus on developing cost-effective solutions and addressing the skill gaps in the industry.

In conclusion, building automation systems hold significant potential for improving building efficiency and comfort. The study's findings underscore the importance of continued research and development in this field, particularly in leveraging advanced technologies to overcome current limitations and maximize the benefits of BAS.

The papper written by Aliabadi *et al.* (2021) delves into the concept of coordinating HEMS to mitigate the adverse effects caused by selfish systems in distribution grid regions. It discusses how coordination can alleviate issues like rebound peaks, instabilities, and contingencies, emphasizing its significance in achieving grid objectives such as load profile flattening, cost reduction, and energy trading facilitation. The review explores recent investigations into

coordinated HEMS, detailing the necessary steps for implementation, including coordination topologies and techniques.

A key focus of the paper is the classification of coordination approaches based on their utilization of decomposition algorithms. It examines the major features, advantages, and disadvantages of these methods while analyzing coordination process characteristics, mathematical issues, and player concerns. Specific applications of coordination designs are discussed and categorized, aiming to provide insights into critical gaps in existing studies and propose practical solutions.

Unlike other reviews, this survey concentrates on effective frameworks to make coordinated HEMS feasible, aiming to identify research gaps, future opportunities, and implementation challenges. The paper concludes by highlighting the potential benefits of coordinated HEMS, including significant reductions in electricity bills, and presents a roadmap for future research in this area.

The authors in Merabet *et al.* (2021) conducts a comprehensive review of AI techniques utilized in building control systems to enhance energy efficiency while maintaining thermal comfort. It addresses the conflicting objectives of reducing energy consumption in HVAC systems while ensuring comfortable indoor conditions. The review encompasses methodologies deployed over the past decade, evaluating their outputs, implementations, and abilities to improve energy efficiency and comfort levels.

Among the twenty AI tools analyzed, functions such as pattern identification, optimization, and predictive control are highlighted for their contributions to energy consumption and comfort control. The review underscores the ongoing nature of AI-based control system performance improvement, attributed in part to the requirement for large amounts of high-quality real-world data.

The paper presents findings indicating significant energy savings and comfort improvements achieved through the application of AI techniques and personalized comfort models. It discusses challenges faced in utilizing AI for energy productivity and comfort improvement, highlighting future research directions in AI-based building control systems for enhanced human comfort and energy efficiency management.

The paper written by Balakrishnan e Geetha (2021) conducts a comprehensive review of HEMS, addressing the increasing energy demand and distribution issues. HEMS are designed to optimize energy usage in homes, identifying areas of energy wastage and facilitating

better energy utilization. They also enable two-way communication between consumers and distribution centers, considering both energy generation and consumption.

The review focuses on various aspects of HEMS, including different climate conditions, appliances, controllers with algorithms, and the lifestyles of home occupants. It discusses research papers related to HEMS implementation in diverse scenarios, aiming to improve energy efficiency without compromising consumer quality of experience (QoE). Different pricing techniques employed by utility centers, such as ToU, RTP, and fixed plan (FP), are also examined.

The development of HEMS aims to enhance QoE by managing energy generation and conservation, integrating renewable energy sources, and utilizing battery storage. By optimizing energy usage, HEMS not only saves money but also conserves natural resources and reduces the need for additional power generation. The review provides insights into the components and functionalities of HEMS, offering a holistic understanding of its applications in various home environments.

A smart home enhances residents' quality of life by incorporating technologies for monitoring, promoting independence, and automating home environment operations to suit inhabitants' needs is the goal of authors in Mekuria *et al.* (2021). The Smart Home Reasoning System (SHRS) plays a crucial role in determining automatic control and adaptation processes within the home. Despite extensive research on various aspects of SHRS, there's a notable lack of systematic investigation into these systems.

To address this gap, their paper conducts a SLR through automatic and manual searches across six electronic databases, analyzing 135 literature sources. The SLR reveals that approximately 43% of smart homes aim to offer general home automation services. It also identifies twelve major requirements of an SHRS.

Furthermore, the study highlights that 55.5% of research contributions in the SHRS domain are conceptual, with 51.5% relying on symbolic artificial intelligence techniques. It examines the usage and application trends of different reasoning techniques in the smart home domain, assessing the assumptions, strengths, and limitations of proposed systems in the literature.

Additionally, their study discusses the challenges of reasoning in ambient assisted living environments and emphasizes the importance of utilizing hybrid reasoning approaches. It underscores the necessity of addressing overlapping, simultaneous, and conflicting activities and goals of multiple inhabitants.

The authors in Mischos *et al.* (2023) thoroughly examine the pressing issue of energy

waste and its contribution to climate change, particularly focusing on residential, commercial, and educational buildings. It underscores the significance of implementing intelligent energy management systems (IEMS) to monitor and regulate energy consumption effectively. Notably, it introduces a classification system that categorizes IEMS into two main types: direct control systems, which offer automation to control various functionalities, and indirect control systems, which target behavioral modification among occupants.

In residential and commercial contexts, where energy usage is substantial, direct control systems are emphasized due to their capacity to provide automation, offering convenience and efficiency. These systems enable real-time monitoring and adjustments, optimizing energy consumption without significant user intervention. Conversely, in educational buildings, where fostering awareness and instigating long-term behavioral changes are paramount, indirect control systems may be more fitting. By influencing occupants' behavior and habits, these systems aim to cultivate sustainable energy practices that extend beyond immediate efficiency gains.

Despite the advantages presented by both approaches, the text also highlights vulnerabilities inherent in these systems. For instance, direct control systems are susceptible to cyberattacks, posing risks such as false data injection that could lead to increased energy consumption or system malfunctions. On the other hand, indirect control systems may encounter challenges like the cold start problem, which arises when new users or actions are introduced, affecting the system's effectiveness until sufficient data accumulates.

The review concludes by suggesting avenues for further research and development in the field of IEMS. It proposes exploring reinforcement learning techniques to enhance the capabilities of direct control systems, addressing issues such as slow training rates to improve their efficiency and adaptability. Additionally, there's a call for creating engaging applications or serious games to bolster user engagement in indirect control systems, facilitating behavioral changes and promoting energy awareness. Ultimately, the text advocates for ongoing advancements in IEMS, particularly emphasizing the need for more accessible and affordable indirect control applications in residential settings to democratize energy management and sustainability efforts.

3 LOAD MODEL

During the bibliographic research, we detected that there is no standard for load modeling or classification. However many authors use similar terms like (non)controllable (Albuquerque, 2018; Santos, 2019; Costa *et al.*, 2023), (un)interruptible (Venkatesh, 2015; Wang *et al.*, 2015), single/multi-period (Mohsenzadeh *et al.*, 2013; Farrokhifar *et al.*, 2018) etc. In this thesis, loads are classified into two categories, following the stated in Albuquerque *et al.* (2018):

1. **Controllable load (CL):** encompasses a wide array of devices allowing for manual or remote manipulation. They utilize switches, dials, or digital interfaces to adjust operations. Integrated into SH ecosystems, users can oversee appliances using smartphones or voice assistants, enhancing convenience and energy efficiency. Examples of CL are air conditioners, pool filter pumps, non-programmable washing machines, dishwashers, irons, or even outdoor lighting.
2. **Detectable load (DL):** refers to an electrical device or equipment that can be identified and monitored within a SH ecosystem. Unlike CL, detectable ones are not typically designed for remote manipulation or control. However, we can estimate their energy consumption by comparing the energy measurements of the smart meter (SM) and all other devices connected to a HEMS. Examples of DL are audiovisual equipment; personal computer systems; indoor lighting; toasters, refrigerators, and freezers.

The parameters of the i^{th} CL in a set, which were used to structure the programmer model and simulations, are presented in Table 2 and are closely related to scheduling problem modeling (Coutinho, 2013).

Figure 2 provides an overview of the load parameters listed in Table 2, illustrating their positioning over time for a generic or randomly drawn load with multiple discreet power stages (gray object).

On the left side of Figure 2, the release $L_i.r$ and expected activation time $L_i.e$ instants are shown. On its right side, the deadline $L_i.d$ and the range of power over time $L_i.P(t)$ are depicted. Above the gray area, the load length $L_i.W$ is shown. Below it, one possible start $L_i.s$ and its respective finishing time $L_i.f$ instants are marked. Finding the correct index of the start instant array that balances cost under white tariff scenario and user comfort due to this scheduling point is the goal of this work. Details of the code that realizes this structure in Julia language can be found in the link provided in Appendix A.

In this study, we considered that a complex load can be represented by its highest

Table 2 – List of symbols that define parameters of a *BasicLoad* structure in Julia language for each load L_i.

Id	Description
$L_i.r$	release time of the i^{th} load
$L_i.e$	expected on time of the i^{th} load by user
$L_i.d$	deadline instant of the i^{th} load
$L_i.W$	width of the i^{th} load, usually measured in minutes
$L_i.W\Delta$	discrete load width
$L_i.s$	array with all possible start times of the i^{th} load, $L_i.s \geq L_i.r$
$L_i.f$	finishing time of the i^{th} load, $L_i.f = L_i.s + L.W \leq L_i.d$
Δt	discrete step in which a load could move through time, common to all loads in set
$L_i.P(t)$	behavior of the i^{th} load through time
$L_i.\bar{P}$	average power of the i^{th} load
$L_i.\hat{P}$	peak power of the i^{th} load
$L_i.\mu$	relevance of the i^{th} load, $\in [0,1]$
k	proportion of discrete time related to 1 hour, $k = \left(\frac{60}{\Delta t}\right)$

Source: Prepared by the author.

Figure 2 – Load model and timing parameters

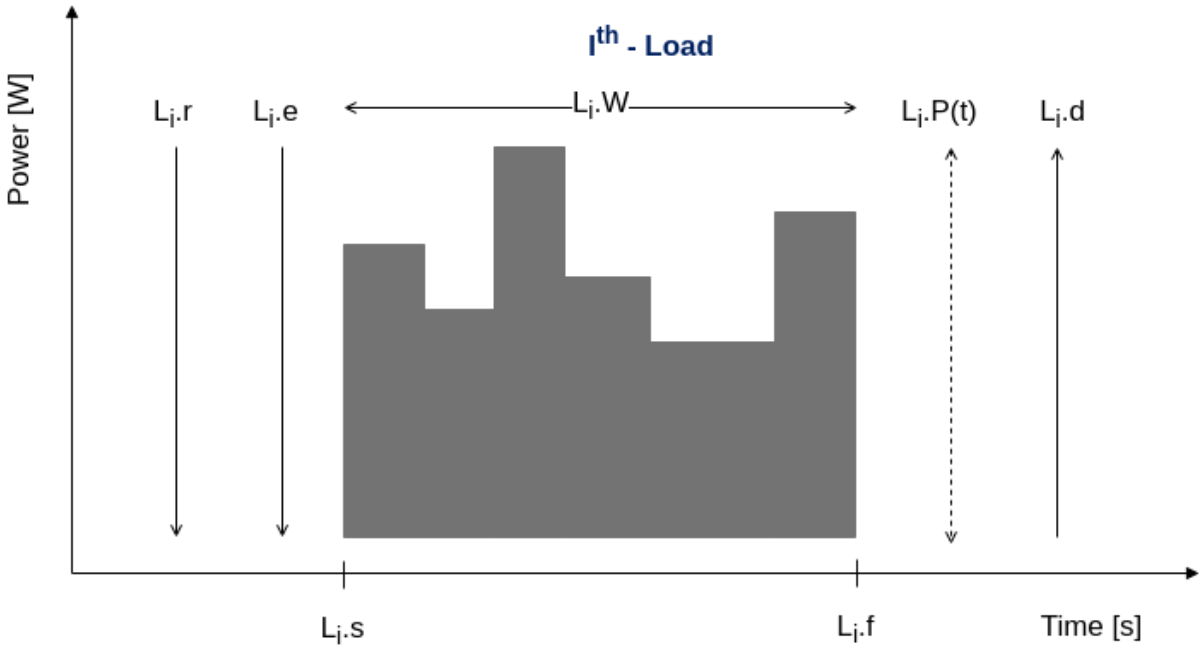

Source: Prepared by the author.

power consumption ($L_i.\hat{P}$), as suggested in Coutinho (2013), which serves as an asymptotic reference scenario for modeling purposes. For instance, an inverter air-conditioner with a peak power of 3.5 kW can be modeled as a rectangle with a constant height of 3.5 kW. However, in practice, this power is often lower and varies depending on climatic conditions. That way, the energy cost evaluated by this work methodology will be greater than or equal to the real scenario.

We also consider that a multistage load could be simplified as a combination of single small loads (Farrokhifar *et al.*, 2018), also estimated by their peak value. This consideration is needed to model loads that could be interrupted or have large stages with different power

peaks and off gaps between them. A practical example of this kind of load is a washing machine. Figure 3 demonstrates this process for a two-stage load L_i.

Figure 3 – Modeling multiple stage load to multiple simple loads

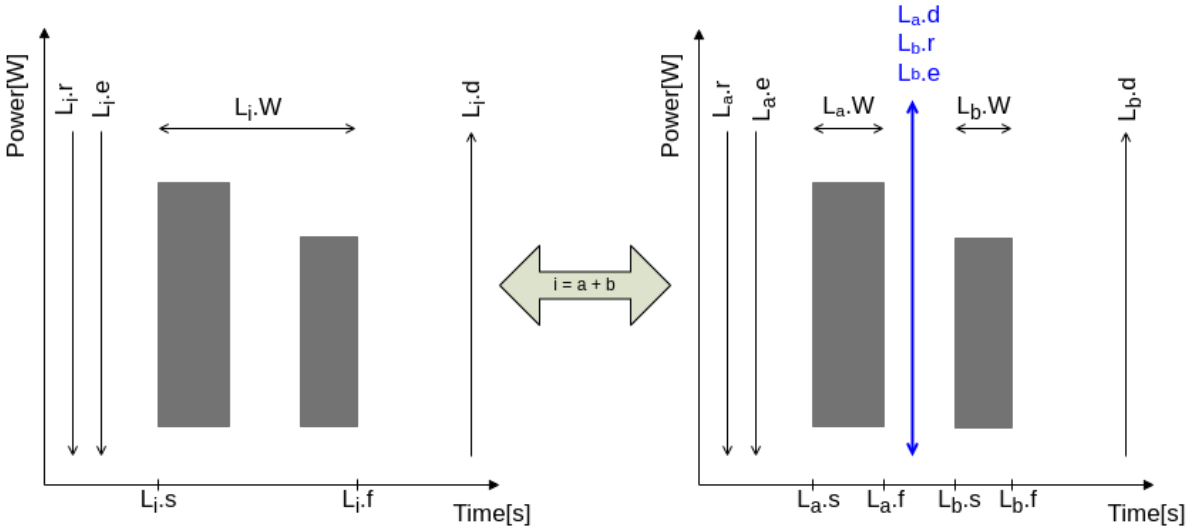

Source: Prepared by the author.

In this example, we split its duration into stages, each with its own start and finish times. We then adjusted the parameters for the release ($L_b.r$) and expected time ($L_b.e$) of the second stage to align with the deadline ($L_a.d$) of the first stage and into the off gap. Moreover, the first stage inherits the release ($L_a.r = L_i.r$) and expected time ($L_a.e = L_i.e$) from the original load L_i, while the second stage inherits its deadline ($L_b.d = L_i.d$).

The simulation step or sampling rate is also an important variable and should be considered as minimum as possible to achieve flexibility in scheduling (Lu *et al.*, 2020). All simulations and benchmark results were obtained using $\Delta t = 5\ min$. However, for some later illustrations, it will be stated as $\Delta t = 30\ min$ for better graphical comprehension.

3.1 Simulation Scenarios

Nine simulation scenarios are proposed in this work. The first one is related to a real house described in Albuquerque *et al.* (2018) and also studied in Albuquerque (2018), Santos (2019), Costa *et al.* (2023). The details of appliances are described in Table 3. This set of loads has been considered due to the known results by the author of this thesis from previous works, serving as a compass to ensure the methodology presented in this present work.

The last eight sets of loads were **randomly generated** and utilized to collect benchmarks for execution time and memory usage, corresponding to load quantities of 10, 25, 50,

75, 100, 250, 500, and 750. These specific load quantities were chosen to assess the impact of increasing load set sizes on performance parameters. All benchmark output details are described in Appendix D.

Table 3 – Reference loads in an actual residence.

ID	Load	Cycles	$\Delta t(min)$	$\bar{P}^*$	$\hat{P}^*$	Expected Time	Release Time	Deadline Time	μ_i
1	Water tank pump	1	20	2	3	8h	7h	17h	0.1
2	Pool filter pump	1	120	0.75	1.5	8h	7h	17h	0.1
3	Iron	1	120	1	1.2	16h	14h	17h	0.3
4	Washing machine	8	10 10 4 6 2 2 2 7	0.13 0.51 0.30, 0.26 0.15 ··· 0.22	0.70 0.50 0.30 0.26 0.15 ··· 0.30	8h	7h	17h	0.5
5	External lamps	1	270	0.3	0.3	18h	17h	24h	0.3
6	Indoor lamps	1	270	0.15	0.3	18h	17h	23h	0.7
7	Air Conditioning 1	14	[10 5 5 ··· 5]	[1.3 ··· 1.3]	[1.7 1.3 ... 1.3]	16h	15h	24h	1.0
8	Air Conditioning 2	7	[30 20 5 ··· 5]	[2 ··· 2]	[2.1 ··· 2.1]	20h	17h	24h	1.0
9	Air Conditioning 3	1	240	1.1	1.2	20h	17h	24h	1.0
10	Air Conditioning 4	7	[10 10 5··· 5]	[0,9 ··· 0.9]	[1,1 ··· 1.1]	20h	17h	24h	1.0
11	Dishwasher	5	5, 10, 15, 5, 10	0.03, 1.76, 0.03, 1.76, 0.03	0.03, 1.76, 0.03, 1.76, 0.03	21h	18h	22h	0.3

Source: Prepared by the author, adapted from Albuquerque (2018)
Note: * Average and Peak Power are measured in kW.

The common attributes across all simulation scenarios are as follows: a) The sampling interval, denoted as Δt, is fixed at 5 minutes; b) Each ensemble of ten loads adheres to a daily demand threshold of 4.0 kW. This threshold is depicted by an inverted Gaussian distribution centered at 18:30h, with a negative amplitude of 25%, serving to simulate a reduction in the demand threshold to accommodate the DL; c) the Brazilian ToU tariffs: constant and white.

For each load in any random scenario, the restrictions from Equations (3.1) and (3.2) were applied. Additionally, the relevance factor μ previously defined in Table 2 has been set to one to avoid any attenuation on the evaluation process of the comfort goal.

$$L_i.W \leq 6h \tag{3.1}$$

$$L_i.r \leq L_i.e \leq L_i.d - L_i.W \tag{3.2}$$

For each controllable load L_i in a SH context, the threshold in Equation (3.1) has been established based on the authors' common understanding that a controllable appliance would rarely operate for more than 6 hours. This time length is represented by the variable $L_i.W$. Nevertheless, this value could have been set to any appropriate value. The constraints outlined in Equation (3.2) specify that the expected activation time ($L_i.e$) for a load must fall within the release time ($L_i.r$) and its deadline ($L_i.d$), adjusted by the duration of the load ($L_i.W$). All these variables have been previously defined in Table 2.

All scheduling simulation results for all procedures listed in Chapter 6 and the simulated user expected activation time are graphically illustrated at Appendix C.

4 CLASSIC SHC

In this thesis, we assume that a SHC is connected to all controllable loads and is capable of performing their scheduling. For this control to be possible, the SHC must receive information about energy billing, white tariff ($C_w[t] \in \{T_f, T_i, T_p\}$) and constant tariff ($T_c$), controllable residential loads set (L_m), residential load activation preferences ($L_m.e$, $L_m.r$, $L_m.d$), and comfort level ($L_m.\mu$). To achieve this goal, we model the data related to residential loads, including the consumption profile (f_1) and the residential comfort profile (f_2). This modeling process enables us to understand consumption patterns, identify potential savings, and optimize comfort levels through a day-ahead load schedule.

4.1 Cost model - f_1

The mathematical definitions related to residential load at the grid level employed in this thesis are akin to those presented in prior works (Giorgio e Pimpinella, 2012; Albuquerque *et al.*, 2018; Rajasekhar *et al.*, 2019). The mathematical model for cost of residential loads corresponds to Equation (4.1), which incorporates the following premises: M schedulable loads, N daily samples, a sampling interval Δt. N index in sum is restricted to start ($L_i.s$) and finishing ($L.i_f$) instants. All these variables follows the notation described in the Load Model Chapter.

$$f_{Fcost} = \sum_{i=1}^{M} \sum_{j=L_i.s}^{L_i.s+L_i.W} (L_i.\bar{P}[j] \frac{\Delta t}{60} C_w[j]) \tag{4.1}$$

subject to the following constraints:

$$L_i.r \leq L_i.s \leq L_i.d - L_i.W, \forall\, i \in M \tag{4.2}$$

$$\sum_{i=1}^{M} L_i.\hat{P}[j] \leq \hat{P}_j, \forall\, j \in N \tag{4.3}$$

where $L_i.\bar{P}[j]$ and $L_i.\hat{P}[j]$ are respectively average power and the peak power of the i^{th} load L at instant j, and $\hat{P}_j$ is the total maximum demand restriction for the same moment.

The bounds outlined in Equation (4.2) specify that the timing of activation for the i^{th} load must fall within the user-defined release and deadline time instants, in the same terms as Equation (3.2) was defined. Additionally, the loads must not surpass the threshold demand ($\hat{P}_j$) at the j^{th} activation time, as indicated by the constraints presented in Equation (4.3).

The cost function (f_1) defines the economic savings due to SHC normalized by the cost in constant tariff. The first and second terms in Equation (4.4) correspond to the costs resulting from the user preference profile and the SHC scheduling, respectively.

The normalized economic savings, denoted by the cost function (f_1), articulate the financial benefits of dynamic tariff attributed to the SHC, normalized against the costs in a constant tariff setting. The initial and subsequent elements in the numerator of Equation (4.4) represent the costs associated with the user preference profile and the scheduling facilitated by the SHC, respectively, considering ToU white tariff.

$$f_1 = \frac{\sum_{i=1}^{M} \left(\sum_{j=L_i.e}^{L_i.e+L_i.W} (L_i.\bar{P}[j] \frac{\Delta t}{60} C_w[j]) - \sum_{j=L_i.s}^{L_i.s+L_i.W} (L_i.\bar{P}[j] \frac{\Delta t}{60} C_w[j]) \right)}{\sum_{i=1}^{M} \sum_{j=L_i.s}^{L_i.s+L_i.W} (L_i.\bar{P}[j] \frac{\Delta t}{60} T_c)} \tag{4.4}$$

In this context, $f_1 \geq 0$ ensures that the schedule proposed by the SHC is deemed acceptable by the algorithm as a valid solution for the user. Also note that f_1 is subjected to the same restrictions of Equation (4.1).

4.2 Comfort model - f_2

The comfort model, adapted from Albuquerque *et al.* (2018), Rajasekhar *et al.* (2019), takes into account the comfort relevance level of a load i as a measure of how much it deviates from the expected activation time by the user. To facilitate this, users are required to register residential loads eligible for scheduling in the SHC, along with specifying comfort relevance values ($0 \leq L_i.\mu \leq 1$) and the load activation parameters in terms of release ($L_i.r$), deadline ($L_i.d$), and expected ($L_i.e$) time instants.

Equation (4.5) delineates the comfort function. The initial term signifies the activation window of a load i concerning the user's preferences, serving as a benchmark for computing normalized comfort. The subsequent term quantifies the discrepancy between the time instant ($L_i.s$) chosen by the SHC and the user's preferred time ($L_i.e$). This difference is adjusted by the comfort relevance ($L_i.\mu$) associated with the i^{th} load. Note that if $L_i.\mu$ equals zero, the scheduling of this load becomes irrelevant since the comfort associated with it is maximized and set to a value of one.

$$f_2 = \frac{1}{M}\sum_{i=1}^{M}\left(\frac{\left[max(|L_i.r - L_i.e|, |(L_i.d - L_i.W) - L_i.e|)\right] - L_i.\mu\,|L_i.s - L_i.e|}{\left[max(|L_i.r - L_i.e|, |(L_i.d - L_i.W) - L_i.e|)\right]}\right) \tag{4.5}$$

For a specific load i with a comfort relevance of $L_i.\mu = 1$, this parameter attains its highest value when the scheduled time by the SHC aligns closely with the user's preferred time ($L_i.s \approx L_i.e$). However, if $L_i.s \approx L_i.r$ or $L_i.s \approx (L_i.d - L_i.W)$ (at the opposite end of the load activation window), the comfort level will be minimal. This occurs because the operation cycle commences at a time furthest from the one designated by the user as the preferred time.

4.3 JuMP and Hierarchical Algorithm

Julia Modeling Language for mathematical optimization (JuMP) is a modeling language (Lubin *et al.*, 2023) that condenses a collection of supporting libraries and packages running in Julia language (Bezanson *et al.*, 2017) that makes it prone to formulate and solve different problem classes related to optimization. The Multi-Objective Algorithms package (DOWNSON, O et al., 2023) provides many classic implementations ready to use. The best benchmark results were achieved with the hierarchical algorithm.

The hierarchical multi-objective algorithm organizes its approach to return a single point via an iterative scheme. First, it partitions the objectives into sets according to the objective priority. Then, in descending order of priority, it formulates a single-objective problem by scalarizing all objectives with equal weights. Next, it constrains these objectives to be at most relative tolerance worse than optimal in future solves.

In other words, it solves the model up to a given MIP gap to obtain an optimal value for the first objective function. Then, given the model restrictions, it optimizes the second objective using the first set of values of optimization variable to constraint the feasible set of the next optimization, such that the evaluated solution cannot get worse than first taking into account some predefined tolerance.

Finally, it proceeds to the next set of prioritized objectives. The solution represents a single point that trades off the various objectives. To save memory space, the implementation of this algorithm in JuMP development framework does not record the partial solutions found along the way (Lubin e Dunning, 2015; Dunning *et al.*, 2017; Lubin *et al.*, 2023).

All code related to the implementation of SHC Classic Model can be found in the link provided in Appendix A.

5 PROPOSED DEFINITIONS AND METHODOLOGY

The reader is now invited to look at Figure 4. The squared chart represents a zoom-around peak post of white tariff over time. The white outer regions are related to off-peak post, while the two thin yellow regions are related to the intermediate post and the central red area represents the peak post. Each square along the chart represents a sample period, which, for didactic purposes, has been set to 30 minutes. The long blue rectangles represent a generic four-hour-long load started in three different instants. For the purposes of this analysis, the vertical axis dimension of the time chart is considered irrelevant.

Figure 4 – Three different startup times for a 4 hours load around intermediate and peak post tariffs.

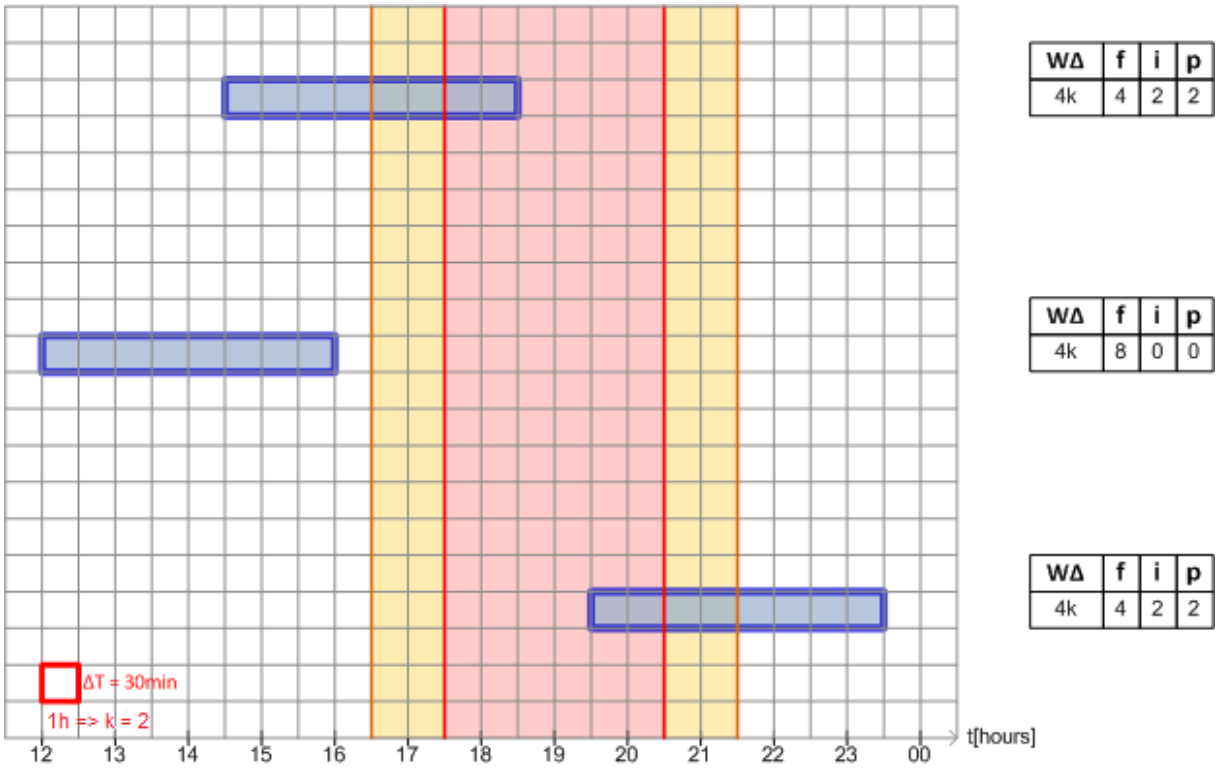

Source: Prepared by the author.

Note that while the four-hour-long load crosses the tariff posts, it is possible to evaluate how many discrete samples fit in each time post. For instance, the first load has four time units in off-peak post, two in intermediate post and two in peak post. These quantities are shown on the right side of each load representation in Figure 4.

From now, we assume that each time (or region) post in white tariff could be modeled as an independent dimension so that we could create a three-dimensional vector with components $(\hat{f}, \hat{i}, \hat{p})$ respectively to white tariff off-peak post, intermediate post, and peak post, whose lengths

are the load length portion that fits inside of each post region. This vector space is named here as **Tariff Space**.

The process for a load L, which quantifies how many discrete samples will fit in each time post according to load length ($L.W$ - continuous, $L.W\Delta$ - discreet) and its start time ($L.s$), is defined as **time decomposition into tariff space**. Its output is a vector in Tariff Space, as shown on the right side of Figure 4.

The code related to time decomposition into tariff space and its reverse operation can be found in the link provided in Appendix A. As the vector resulting from time decomposition has been stated, we now can evaluate the cost of a load, according to it start time, into a white tariff scenario using dot product:

$$C_w = k \cdot L.\hat{P} \cdot [(\hat{f}, \hat{i}, \hat{p}) \centerdot (T_f, T_i, T_p)] \tag{5.1}$$

where:

$$|\hat{f}| + |\hat{i}| + |\hat{p}| = L.W\Delta; \tag{5.2}$$

$$k = \left(\frac{60}{\Delta t}\right); \tag{5.3}$$

$L.\hat{P}$ is the peak power of a load and k is the discrete amount of time related to one hour due to sample rate Δt. All these symbols were defined in Table 2. The values in vector (T_f, T_i, T_p) represent the white tariff post costs, as previously stated in Table 1.

The minimum, maximum, and normalized costs of a load can also be written as:

$$C_{min} = k \cdot L.\hat{P} \cdot L.W\Delta \cdot T_f \tag{5.4}$$

$$C_{max} = k \cdot L.\hat{P} \cdot L.W\Delta \cdot T_c \tag{5.5}$$

$$C_{norm} = \left(\frac{C_w}{C_{max}}\right) \tag{5.6}$$

where C_w is the cost of a load under white tariff, as defined in Equation (5.1), and $L.W\Delta$ is the discrete value of load length due to sample rate Δt.

Note that the maximum is a relative value and is evaluated using constant tariff value because our goal is to reduce the bill relative to this reference value.

$$C_{min} \leq C_w \leq C_{max} \longleftrightarrow L.W\Delta \cdot T_f \leq [\hat{f} \cdot T_f + \hat{i} \cdot T_i + \hat{p} \cdot T_p] \leq L.W\Delta \cdot T_c \tag{5.7}$$

As cost margins have been defined, we can analyze the extreme points of Equation (5.7). Solving the equality at the lower bound yields the expression seen in (5.8). This indicates that to achieve this threshold, the total load length should fall within the off-peak post or, in other words, the point ($L.W\Delta$,0,0). Solving the equality at the upper bound, together with Equation (5.2), yield the two points expressed in (5.9). These three points delimit a region into tariff space in which the cost of a load in the white tariff scenario is less than or equal to the constant tariff, as points in Equation (5.9) delimit a line of this equality.

$$\hat{i} = -\hat{p}\frac{T_p - T_f}{T_i - T_f} < 0 \tag{5.8}$$

$$\begin{cases} if\ \hat{i} = 0 \quad \hat{p} = L.W\Delta\frac{T_c - T_f}{T_p - T_f} \quad \hat{f} = L.W\Delta - \hat{p} = L.W\Delta\frac{T_p - T_c}{T_p - T_f} \quad (point\ Q1) \\ if\ \hat{p} = 0 \quad \hat{i} = L.W\Delta\frac{T_c - T_f}{T_i - T_f} \quad \hat{f} = L.W\Delta - \hat{i} = L.W\Delta\frac{T_i - T_c}{T_i - T_f} \quad (point\ Q2) \end{cases} \tag{5.9}$$

Furthermore, it is important to consider that Equation (5.2) represents an equilateral triangle encompassing all possible combinations for $(\hat{f}, \hat{i}, \hat{p})$ within the constraints of $L.W\Delta$. However, it is possible for this representation to yield infeasible combinations, either due to one of the dimensions potentially being shorter than the length of a load itself or because of adjacent displacements in time imposed by the white tariff definition. For simpler examples, readers can refer to Appendix E, which contains applications demonstrating various binomial tariff patterns.

All these regions, along the points related to a one-hour-long load crossing the tariff regions, can be seen in Figure 5. The points related to the load movement have been colored according to their normalized cost, so the reader can see how their price change over the gray triangle plane surface. The region delimited by a red triangle represents the region of lower cost, which is composed by the two points in Equation (5.9) and the point that represents a load fully into $\hat{f}$ space.

Observe that the one-hour-load "walks" through the side of the triangle only. This occurs because time decomposition for this load would never have three components as its length fits entirely into all three tariff regions or between its adjacent transitions in pairs. For loads with length less than or equal to $L.\Delta t$ only the vertices of the triangle should be considered.

The next relevant load movement graphic is shown in Figure 6 and represents a six-hour-long load. Note that the behavior in tariff space is quite different from the one observed in Figure 5. This behavior can easily be modeled accordingly only to the load length. Those patterns, called here geometric *locus* of a load, are condensed in the six equations that follow for all sizes of $L.W$ between $L.\Delta t$ and a full day (24h). More examples of load decomposition into time space can be found in Appendix B.

$$(L.W\Delta,0,0);(0,L.W\Delta,0);(0,0,L.W\Delta) \tag{5.10}$$

$$\hat{i} = L.W\Delta - \hat{p} \leq k; \hat{f} = 0 \tag{5.11}$$

$$\hat{i} = L.W\Delta - \hat{f} \leq k; \hat{p} = 0 \tag{5.12}$$

$$\hat{i} = k, \hat{f} = L.W\Delta - \hat{p} - k; \tag{5.13}$$

$$\hat{i} = (L.W\Delta - 3 \cdot k) - \hat{f}; \hat{p} = 3k \tag{5.14}$$

$$\hat{i} = 2k; \hat{p} = 3k; \hat{f} = L.W\Delta - 5 \cdot k \tag{5.15}$$

Before analyzing each of these six equations, it's important to note that they are all confined to the region inside the triangle defined in Equation (5.2). We will frequently refer to the edges or vertices of this triangle to better understand the position of each locus.

The points shown in Equation (5.10) are related to a load whose length is less or equal to Δt, as mentioned before. Equation (5.11) represents a triangle side that connects axis $\hat{p}$

Figure 5 – All startup times for a 1 hour load crossing intermediate and peak post tariffs.

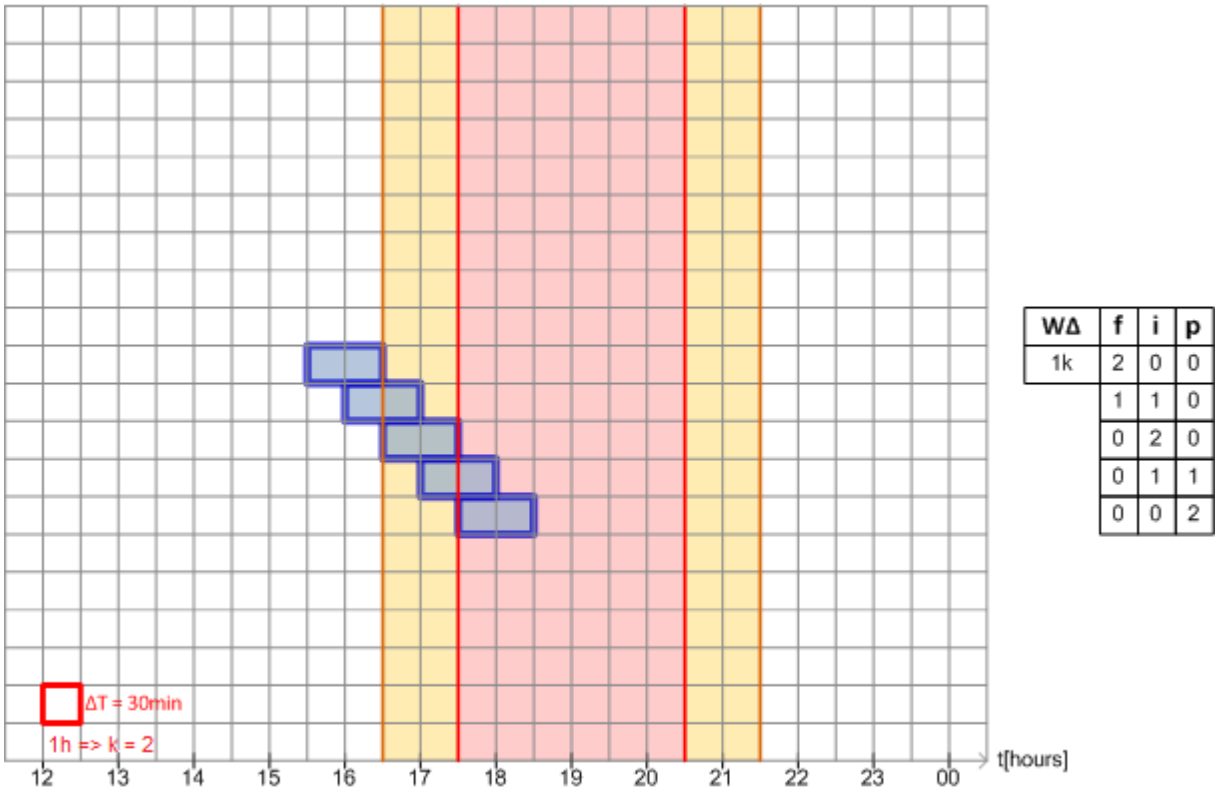

WΔ	f	i	p
1k	2	0	0
	1	1	0
	0	2	0
	0	1	1
	0	0	2

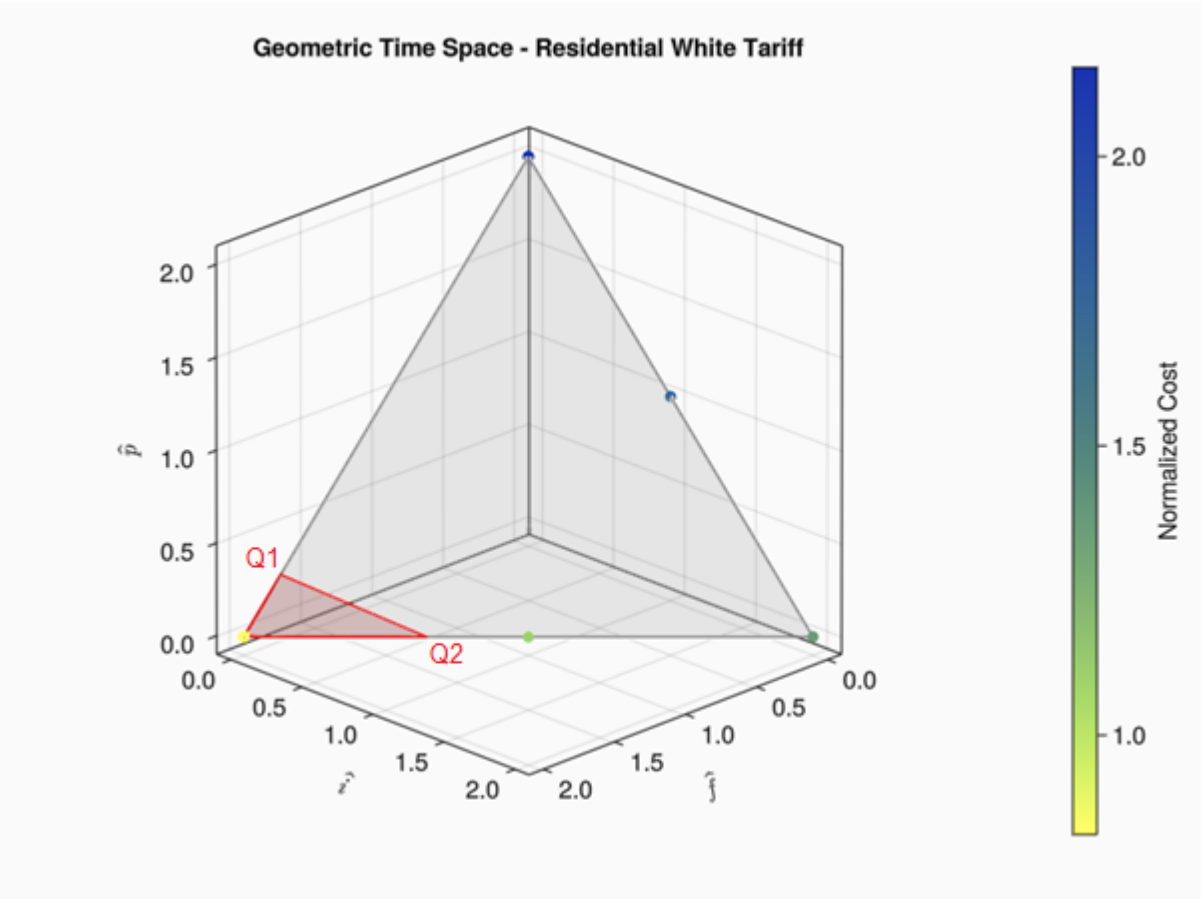

Source: Prepared by the author.

Figure 6 – Example of startup times for a 6 hours load crossing intermediate and peak post tariffs.

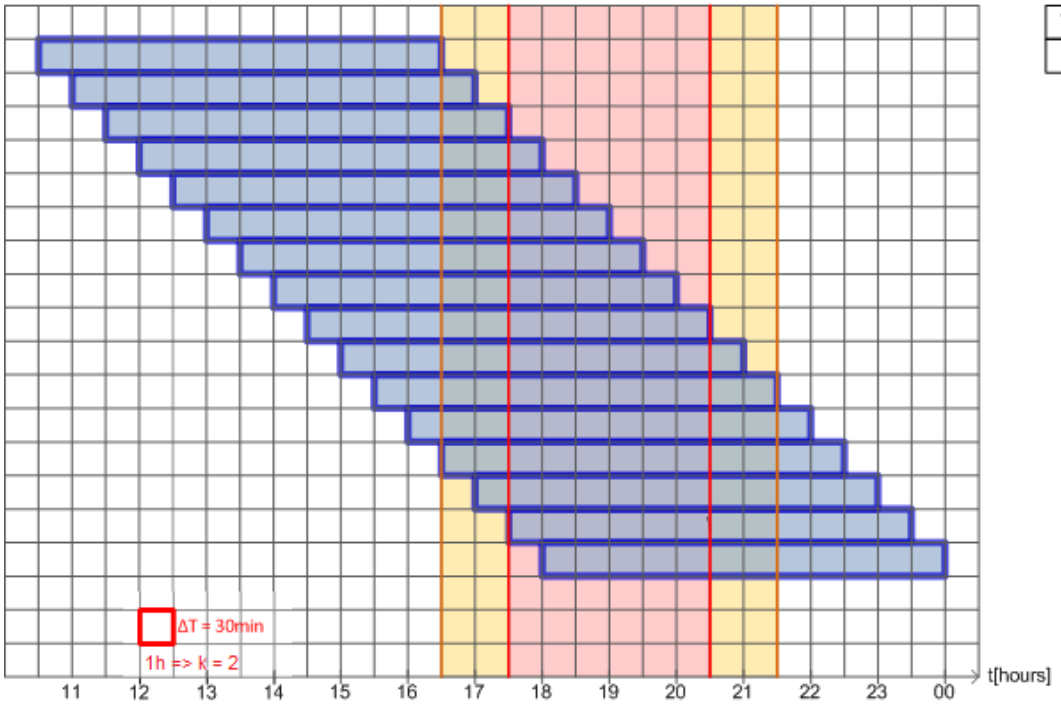

WΔ	f	i	p
6k	12	0	0
	11	1	0
	10	2	0
	9	2	1
	8	2	2
	7	2	3
	6	2	4
	5	2	5
	4	2	6
	3	3	6
	2	4	6
	2	4	6
	2	4	6
	3	3	6
	4	2	6
	5	2	5

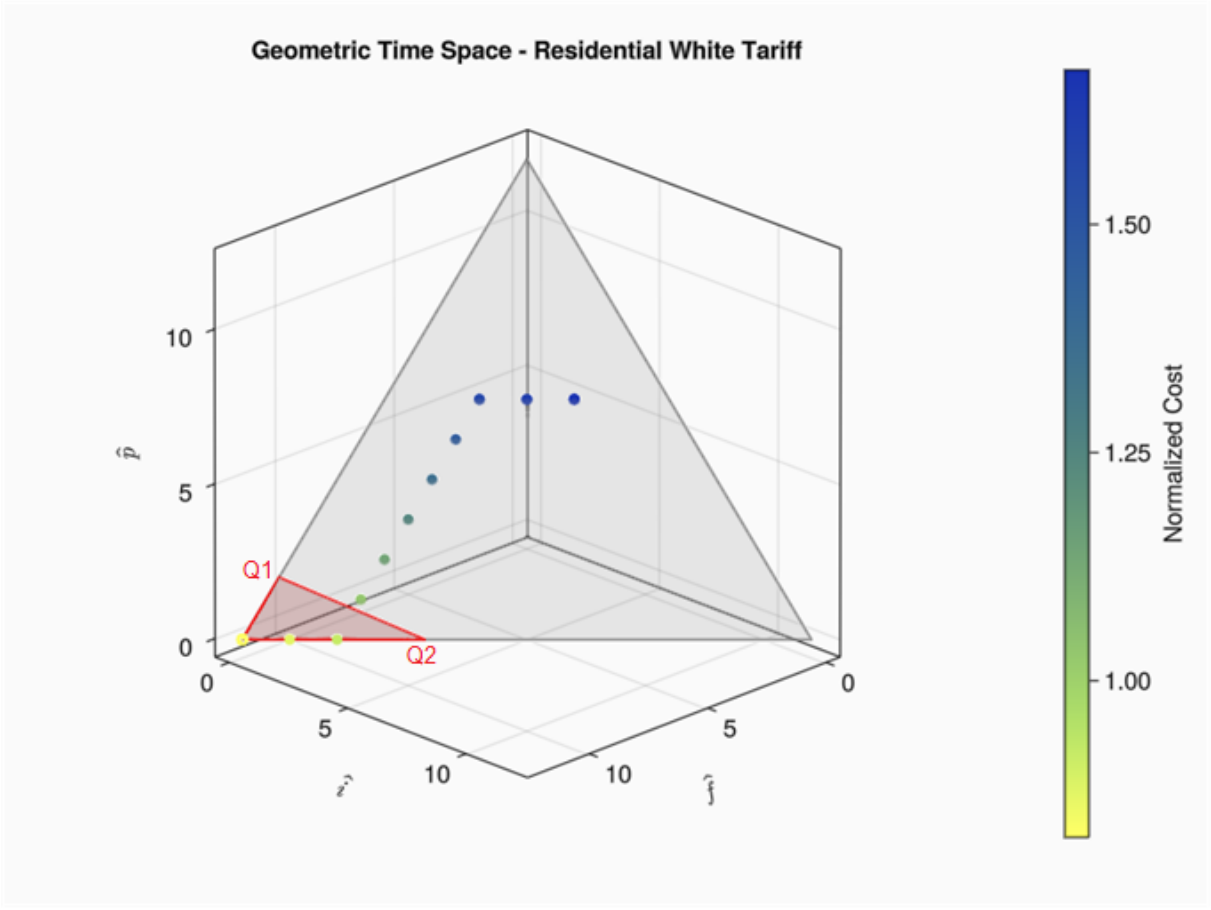

Source: Prepared by the author.

to $\hat{i}$ and signifies a linear trade-off for a load whose length is lower than or equal to an hour. A similar case occurs in Equation (5.12) that represents the triangle side that connects axis $\hat{f}$ to $\hat{i}$.

Equation (5.13) is applied when the load length is greater than an hour but less than or equal to four hours. It represents a parallel line to the triangle side that connects the axis $\hat{f}$ to $\hat{p}$. Note that, while a load longer than an hour crosses the intermediate post, that component remains constant and equal to an hour in size (represented by variable k, defined in Table 2). Additionally, it is important to recognize that this triangle side could never be reached as we could not split a single load into two parts. As stated in the Load Model Chapter, multiple-stage loads should be modeled as an array of single, indivisible loads with a shared deadline and release time.

The last two Equations (5.14),(5.15), are related to loads whose lengths are greater than 4 hours. It's important to note that for loads with a length of 4 hours or longer, as they cross the intermediate and peak posts their respective components should remain constant and equal to the regions occupied. Equation (5.14) models a line parallel to a side that connects axis $\hat{f}$ to $\hat{i}$. Finally, Equation (5.15) is a single point into tariff space that exists while the load is placed through the three-time posts and is also larger than both intermediate and peak posts.

Once we have defined all possible geometric *loci* for an appliance, it is pretty visible that only the lines defined by Equations (5.12) and (5.13) could reach the lower cost region. The analysis of upper bounds in Equation (5.7) gives us two points that could be combined to generate a parametric line Equation (5.16). The intersection between this line and load geometric *locus* will give us the solution to our schedule problem,

$$\begin{cases} \hat{f} = L.W \cdot \frac{T_p - T_c}{T_p - T_f} + \lambda \cdot \left(L.W \cdot \frac{(T_p - T_i)\cdot(T_c - T_f)}{(T_p - T_f)\cdot(T_i - T_f)} \right) \\ \hat{i} = \lambda \cdot L.W \cdot \frac{T_c - T_f}{T_i - T_f} \\ \hat{p} = L.W \cdot \frac{T_c - T_f}{T_p - T_f} \cdot (1 - \lambda) \end{cases} \tag{5.16}$$

where λ is the parametric variable for Equation (5.16)

Equations (5.12) and (5.13) can also be rewritten in parametric form,

$$\begin{cases} \hat{f} = L.W \cdot (1 - \alpha) \\ \hat{i} = \alpha \cdot L.W \\ \hat{p} = 0 \end{cases} \tag{5.17}$$

$$\begin{cases} \hat{f} = \rho \cdot (L.W - k) \\ \hat{i} = k \\ \hat{p} = (L.W - k) \cdot (1 - \rho) \end{cases} \tag{5.18}$$

where α and ρ are parametric variables for Equations 5.17 and 5.18 respectively.

Evaluating the interception point between Equations (5.16) and (5.17), we find a point described in Equation (5.19), which is one of the points that belong to ones listed in Equation (5.9). Graphically, it is indeed the point at lower cost region border where the cost of a load in white tariff is equal to the cost in constant one. As we need a relatively lower cost, we could use the *rounding floor function* to reach the next point inside the triangle. Note that by choosing this first inner point, a load whose expected time is in intermediate or peak post has minimum movement through time space, that way both objectives, cost, and comfort (as defined in section 4.2 and Equation (4.5)), are achieved.

$$P_{best1} = \left(\hat{i} = \lfloor L.W \cdot \frac{T_i - T_c}{T_i - T_f} \rfloor,\ \hat{f} = L.W - \hat{i},\ \hat{p} = 0 \right) \tag{5.19}$$

Calculating the interception point between Equations (5.16) and (5.18), we find the point described in (5.20).

$$P_{best2} = \left(\hat{p} = \lfloor L.W \cdot \frac{k \cdot (T_f - T_i) - L.W \cdot (T_f - T_c)}{T_p - T_f} \rfloor,\ \hat{i} = k,\ \hat{f} = L.W - k - \hat{p} \right) \tag{5.20}$$

The criteria to choose between P_{best1} or P_{best2} depend on the load length relative to k and the sign of $\hat{f}$ component. The flowchart in Figure 7 shows the decision process between the two values. Appendix A has a link to all code for the geometric search process (GeoFind for short).

5.1 Analysis of a load fully into off-peak post

As stated before, the methodology previously discussed is applicable only if the load has its expected start time inside the interval composed of the intermediate and peak posts. If a load is scheduled by a user fully into the off-peak post, no movement should be made with it, as it is already with maximum comfort (see section 4.2 for details) and lower possible cost.

Figure 7 – Geometric Search Flowchart

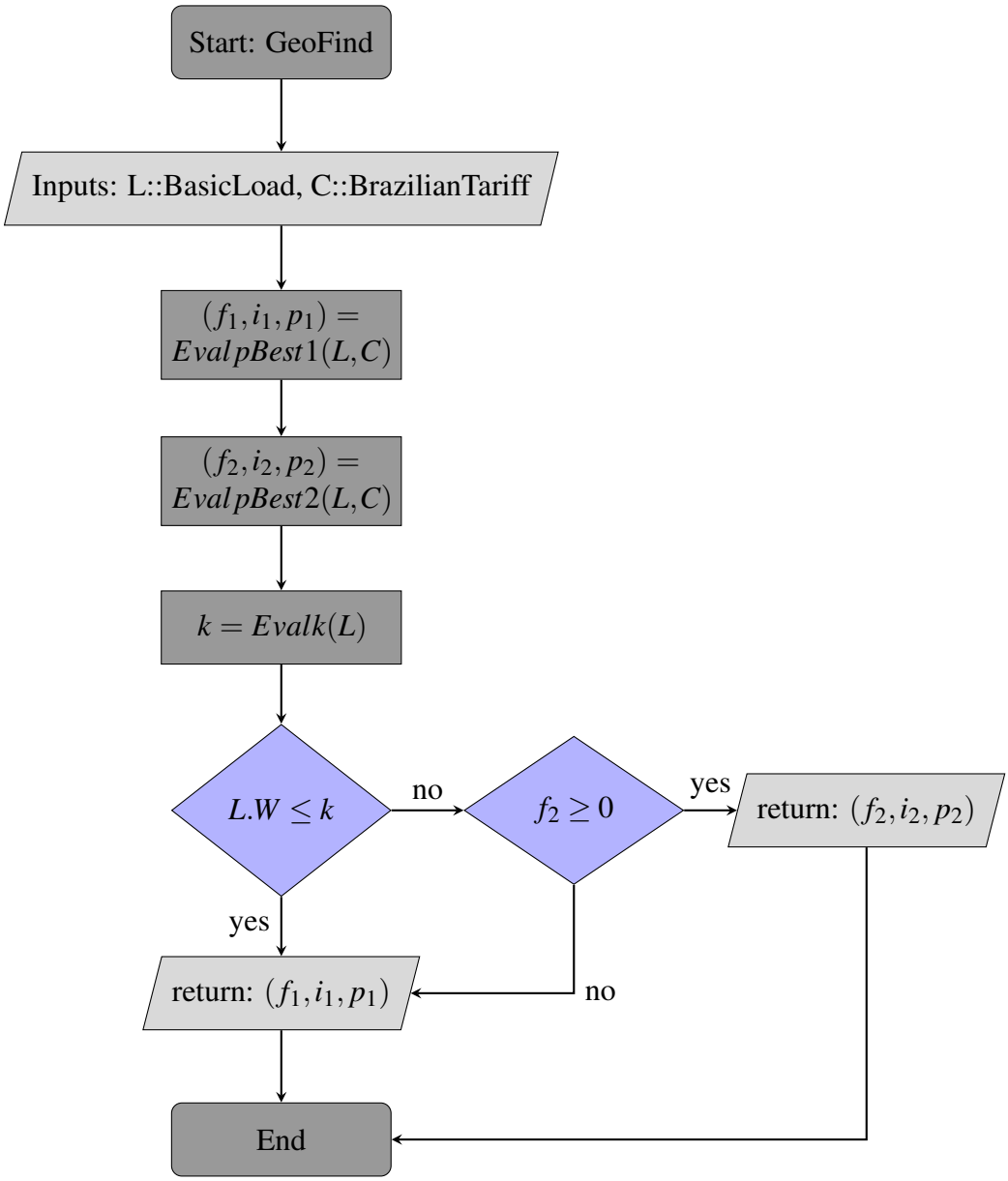

Source: Prepared by the author.

5.2 Analysis over defective geometric locus

Due to restrictions caused by the release or deadline instants, some loads may have not the full capability of moving through their geometric *locus*. As a result, such loads may be considered defective. To illustrate, consider an example of a load whose data could be read in Table 4 and its geometric *locus* seen in Figure 8. Note there is no intersection between the geometric *locus* and the lower cost region. In that specific case, we should look at the edges of the possible start times to find the schedule position with higher component $\hat{f}$, and to the expected schedule time, then evaluate the ratio between cost, Equation (5.1), and comfort, Equation (4.5), for this three instants, as shown in Equation (5.21) or in the flowchart illustrated at Figure 9.

Table 4 – Example of a load with defective geometric locus.

L.r	L.e	L.d	$L.\Delta t$	L.W
16h	18h	23h	5min	3h

Source: Prepared by the author.

Figure 8 – Example of a defective load into tariff space time

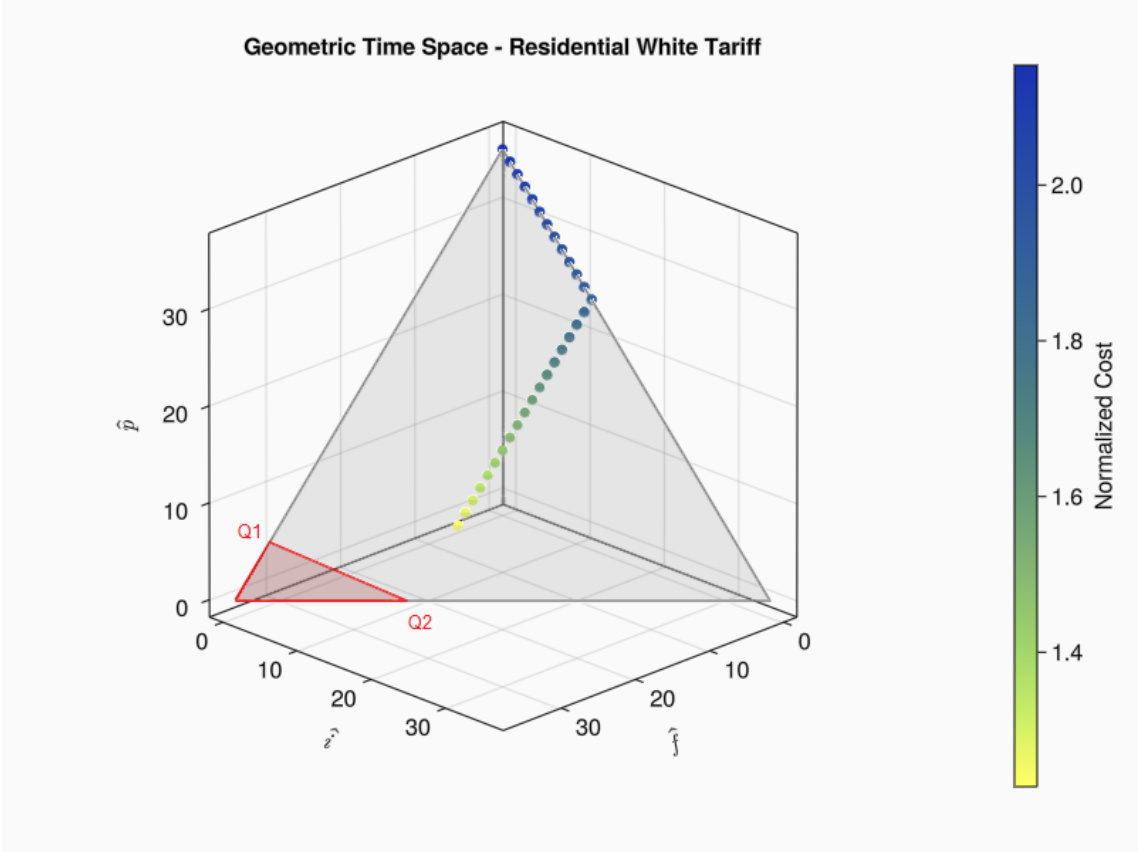

Source: Prepared by the author.

$$\begin{cases} R1 = Comfort(L, L.s[1])/Cost(L, L.s[1]) \\ Rf = Comfort(L, L.s[end])/Cost(L, L.s[end]) \\ Re = Comfort(L, L.e)/Cost(L, L.e) \end{cases}$$

$$\Rightarrow R1 \geq Rf \; ? \; (R1 \geq Re \; ? \; L.s[1] : L.e) \; : \; (Rf \geq Re \; ? \; L.s[end] : L.e) \quad (5.21)$$

In this case, the solution returned should be the best ratio result between comfort and cost. A concise implementation, reflecting the statements from this subsection and subsection 5.1, is demonstrated in Algorithm 1.

Figure 9 – Defective Geometric Locus Analysis Flowchart

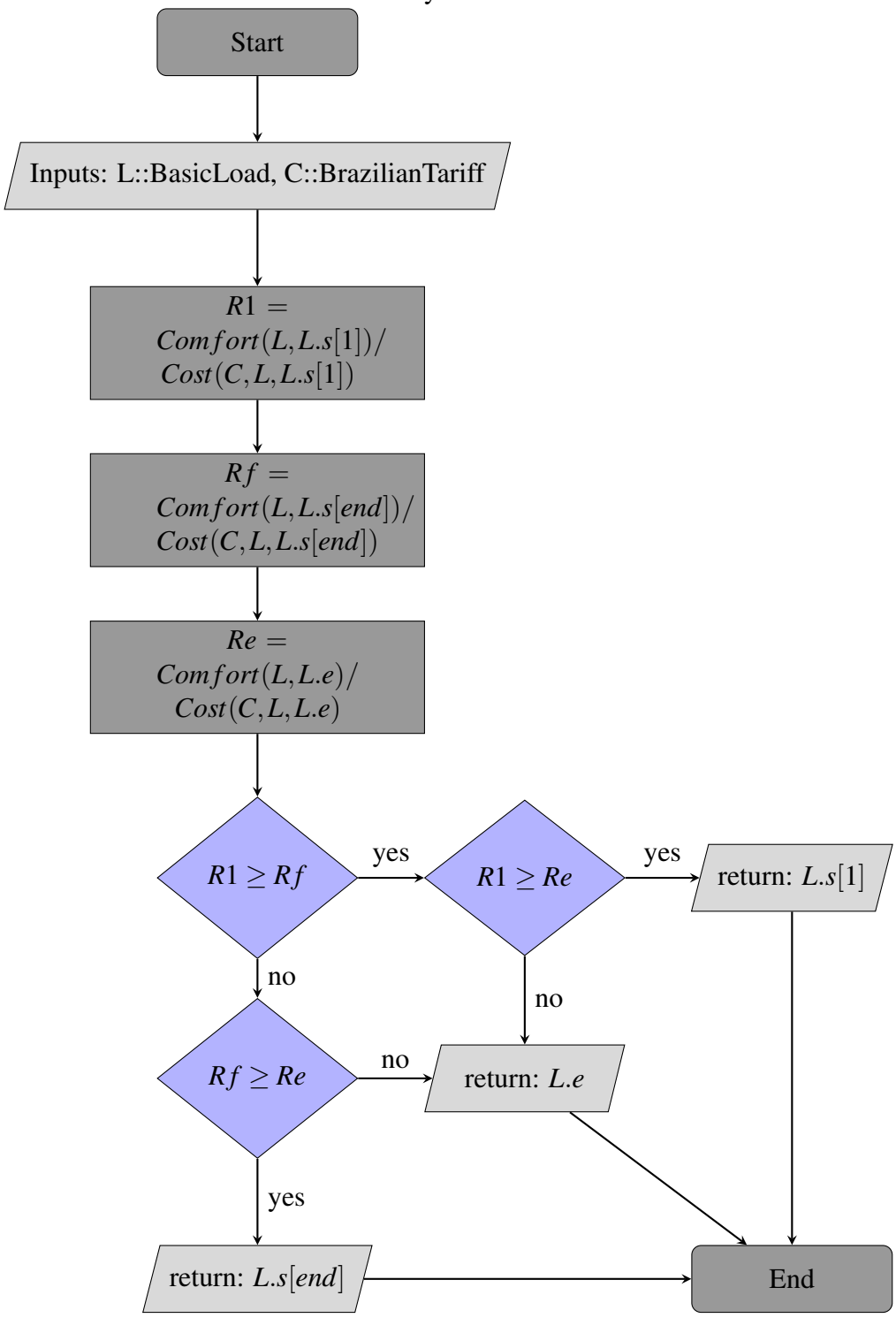

Source: Prepared by the author.

5.3 Analysis of power demand response

So far, all analyses that have been made have focused on only one load. As loads could be considered independent, a feasible solution for an array of loads would be to iterate the geometric search through a loop and return all schedule instants by recomposing time after

finding the points in tariff space. One side effect of this solution is that we cannot yet add any constraint about demand peaks or maximum power over time.

To cover this issue, a few hypotheses have been formulated, and two of them were tested through simulation. Both hypotheses use the hierarchical algorithm in combination with the output results of geometric search to try to speed up their execution and reduce memory usage. Specifically, the first trial consists of initializing the hierarchical algorithm with instant values evaluated using the geometric search.

The second approach iterates through the scheduled loads and locates the ones whose summed power exceeds the demand restriction. After identifying the loads that are causing the surge peak, they are cut from the original problem set and passed as parameters to the hierarchical algorithm, which will attempt to reschedule them within 95% or 90% of the original constraint. This reduction is needed to avoid another demand peak by reinserting the loads into the full set. Then, we check if all loads fit into the demand constraint. In the negative case, another cut is made.

Once all loads fit within the demand constraint, the iterations end. This last methodology has been named the hybrid algorithm. A short version of this method can be seen in Algorithm 2, and its full codification in Julia language can be found in the link in Appendix A. Functions that iterate through a set of loads receive the suffix *Vector*.

Algorithm 1 – Best Geofind

```
function Best_GeoFind(L::BasicLoad)
  Pe = Decompose_Time(L, L.e)
  if Pe[1] == L.C$\Delta$
    return L.e
  end
  A = GeoFind(L)
  t = Recompose_Time(L, A)
  if (L.s[1] <= t) && (t <= L.s[end])
    return t
  end
  C1   = Eval_BasicLoad_Comfort(L, L.s[1])/
     Eval_BasicLoad_Cost(L, L.s[1])
  Ce   = Eval_BasicLoad_Comfort(L, L.e)/Eval_BasicLoad_Cost
     (L, L.e)
  Cend = Eval_BasicLoad_Comfort(L, L.s[1])/
     Eval_BasicLoad_Cost(L, L.s[end])
  val,tempo = C1 >= Cend ? (C1,L.s[1]) : (Cend,L.s[end])
  return Ce >= val ? L.e : tempo
end
```

Algorithm 2 – Hybrid Algorithm

```
function Hybrid(H::Vector{BasicLoad}; demand_scale::Float64
    = 1.0, max_iterations::Int64 = 5)
  t = Best_GeoFindVector(H)
  count::Int64 = 0
  while(true)
    Hcut, B = find_demand_peaks(H, t)
    L = length(B)
    println("Hybrid found $L loads causing excessive power
       demand in iteration $count\n")
    if isempty(B) || (count >= max_iterations)
      return t, count
    end
    tcut = JuMP_MOAVector(Hcut; demand=true, load_size=
       length(H), demand_scale=demand_scale)
    for i in eachindex(B)
      t[B[i]] = tcut[i]
    end
    count+=1
  end
end
```

6 SIMULATIONS AND RESULTS

In Brazil, ANEEL resolution defines that residential consumers are not charged for demand, and only those in the A group have this type of billing (ANEEL: Brazil, 2021). That way, the methodology presented in this topic would be enough for our local situation. Nevertheless, as vastly discussed before, DR is a global concern and should be taken into account.

As mentioned before, the first simulation scenario is related to a reference house with 11 controllable loads whose appliance set is familiar to this thesis's author as it has been studied in previous related works (Albuquerque *et al.*, 2018; Costa *et al.*, 2023; Santos, 2019; Albuquerque, 2018). Figure 10 illustrates the scheduling results in a cumulative or stacked load power. Figure 10(a) represents the house inhabitants' preferences. Figures 10(b) and (c) show the geometric search and hierarchical results, both without demand constraints. At last, Figure 10(d) represents the schedule with demand constraint. The three least methodologies returned the same quantitative result, *videlicet*: hierarchical with DR, hierarchical with DR constraint and initialized with geometric search results, and the hybrid strategy. However, only the two purely based on the hierarchical algorithm were expected to return the same qualitative results. This result has occurred due to the small number of loads in this simulation set and because a significant amount of them were selected to run into hierarchical. In quantitative analysis, only the hybrid strategy has achieved better benchmarks, as hypothetically expected. Also note that no appliance has been turned off or had its usage time shortened in any of the strategies. Only the start time has been changed.

In Table 5, the values of comfort and normalized cost for reference house scenario can be read. Note that the best comfort values are realized by the methodology presented in this thesis.

Table 5 – Mean comfort and cost for reference house appliances.

Algorithm	Comfort	Cost
Expected user time	1.000	1.311
Geofind	**0.873**	1.021
Hierarchical without DR	0.845	**0.965**
Hierarchical with DR	0.813	0.974
Hierarchical with DR[a]	0.813	0.974
Hybrid algorithm	0.813	0.974

Source: Prepared by the author.
Note: [a] Initialized with geometric search results.

The results of the geometric search could be equal to hierarchical by adjusting the

Figure 10 – Reference House loads user schedule and output results

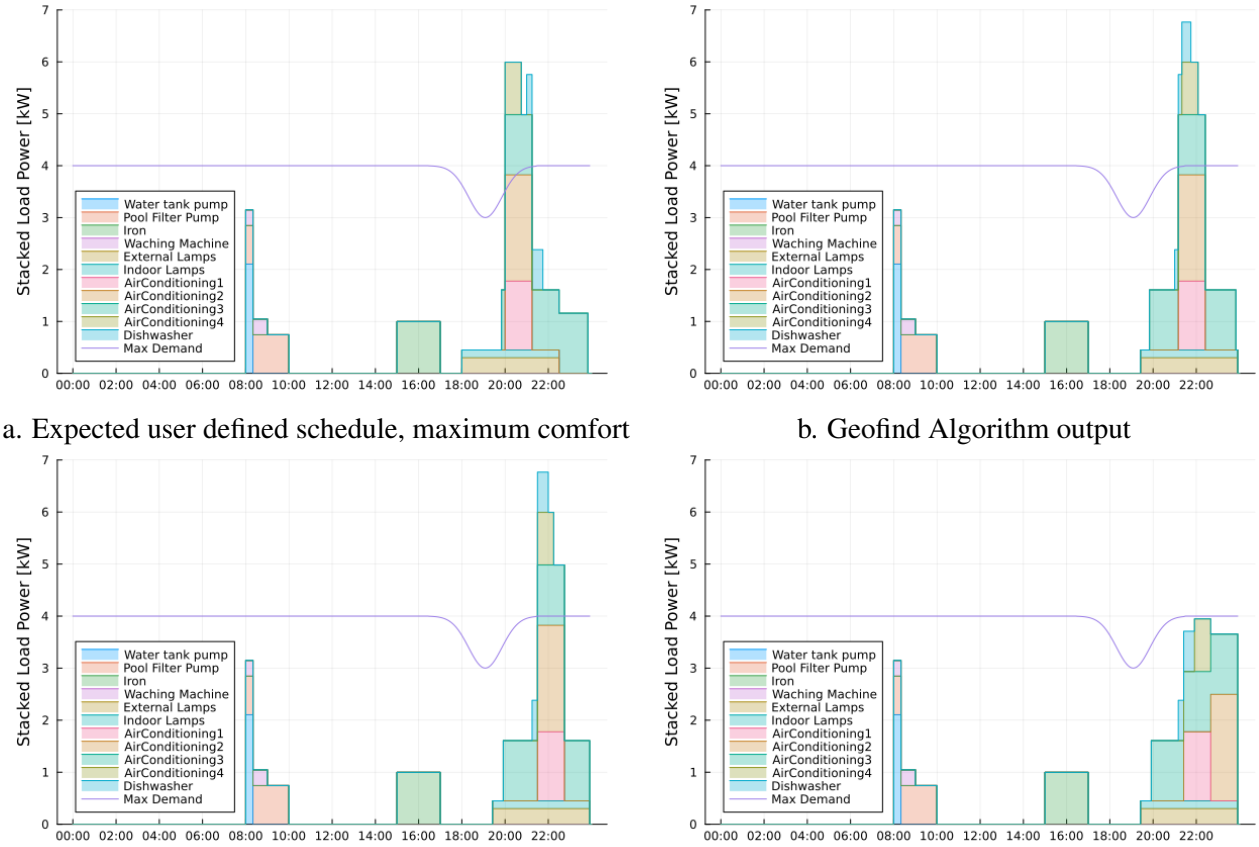

a. Expected user defined schedule, maximum comfort

b. Geofind Algorithm output

c. Hierarchical without demand restriction

d. Hierarchical with demand restriction and Hybrid Strategy

Source: Prepared by the author.

code to return the next inner point in the lower cost region, rather than the first one. All results achieved are compatible with cited previous works.

During experiments with the data from the first scenario, it was noted that the output results of the geometric search were significantly faster compared to those obtained by linear programming tools. Furthermore, less memory was also been allocated during the evaluation. To stand this result and verify its impact with larger sets of data, we proposed to generate eight sets of data with increasing size in log_{10} scale, as described in section Simulation Scenarios into Load Model Chapter. Each set of data has been submitted to five different scheduling procedures:

- Geometric Search;
- Multi-objective Hierarchical without demand constraint;
- Multi-objective Hierarchical with demand constraint;
- Multi-objective Hierarchical with demand constraint and initialized with Geofind solution;
- Hybrid algorithm.

The five scheduling results and the randomly generated expected time schedule can

be examined in detail for each dataset in Appendix C.

All benchmark results presented and discussed here have been run at least 25 times to ensure consistent outcomes. Most data has been collected through 100 or more executions under the same conditions and on the same computer (Intel Core i5-6200U 2.3GHz with 8GB of DDR4 Memory using Windows 10 Home and Julia 1.8). This iteration number has been considered sufficient as all results evaluated in each procedure consistently provided the same solution. Detailed histograms and all benchmark outputs can be found in Appendix D.

The data presented in Table 6 showcases the mean execution time benchmark for all the studied algorithms. Each row of the table corresponds to a different number of random loads, spanning from 10 to 750, while each column represents a specific algorithmic approach. The execution times, measured in microseconds (μs) and seconds (s), offer a comprehensive overview of how each algorithm performs under varying load conditions.

Geometric search emerges as the standout performer in terms of speed, consistently delivering results within microseconds, irrespective of the number of loads. This rapid performance underscores the efficiency of geometric search in swiftly identifying optimal solutions, rendering it particularly well-suited for real-time applications or scenarios with stringent time constraints.

In contrast, the hierarchical algorithm exhibits progressively longer execution times as the number of loads increases. Without any additional techniques, the hierarchical algorithm's performance deteriorates significantly, with execution times reaching several seconds for scenarios involving 500 or more loads.

By incorporating DR constraint, the hybrid methodology demonstrates remarkable improvement over the purely hierarchical approach. With execution times consistently lower than those of the hierarchical algorithm, the hybrid methodology showcases an improvement of about 50

A similar discussion applies to the memory estimate data presented in Table 7. Furthermore, an intriguing observation arises from the hierarchical algorithm initialized with the output of geometric search. This approach yields execution times that are marginally better than the non-initialized version of the hierarchical algorithm. Comparing the three last columns in Table 7, it becomes apparent that the same quantity of memory is allocated for this methodology as for the purely hierarchical approach, indicating that no cuts in the search tree have been effectively made.

Table 6 – Mean execution time benchmarks for random loads scenario.

Random Loads	Geofind without DR	Hierarchical without DR	Hierarchical with DR	Hierarchical with DR[a]	Hybrid algorithm
10	3.005 μs	0.022 s	1.249 s	1.066 s	1.208 s
25	10.074 μs	0.065 s	1.285 s	1.256 s	0.822 s
50	20.748 μs	0.105 s	2.370 s	2.343 s	0.966 s
75	19.975 μs	0.179 s	3.933 s	3.715 s	1.829 s
100	35.647 μs	0.252 s	6.055 s	5.968 s	1.975 s
250	102.471 μs	0.962 s	16.864 s	16.919 s	4.061 s
500	173.276 μs	3.509 s	37.316 s	37.328 s	16.124 s
750	319.320 μs	6.699 s	92.339 s	84.897 s	38.664 s

Source: Prepared by the author.
Note: [a] Initialized with geometric search results.

Table 7 – Memory estimate benchmarks for random loads scenario.

Random Loads	Geofind without DR	Hierarchical without DR	Hierarchical with DR	Hierarchical with DR[a]	Hybrid algorithm
10	1.17 KiB	5.84 MiB	37.84 MiB	37.84 MiB	36.53 MiB
25	3.66 KiB	19.09 MiB	92.67 MiB	92.64 MiB	60.82 MiB
50	5.45 KiB	40.51 MiB	180.14 MiB	180.07 MiB	82.99 MiB
75	7.50 KiB	72.37 MiB	273.62 MiB	273.53 MiB	153.42 MiB
100	15.59 KiB	123.39 MiB	421.92 MiB	421.79 MiB	161.99 MiB
250	31.16 KiB	508.57 MiB	1.21 GiB	1.21 GiB	303.17 MiB
500	68.56 KiB	1.72 GiB	3.13 GiB	3.13 GiB	1.22 GiB
750	97.38 KiB	3.67 GiB	5.93 GiB	5.93 GiB	2.67 GiB

Source: Prepared by the author.
Note: [a] Initialized with geometric search results.
Note: The 'i' vowel in 'iB' is short for integer.

Figure 11 illustrates the benchmark results for time, while Figure 12 provides a close-up view to allow readers to discern the differences between two executions of the hierarchical algorithm and to appreciate the significant improvement achieved by the hybrid solution.

The next data presented here are the values for comfort (Table 8) and normalized cost (Table 9) evaluated for each load set applying all five scheduling methodologies. As occurred in scenario one, the geometric search has a better result in comfort metric than the hierarchical algorithm without DR restriction while achieving the goal to lower the energy cost due to constant tariff. The Hybrid algorithm has also achieved better comfort metrics when compared to hierarchical results while all three algorithms have processed the DR constraint. For a better view of these results, the reader can refer to the graphics available Appendixes C and D.

To finish our discussion about the results, Table 10 presents the dataset that has been processed by the hierarchical algorithm inside the hybrid solution and how many iterations it has executed to comply with the demand constraint.

Excluding the results presented in the first line of Table 10, after the scheduling

Figure 11 – Benchmarks results for execution time.

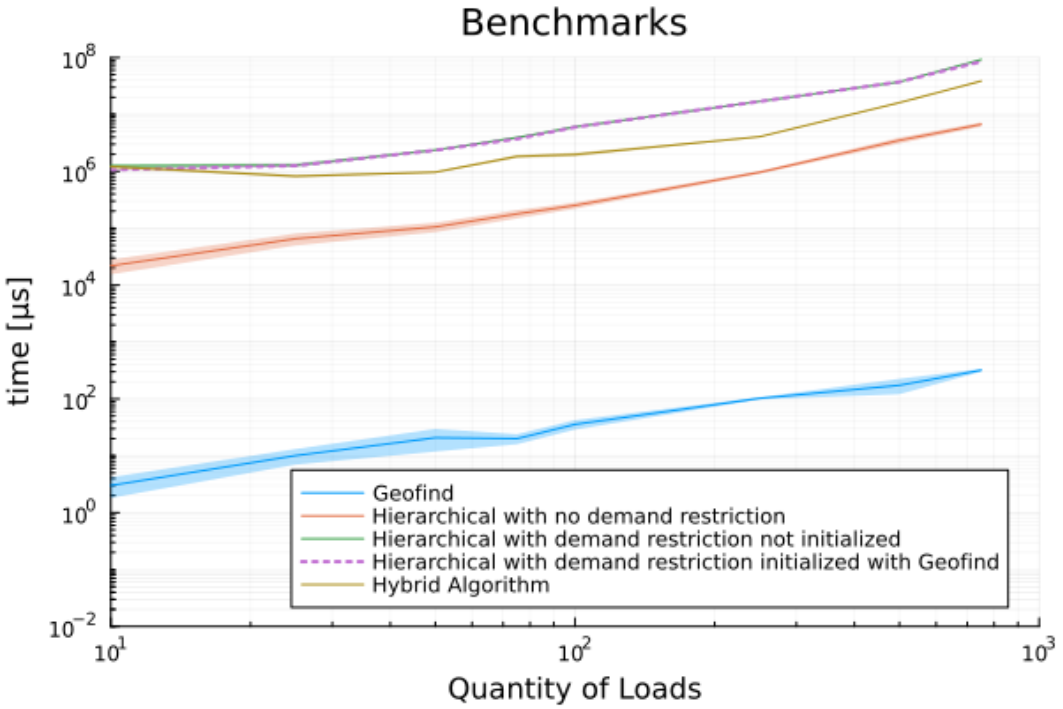

Source: Prepared by the author.

Figure 12 – Benchmarks results for execution time, only algorithms with demand response constraint

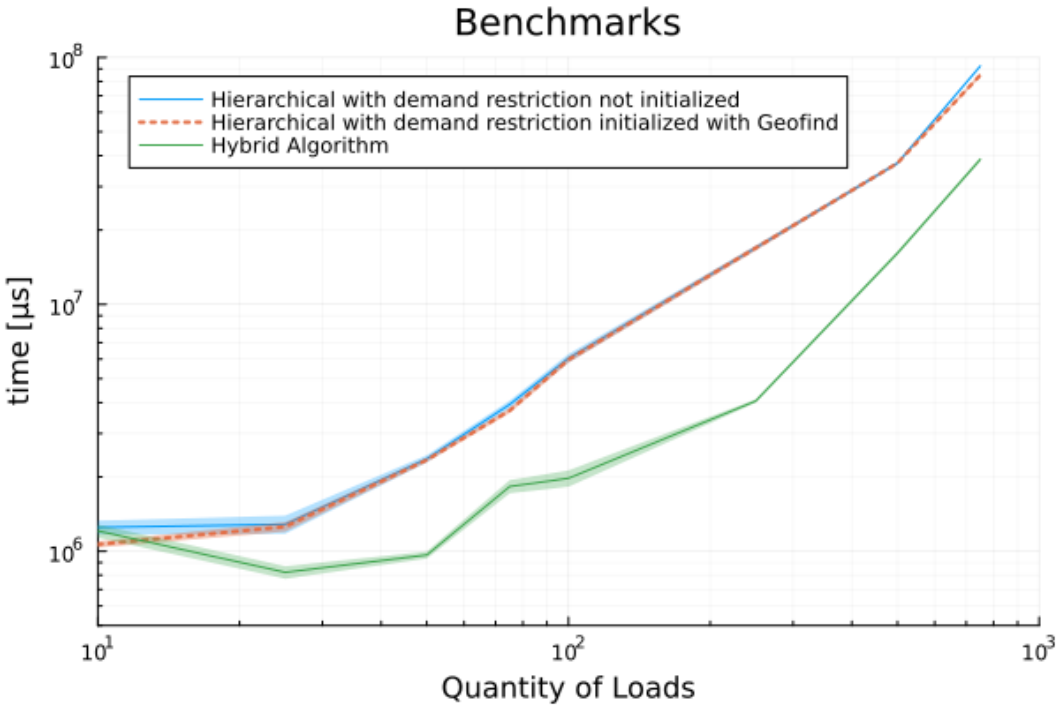

Source: Prepared by the author.

has been processed by geometric search, an amount ranging from a third to a half of the loads in random datasets is agglutinated, causing a demand peak. So, through hybrid methodology, we have been able to reduce the amount of data processed by the LP tool, which explains the

Table 8 – Mean normalized comfort[a] for random loads scenario.

Random Loads	Geofind without DR	Hierarchical without DR	Hierarchical with DR	Hierarchical with DR[b]	Hybrid algorithm
10	0.976	0.974	0.887	0.887	0.887
25	0.963	0.948	0.945	0.945	0.957
50	0.942	0.942	0.941	0.941	0.935
75	0.965	0.964	0.962	0.962	0.963
100	0.941	0.935	0.934	0.9341	0.945
250	0.968	0.959	0.958	0.958	0.967
500	0.947	0.934	0.937	0.937	0.944
750	0.954	0.940	0.941	0.941	0.946

Source: Prepared by the author.
Note: [a] Maximum possible value for comfort metric is one.
Note: [b] Initialized with geometric search results.

Table 9 – Mean normalized cost for random loads scenario.

Random Loads	Geofind without DR	Hierarchical without DR	Hierarchical with DR	Hierarchical with DR[a]	Hybrid algorithm
10	0.871	0.828	0.843	0.843	0.843
25	0.923	0.893	0.893	0.893	0.914
50	0.859	0.833	0.839	0.839	0.839
75	0.873	0.852	0.852	0.852	0.873
100	0.910	0.863	0.863	0.863	0.907
250	0.881	0.847	0.847	0.847	0.881
500	0.897	0.854	0.858	0.858	0.885
750	0.885	0.846	0.848	0.848	0.862

Source: Prepared by the author.

related improvement. Also note that hybrid methodology has done few search iterations, which demonstrates the efficiency of this method too. In the first case, the number of loads causing the demand peak where very close to the total quantity (9 out of 10).

Table 10 – Hybrid algorithm running parameters for random loads scenario.

Random Loads	Loads causing demand peak	Search iterations
10	9	1
25	14	1
50	22	1
75	19	2
100	41	1
250	75	1
500	123	2
750	217	2

Source: Prepared by the author.

That way, the search processing and running the hierarchical algorithm with reinforced constraint due to scale reduction results were similar to the original linear programming tool with 10 loads, so it is a valid effort.

7 CONCLUSIONS

Achieving simultaneous objectives of energy efficiency and comfort is not an easy task, as it represents an intricate trade-off between the need to reduce energy bill and stand for user preferences. The proposed solution performs fast optimization in a SH scenario whose ToU takes into account three tariff posts: off-peak, intermediate, and peak. That stated, the main goal of this work was to present a new methodology for scheduling home electric loads minimizing cost but without sacrificing inhabitants' comfort rate.

To achieve the main goal, the methodology relies on defining tariff space, decomposing the time axis into multiple independent dimensions, and establishing the geometric *locus* of a load. This *locus* models the behavior of an appliance as it progresses through either tariff space or time. It also emphasizes that a set of appliances can be represented as an independent set. Through explanation, examples of each definition have been provided and systematically explored.

A traditional optimization programming tool, like the hierarchical algorithm or any metaheuristic, begins computation from an initial value and explores the solution space to identify an optimal outcome. By employing the new concepts discussed in this paper, we determine the direct evaluation of the optimal solution to the given scheduling problem, eliminating the need for iterative exploration.

The benchmark results for processing time and memory usage, as presented in Tables 6 and 7, respectively, illustrate a significant performance improvement compared to the solution evaluated by the LP multi-objective counterpart. Specifically, the processing time is approximately ten thousand times faster, and the memory usage is significantly reduced. These results underscore the efficiency and effectiveness of the proposed methodology in addressing the load scheduling problem without demand restriction.

The output results for comfort and cost, as presented in Tables 8 and 9, highlight the reliability of proposed methodologies, as outputs for all methods are quite similar. It is anticipated that the new scheduler proposed in this work would achieve better results for the comfort metric. This expectation arises from the concept of the methodology, which aims to provide the shortest distance of movement in time necessary to reduce the energy bill. To ensure a fair comparison, the relevance factor μ, previously defined in Table 2, for all loads and in all simulations has been set to one. This choice prevents the diminishing of the comfort goal, as a relevance factor equal to zero for a load implies that shifting it beyond the expected time would

cause no discomfort.

The presented methodology for scheduling appliances in a SH environment aligns with legal regulations in the Brazilian energy market. However, this new methodology could be applied or extended to other tariff patterns. In Appendix E the reader could find some examples for binomial tariff sets. Moreover, it demonstrates the capability to solve large instances of this problem in less than a few milliseconds. Also, the reduction in memory usage by geometric search holds potential for the practical implementation of this solution in low-cost embedded systems. This advancement could enhance HEMS soon and contribute to popularizing this kind of equipment.

Besides optimization, achieving energy bill savings constrained by flattening demand is important as it contributes to reducing investments of energy suppliers in the distribution network. This helps decrease the constant need to expand the system to maintain the availability of ever-increasing energy consumption (Albuquerque, 2018). While the current state of geometric search is not able yet to directly relate to demand restrictions, the present work has also tested two methodologies to enhance the geometric search methodology so it could also comply with demand response restriction problems.

The proposed hybrid algorithm achieved superior benchmark results than its linear programming counterpart, with improvements of at least 40% for larger load sets. However, better ways to include demand constraints should be also included in future works. Some other hypotheses using Game Theory (Coutinho, 2013) are currently under study.

The analysis of local energy storage, including batteries or electric vehicles EV, and generation methods like photovoltaic PV systems or wind turbines is a crucial aspect of future research endeavors. These investigations are pivotal in understanding the impact of decentralized energy solutions within the context of smart homes and appliance scheduling. By examining the integration of these technologies, we can unveil their potential to enhance energy efficiency, reduce costs, and contribute to sustainable living.

Time itself is a substantially complex subject, and this work may have started to open a window that will allow us to explore its properties even further. The decomposition of time into a geometric space is a new methodology that is far from reaching its full potential. Future research should include extrapolation of tariff space for hour-based tariffs or even continuous ones. The works proposed by Hausmann e Knutson (1996), Hausmann e Knutson (1998) seem to be a key path to continue this discussion.

REFERENCES

AKBARI-DIBAVAR, A.; NOJAVAN, S.; MOHAMMADI-IVATLOO, B.; ZARE, K. Smart home energy management using hybrid robust-stochastic optimization. **Computers Industrial Engineering**, Elsevier, v. 143, 2020.

ALBUQUERQUE, P. U. B.; OHI, D. K. de A.; PEREIRA, N. S.; PRATA, B. de A.; BARROSO, G. C. Proposed architecture for energy efficiency and comfort optimization in smart homes. **Journal of Control, Automation and Electrical Systems**, Springer, v. 29, n. 6, p. 718–730, 2018.

ALBUQUERQUE, P. U. B. de. **Estudo e Desenvolvimento de Abordagens Multiobjetivo Baseadas em Programação Linear e em Metaheurísticas para Otimização do Custo com Energia Elétrica e do Conforto do Usuário**. Tese (Doutorado em Engenharia de Teleinformática) – Universidade Federal do Ceará, Fortaleza, Brazil, 2018.

ALI, S. Demand response program for efficient demand-side management in smart grid considering renewable energy sources. **IEEE Access**, IEEE, v. 10, 2022.

ALIABADI, F. E.; AGBOSSOU, K.; KELOUWANI, S.; HENAO, N.; HOSSEINI, S. S. Coordination of smart home energy management systems in neighborhood areas: A systematic review. **IEEE Access**, IEEE, v. 9, p. 36417–36443, 2021.

ANEEL: Brazil. **Resolução Normativa ANEEL Nº 1.000, de 7 de Dezembro e 2021**. 2021. Available in: https://www2.aneel.gov.br/cedoc/ren20211000.pdf. Accessed: 15 fev. 2024.

ANEEL: Brazil. **Base de Dados das Tarifas das Distribuidoras de Energia Elétrica**. 2023. Available in: https://portalrelatorios.aneel.gov.br/luznatarifa/basestarifas. Accessed: 15 fev. 2024.

ASHRAE. **ASHRAE Handbook Fundamentals, SI edition**. Atlanta, GA: ASHRAE, 2017.

BALAKRISHNAN, R.; GEETHA, V. Review on home energy management system. **Materials Today: Proceedings**, Elsevier, 4 2021.

BEZANSON, J.; EDELMAN, A.; KARPINSKI, S.; SHAH, V. B. Julia: A fresh approach to numerical computing. **SIAM Review**, v. 59, n. 1, p. 65–98, 2017.

BEZERRA FILHO, P.; ALBUQUERQUE, P.; PRATA, B.; BARROSO, G. A smart home controller using an integer programming approach for the optimization of consumer economic saving and comfort. In: SBA, 2015, Natal. **Proceedings of the XII SBAI Simpósio Brasileiro de Automação Inteligente (Brazilian Symposium in Intelligent Automation)**. Natal-RN, Brazil, 2015. v. 25.

BLEVISS, D. L. Transportation is critical to reducing greenhouse gas emissions in the united states. **Wiley Interdisciplinary Reviews: Energy and Environment**, Wiley, v. 10, n. 2, 2021.

BYRNE, Z. H. J. ho K. J. W. J. Review of dynamic pricing programs in the us and europe: Status quo and policy recommendations. **Renewable and Sustainable Energy Reviews**, Elsevier, v. 42, p. 743–751, 2015.

CHEKIRED, F.; MAHRANE, A.; SAMARA, Z.; CHIKH, M.; GUENOUNOU, A.; MEFLAH, A. Fuzzy logic energy management for a photovoltaic solar home. **Energy Procedia**, Elsevier, v. 134, 2017.

CHEN, X.; WEI, T.; HU, S. Uncertainty-aware household appliance scheduling considering dynamic electricity pricing in smart home. **IEEE Transactions Smart Grid**, IEEE, v. 4, p. 932–941, 2013.

CHEN, Z.; CHEN, Y.; HE, R.; LIU, J.; GAO, M.; ZHANG, L. Multi-objective residential load scheduling approach for demand response in smart grid. **Sustainable Cities and Society**, Elsevier, v. 76, 2022.

CLEMENT-NYNS, K.; HAESEN, E.; DRIESEN, J. The impact of charging plug-in hybrid electric vehicles on a residential distribution grid. **IEEE Transactions Power Systems**, IEEE, v. 25, n. 1, p. 371–380, 2009.

COSTA, J. R. D.; BARROSO, G. C.; SOUZA, D. A. D.; BATISTA, J. G.; JUNIOR, A. B. D. S.; RIOS, C.; VASCONCELOS, F.; JúNIOR, J.; BEZERRA, I. D. S.; LIMA, A. F. D.; SANTANA, K. A. D.; JúNIOR, J. R. D. O. An improved optimization function to integrate the user's comfort perception into a smart home controller based on particle swarm optimization and fuzzy logic. **Sensors**, MDPI, v. 23, n. 6, 2023.

COUTINHO, L. R. R. **Método de Ordenação de Eventos para Sistemas Embarcados Multitarefa com Múltiplos Níveis Críticos.** Dissertação (Mestrado em Computação Aplicada) – Universidade Estadual do Ceará, Fortaleza, Ceará, 2013.

DOWNSON, O et al. **MultiObjectiveAlgorithms.jl (MOA) is a collection of algorithms for multi-objective optimization.** 2023. Avaliable in: https://github.com/jump-dev/MultiObjectiveAlgorithms.jl. Accessed: 15 fev. 2024. MultiObjectiveAlgorithms.jl is licensed under the MPL 2.0 License.

DUNNING, I.; HUCHETTE, J.; LUBIN, M. JuMP: A Modeling Language for Mathematical Optimization. **SIAM Review**, SIAM, v. 59, n. 2, p. 295–320, 2017.

ENEL (Ceará). **Tarifa de fornecimento - Baixa tensão**. 2023. Available in: https://www.enel.com.br/content/dam/enel-br/megamenu/taxas,-tarifas-e-impostos/Tarifas-ENELCE_Hist_Verde_REH.3.185_22042023.pdf. Accessed: 15 fev. 2024.

FARROKHIFAR, M.; MOMAYYEZI, F.; SADOOGI, N.; SAFARI, A. Real-time based approach for intelligent building energy management using dynamic price policies. **Sustainable Cities and Society**, Elsevier, v. 37, p. 85–92, 2018.

GARCíA, O.; PRIETO, J.; ALONSO, R. S.; CORCHADO, J. M. A framework to improve energy efficient behaviour at home through activity and context monitoring. **Sensors**, MDPI, v. 17, 2017.

GAZAFROUDI, A. S.; SHAFIE-KHAH, M.; HEYDARIAN-FORUSHANI, E.; HAJIZADEH, A.; HEIDARI, A.; CORCHADO, J. M.; CATALãO, J. P. Two-stage stochastic model for the price-based domestic energy management problem. **International Journal of Electrical Power and Energy Systems**, Elsevier Ltd, v. 112, p. 404–416, 11 2019.

GELLINGS, C. W.; SAMOTYJ, M. Smart grid as advanced technology enabler of demand response. **Energy Efficiency**, Springer, v. 6, n. 4, p. 685–694, 2013.

GIORGIO, A.; PIMPINELLA, L. An event driven smart home controller enabling consumer economic saving and automated demand-side management. **Applied Energy**, Elsevier, v. 96, 2012.

GONZáLEZ-BRIONES, A.; PRIETO, J.; PRIETA, F.; HERRERA-VIEDMA, E.; CORCHADO, J. M. Energy optimization using a case-based reasoning strategy. **Sensors**, MDPI, v. 18, 2018.

HAUSMANN, J.-C.; KNUTSON, A. Polygon spaces and grassmannians. **arXiv: Differential Geometry**, 1996.

HAUSMANN, J.-C.; KNUTSON, A. The cohomology ring of polygon spaces. **Annales de l'institut Fourier**, Numdam, v. 48, n. 1, p. 281–321, 1998.

HUANG, Y.; WANG, L.; GUO, W.; KANG, Q.; WU, Q. Chance constrained optimization in a home energy management system. **IEEE Transactions Smart Grid.**, IEEE, v. 9, 2016.

IPAKCHI, A.; ALBUYEH, F. Grid of the future. **IEEE Power Energy Magazine**, IEEE, v. 7, n. 2, p. 52–62, 2009.

KIM, T. T.; POOR, H. V. Scheduling power consumption with price uncertainty. **IEEE Transactions Smart Grid**, IEEE, v. 2, n. 3, p. 519–527, 2011.

LIN, Y.-H.; HU, Y.-C. Residential consumer-centric demand-side management based on energy disaggregation-piloting constrained swarm intelligence: Towards edge computing. **Sensors**, MDPI, v. 18, n. 5, 2018.

LU, Q.; ZHANG, Z.; Lü, S. Home energy management in smart households: Optimal appliance scheduling model with photovoltaic energy storage system. **Energy Reports**, Elsevier, v. 6, p. 2450–2462, 2020.

LUBIN, M.; DOWSON, O.; Dias Garcia, J.; HUCHETTE, J.; LEGAT, B.; VIELMA, J. P. JuMP 1.0: Recent improvements to a modeling language for mathematical optimization. **Mathematical Programming Computation**, Springer, n. 15, p. 581–589, 2023.

LUBIN, M.; DUNNING, I. Computing in Operations Research Using Julia. **INFORMS Journal on Computing**, INFORMS, v. 27, n. 2, p. 238–248, 2015.

LUO, F.; KONG, W.; RANZI, G.; DONG, Z. Y. Optimal home energy management system with demand charge tariff and appliance operational dependencies. **IEEE Transactions on Smart Grid**, IEEE, v. 11, n. 1, p. 4–14, 2020.

MA, K.; YAO, T.; YANG, J.; GUAN, X. Residential power scheduling for demand response in smart grid. **International Journal of Electrical Power & Energy Systems**, Elsevier, v. 78, p. 320–325, 6 2016.

MANSOURI, S. A.; AHMARINEJAD, A.; NEMATBAKHSH, E.; JAVADI, M. S.; NEZHAD, A. E.; CATALãO, J. P. A sustainable framework for multi-microgrids energy management in automated distribution network by considering smart homes and high penetration of renewable energy resources. **Energy**, Elsevier, v. 245, 2022.

MANZOOR, A.; JAVAID, N.; ULLAH, I.; ABDUL, W.; ALMOGREN, A.; ALAMRI, A. An intelligent hybrid heuristic scheme for smart metering based demand side management in smart homes. **Energies**, MDPI, v. 10, n. 9, 2017.

MEKURIA, D. N.; SERNANI, P.; FALCIONELLI, N.; DRAGONI, A. F. Smart home reasoning systems: a systematic literature review. **Journal of Ambient Intelligence and Humanized Computing**, Springer Science and Business Media Deutschland GmbH, v. 12, n. 4, p. 4485–4502, 2021.

MERABET, G. H.; ESSAAIDI, M.; HADDOU, M. B.; QOLOMANY, B.; QADIR, J.; ANAN, M.; AL-FUQAHA, A.; ABID, M. R.; BENHADDOU, D. Intelligent building control systems for thermal comfort and energy-efficiency: A systematic review of artificial intelligence-assisted techniques. **Renewable and Sustainable Energy Reviews**, Elsevier, v. 144, 7 2021.

MISCHOS, S.; DALAGDI, E.; VRAKAS, D. Intelligent energy management systems: a review. **Artificial Intelligence Review**, Springer, v. 56, n. 10, p. 11635–11674, 2023.

MOHSENZADEH, A.; SHARIATKHAH, M. H.; HAGHIFAM, M.-R. Applying fuzzy techniques to model customer comfort in a smart home control system. In: CIRED, 22., 2013, Stockholm. **22nd International Conference and Exhibition on Electricity Distribution**. Stockholm, Sweden, 2013. p. 1–4.

O'GRADY, T.; CHONG, H. Y.; MORRISON, G. M. A systematic review and meta-analysis of building automation systems. **Building and Environment**, Elsevier, v. 195, 5 2021.

OGUNJUYIGBE, A. S. O.; AYODELE, T. R.; AKINOLA, O. A. User satisfaction-induced demand side load management in residential buildings with user budget constraint. **Applied Energy**, Elsevier, v. 187, p. 352–366, 2017.

PERERA, A.; KAMALARUBAN, P. Applications of reinforcement learning in energy systems. **Renewable and Sustainable Energy Reviews**, Elsevier, v. 137, 2011.

RAHMANI-ANDEBILI, M. Scheduling deferrable appliances and energy resources of a smart home applying multi-time scale stochastic model predictive control. **Sustainable Cities and Society**, Elsevier, v. 32, 2017.

RAJASEKHAR, B.; PINDORIYA, N.; TUSHAR, W.; YUEN, C. Collaborative energy management for a residential community: A non-cooperative and evolutionary approach. **IEEE Transactions on Emerging Topics in Computational Intelligence**, IEEE, v. 3, n. 3, p. 177–192, 6 2019.

SANGHVI, A. Flexible strategies for load/demand management using dynamic pricing. **IEEE Transactions on Power Systems**, IEEE, v. 4, n. 1, p. 83–93, 1989.

SANTOS J M SOARES, G. C. B. S A B dos; PRATA, B. de A. Demand response application in industrial scenarios: A systematic mapping of practical implementation. **Expert Systems with Applications**, Elsevier, v. 215, 2023.

SANTOS, S. A. B. dos. **Utilização da meta-heurística PSO para otimização multiobjetivo de um SMART HOME CONTROLLER**. Dissertação (Mestrado em Engenharia de Teleinformática) – Universidade Federal do Ceará, Fortaleza, Ceará, 2019.

SCHIRMER, P. A.; MPORAS, I. Non-intrusive load monitoring: a review. **IEEE Transactions Smart Grid**, IEEE, v. 14, 2023.

SORTOMME, E.; EL-SHARKAWI, M. A. Optimal charging strategies for unidirectional vehicle-to-grid. **IEEE Transactions Smart Grid**, IEEE, v. 2, n. 1, p. 131–138, 2010.

UNITED STATES. Congress. **H.R. 6 (110th): Energy Independence and Security Act of 2007**. 2007. Available in: https://www.govtrack.us/congress/bills/110/hr6. Accessed: 15 fev. 2024.

VENKATESH, F. A. Q. M. N. A. S. K. A. A. L. G. B. Appliance scheduling optimization in smart home networks. **IEEE Access**, IEEE, v. 3, p. 2176–2190, 2015.

WANG, C.; ZHOU, Y.; JIAO, B.; WANG, Y.; LIU, W.; WANG, D. Robust optimization for load scheduling of a smart home with photovoltaic system. **Energy Convers. Manag.**, Elsevier, v. 102, 2015.

ZEYNALI, S.; ROSTAMI, N.; AHMADIAN, A.; ELKAMEL, A. Two-stage stochastic home energy management strategy considering electric vehicle and battery energy storage system: An ann-based scenario generation methodology. **Sustainable Energy Technologies and Assessments**, Elsevier Ltd, v. 39, 6 2020.

ÇIMEN, H.; BAZMOHAMMADI, N.; LASHAB, A.; TERRICHE, Y.; VASQUEZ, J. C.; GUERRERO, J. M. An online energy management system for ac/dc residential microgrids supported by non-intrusive load monitoring. **Applied Energy**, Elsevier, v. 307, 2022.

APPENDIX A – GITHUB PROJECT PAGE

The GitHub link bellow has all extra information needed to follow all procedures in this thesis.

https://github.com/rodolforbcoutinhoUFC/GeoFind_SHC

APPENDIX B – TIME DECOMPOSITION INTO TARIFF SPACE EXAMPLES

Figure 13 – All startup times for a 30 min load crossing intermediate and peak post tariffs.

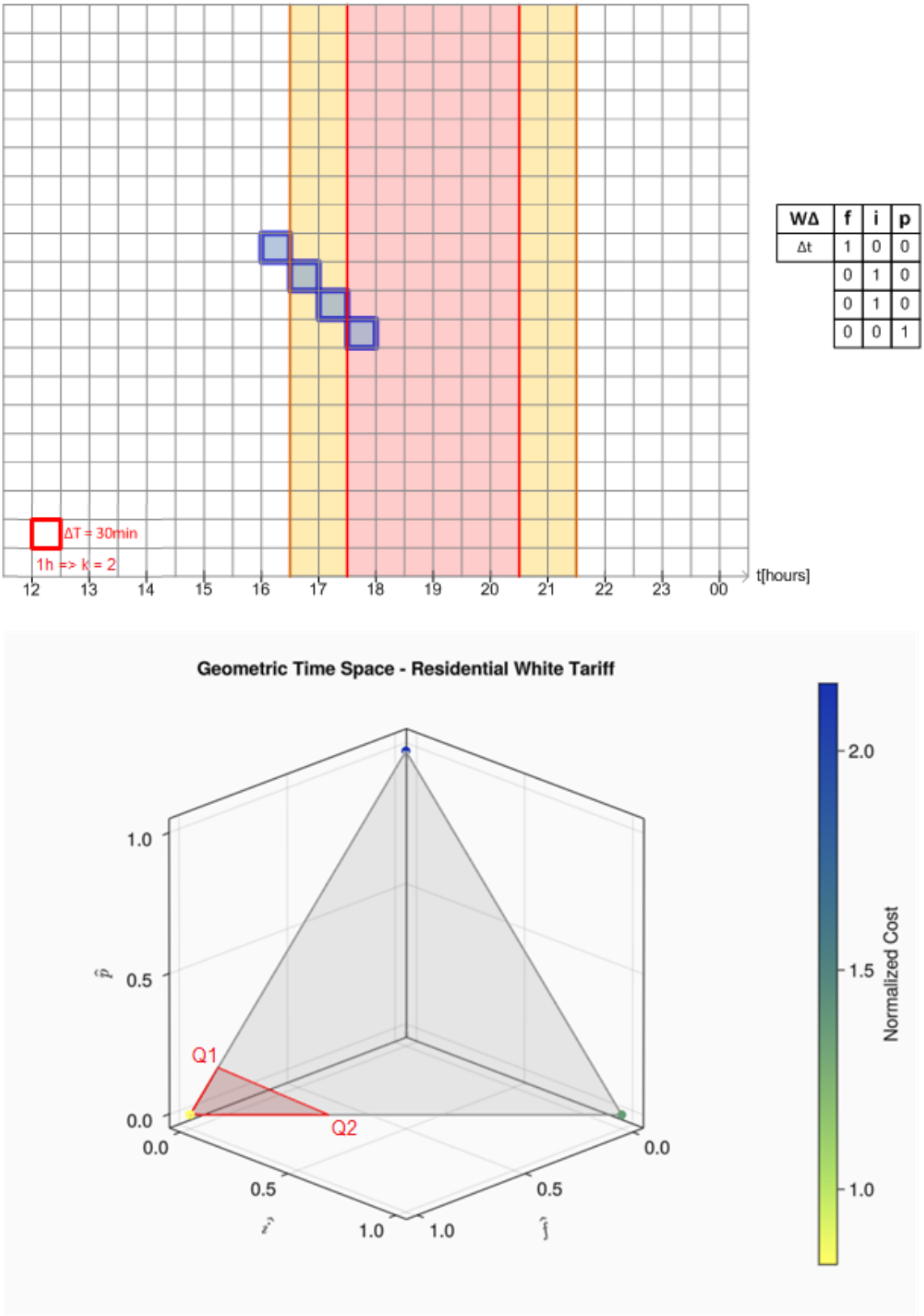

Source: Prepared by the author.

Figure 14 – All startup times for a 1 hour load crossing intermediate and peak post tariffs.

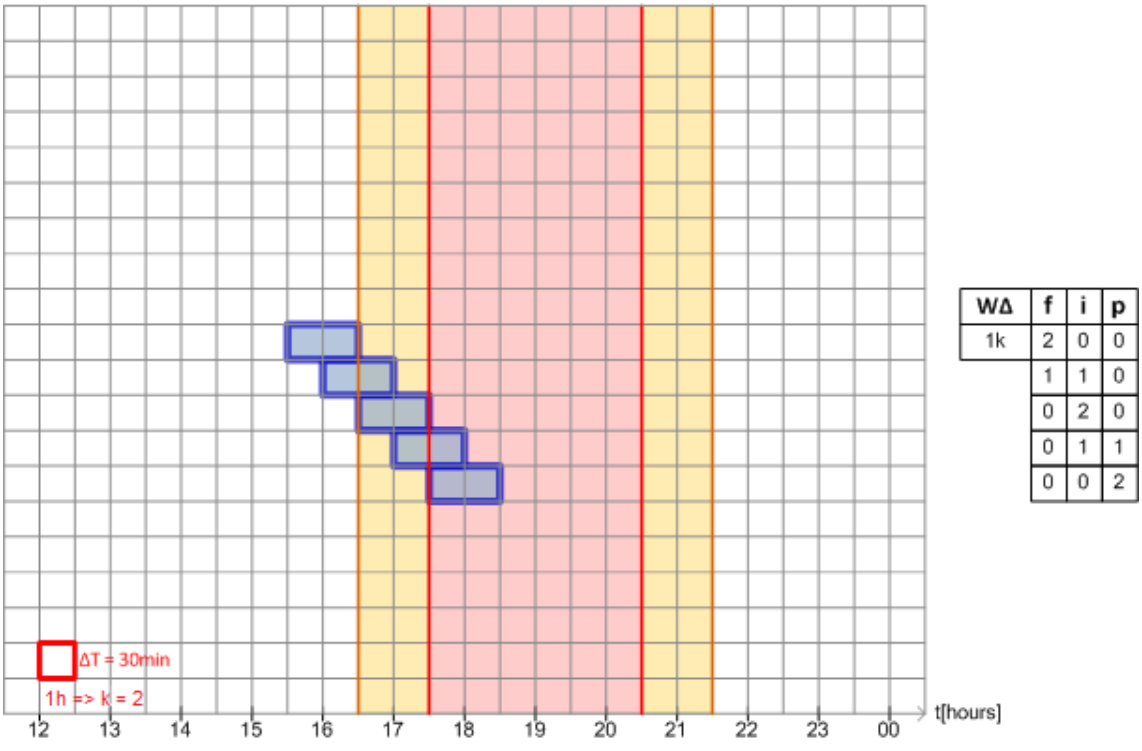

WΔ	f	i	p
1k	2	0	0
	1	1	0
	0	2	0
	0	1	1
	0	0	2

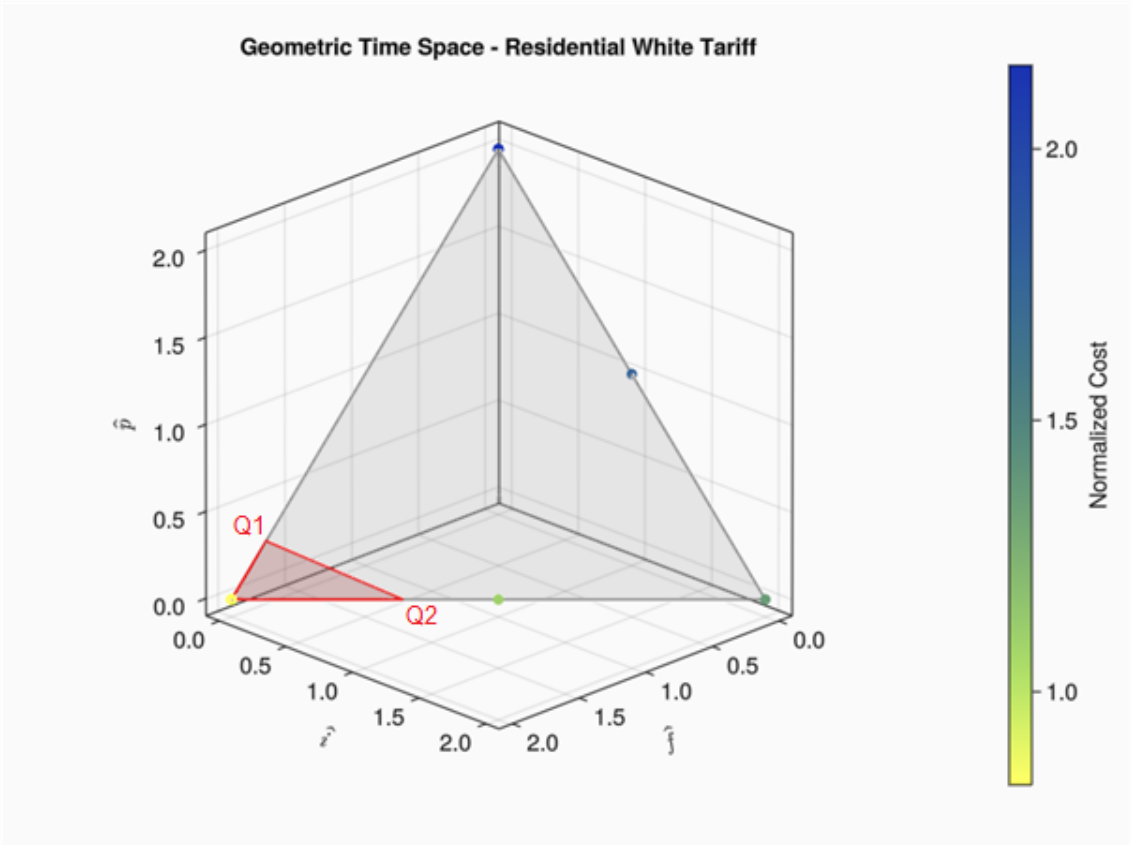

Source: Prepared by the author.

Figure 15 – All startup times for a 2 hour load crossing intermediate and peak post tariffs.

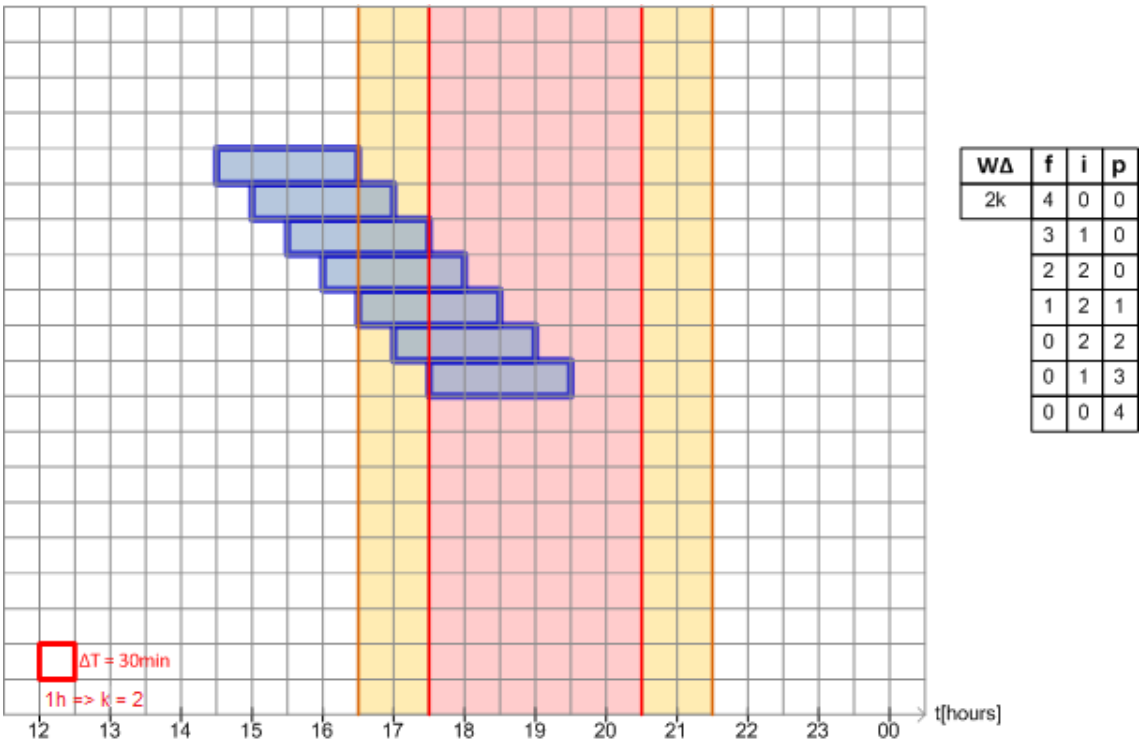

WΔ	f	i	p
2k	4	0	0
	3	1	0
	2	2	0
	1	2	1
	0	2	2
	0	1	3
	0	0	4

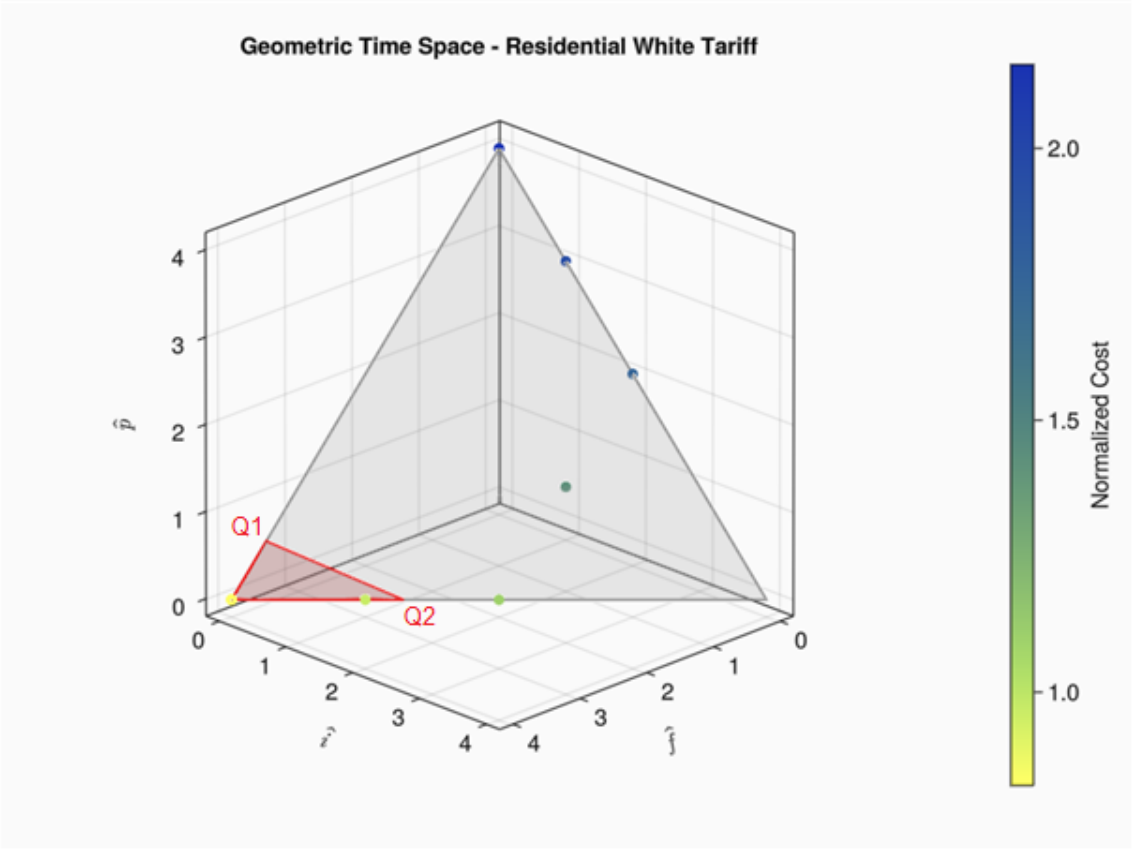

Source: Prepared by the author.

Figure 16 – All startup times for a 3 hour load crossing intermediate and peak post tariffs.

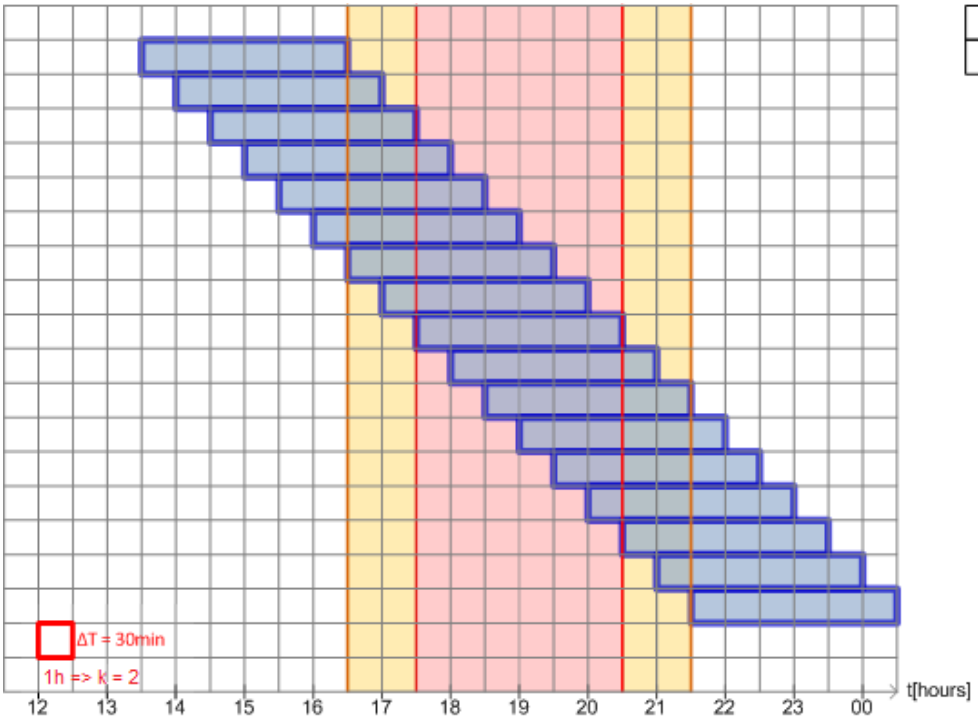

WΔ	f	i	p
3k	6	0	0
	5	1	0
	4	2	0
	3	2	1
	2	2	2
	1	2	3
	0	2	4
	0	1	5
	0	0	6
	0	1	5
	0	2	4
	1	2	3
	2	2	2
	3	2	1
	4	2	0
	5	1	0
	6	0	0

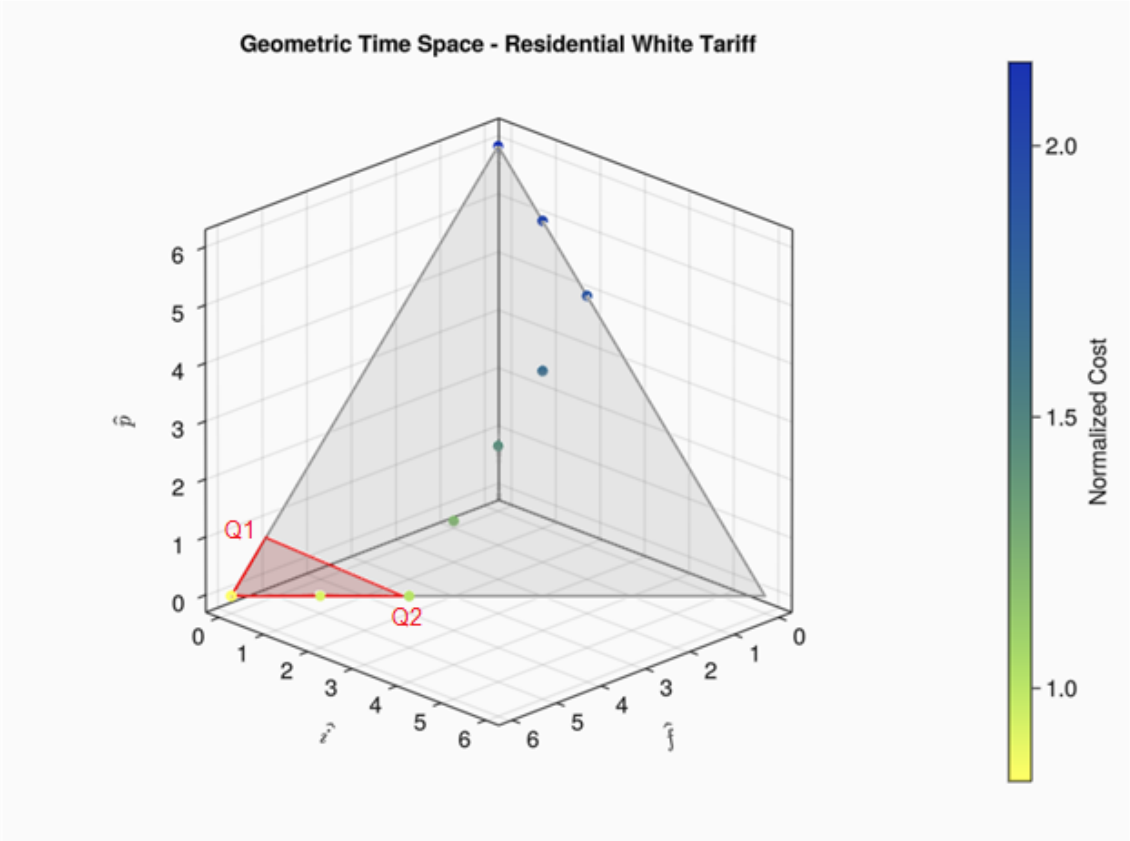

Source: Prepared by the author.

Figure 17 – All startup times for a 4 hour load crossing intermediate and peak post tariffs.

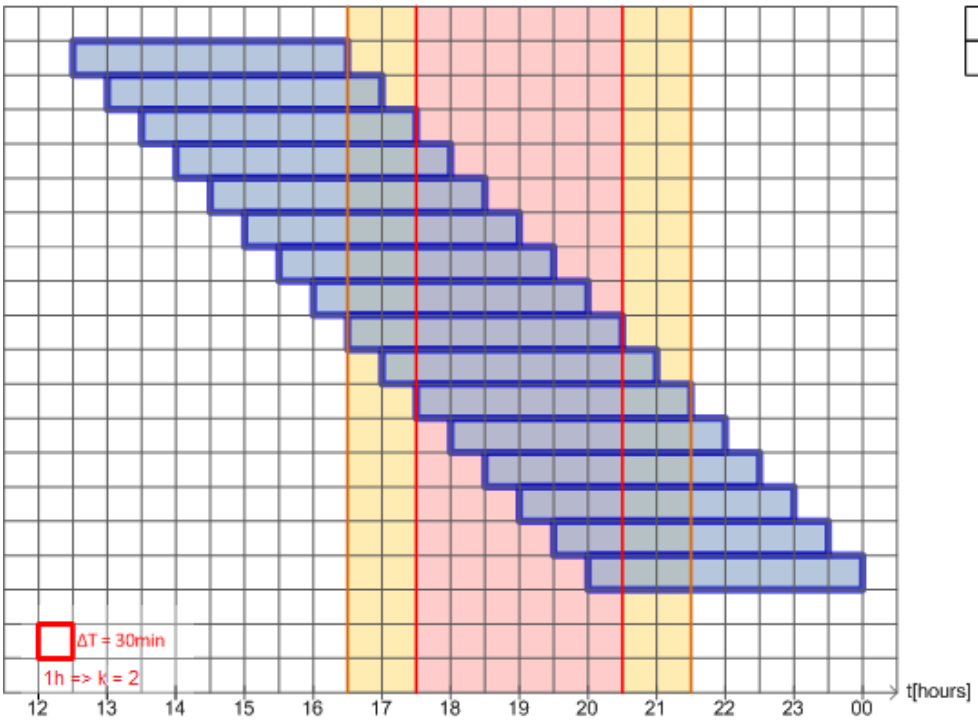

WΔ	f	i	p
4k	8	0	0
	7	1	0
	6	2	0
	5	2	1
	4	2	2
	3	2	3
	2	2	4
	1	2	5
	0	2	6
	0	2	6
	0	2	6
	1	2	5
	2	2	4
	3	2	3
	4	2	2
	5	2	1

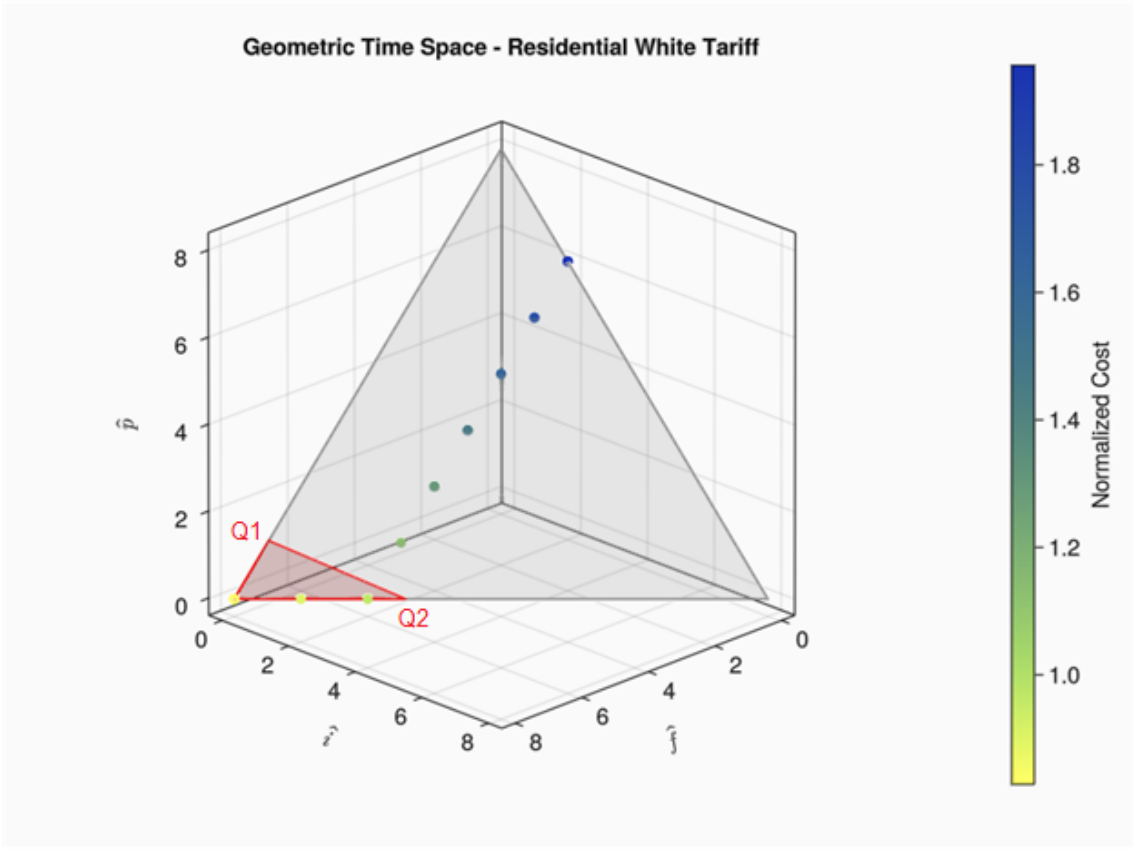

Source: Prepared by the author.

Figure 18 – All startup times for a 6 hour load crossing intermediate and peak post tariffs.

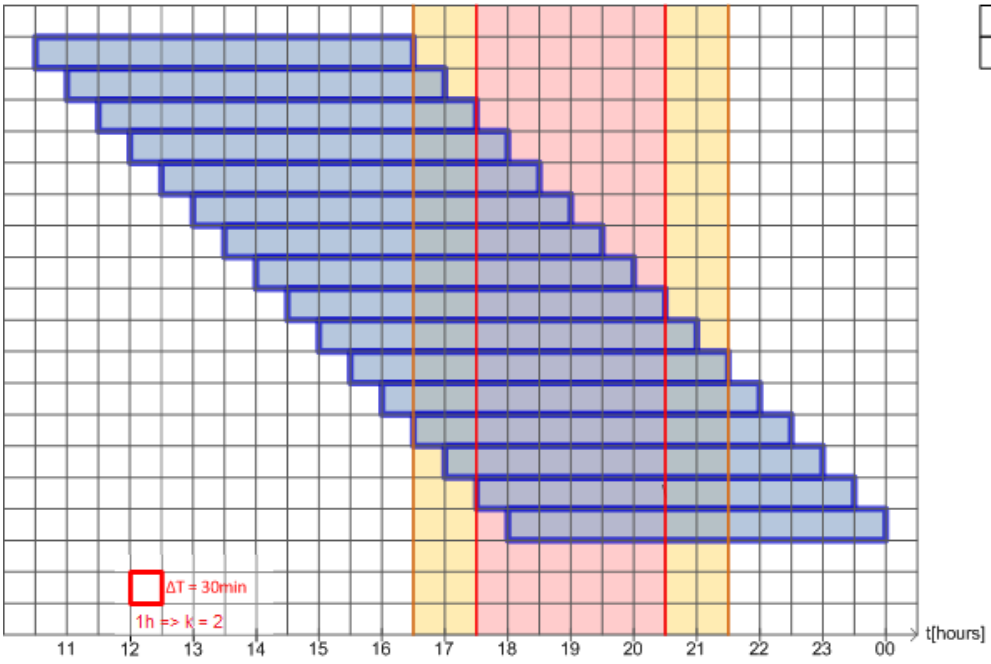

WΔ	f	i	p
6k	12	0	0
	11	1	0
	10	2	0
	9	2	1
	8	2	2
	7	2	3
	6	2	4
	5	2	5
	4	2	6
	3	3	6
	2	4	6
	2	4	6
	2	4	6
	3	3	6
	4	2	6
	5	2	5

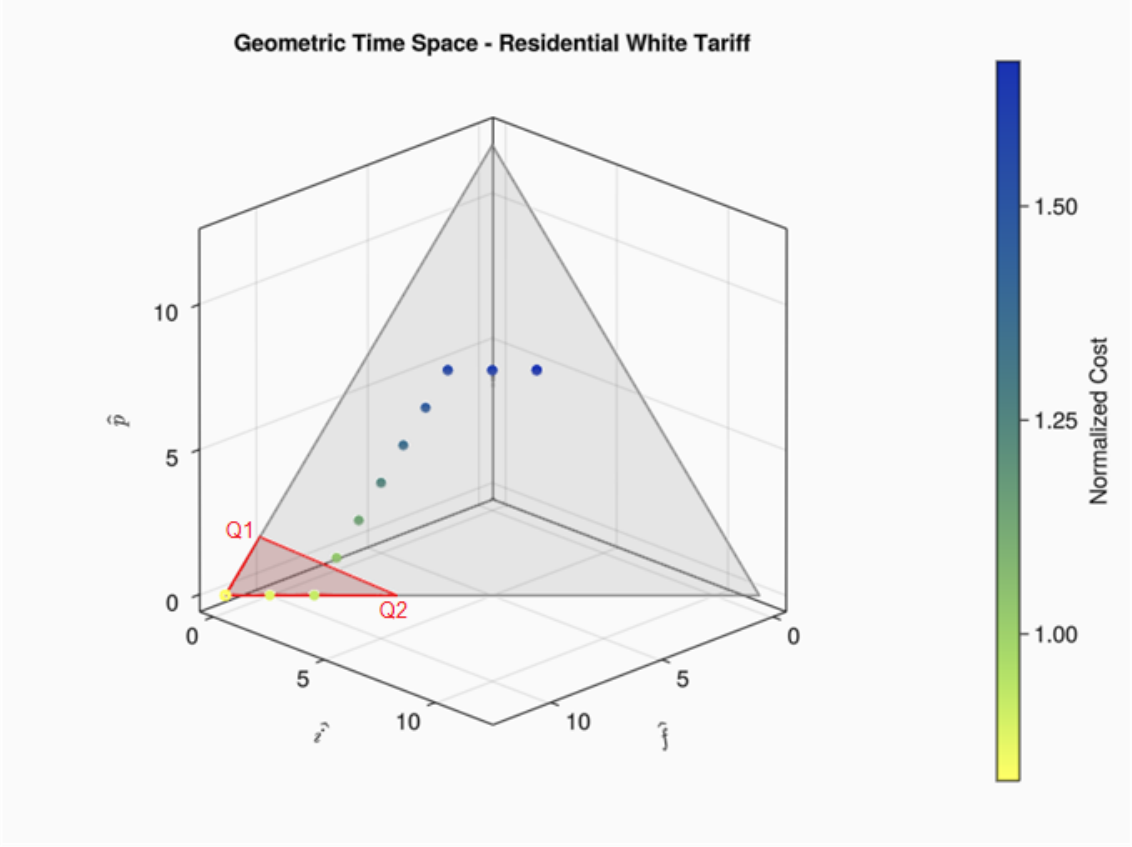

Source: Prepared by the author.

APPENDIX C – SCHEDULING RESULTS FOR ALL RANDOM LOADS SCENARIOS

Figure 19 – 10 Random Loads Schedule Results.

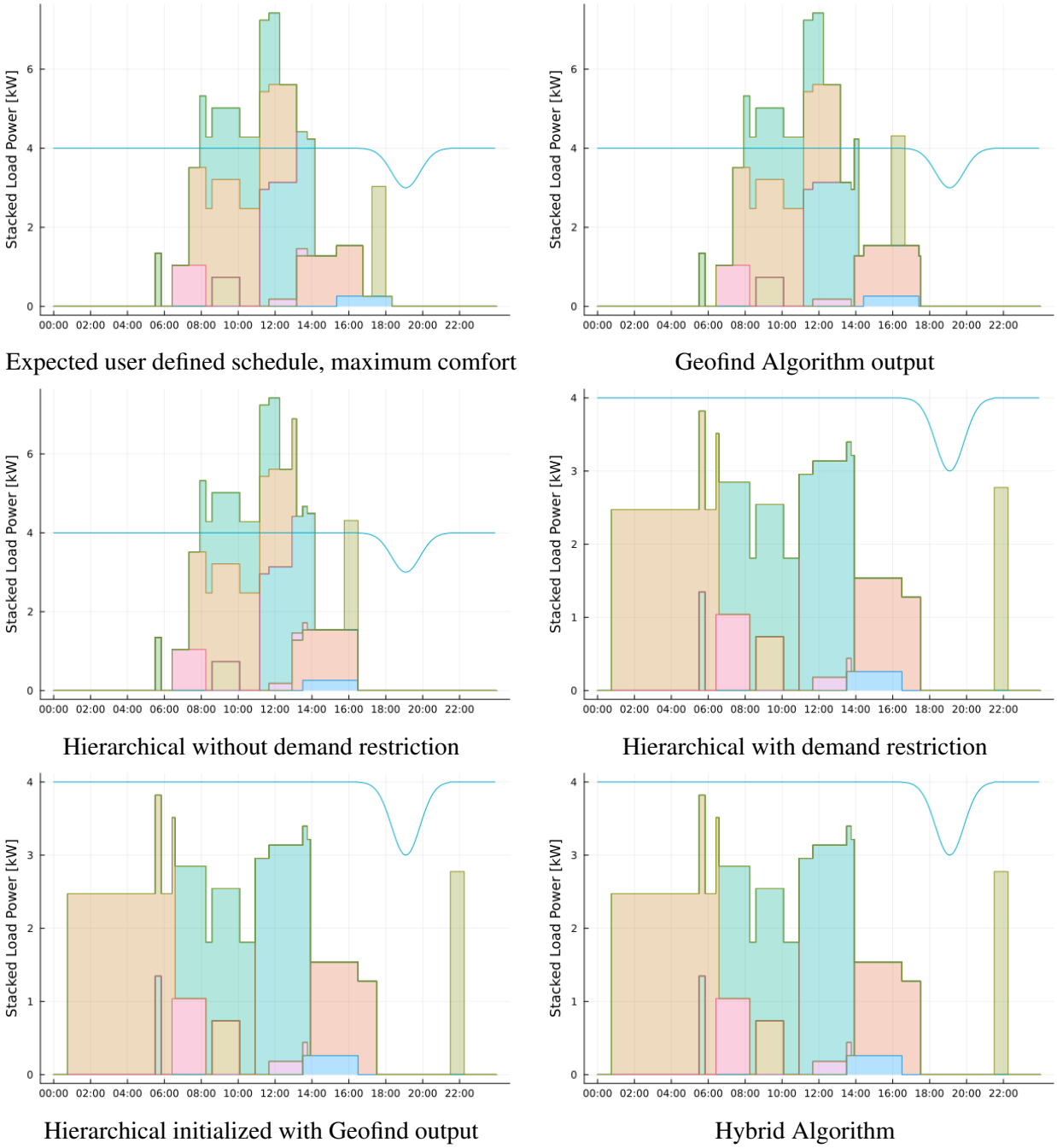

Expected user defined schedule, maximum comfort

Geofind Algorithm output

Hierarchical without demand restriction

Hierarchical with demand restriction

Hierarchical initialized with Geofind output

Hybrid Algorithm

Source: Prepared by the author.

Figure 20 – 25 Random Loads Schedule Results.

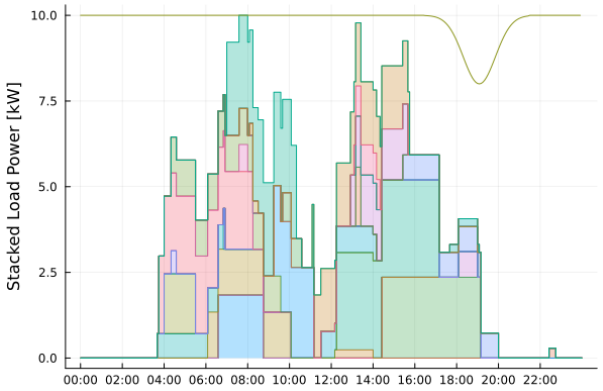

Expected user defined schedule, maximum comfort

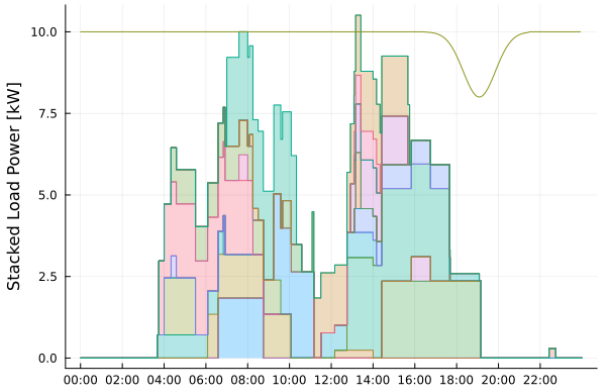

Geofind Algorithm output

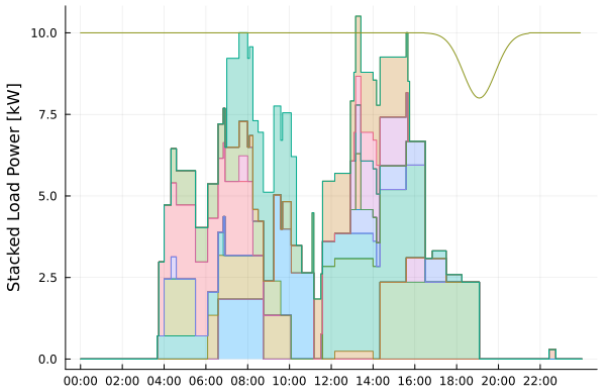

Hierarchical without demand restriction

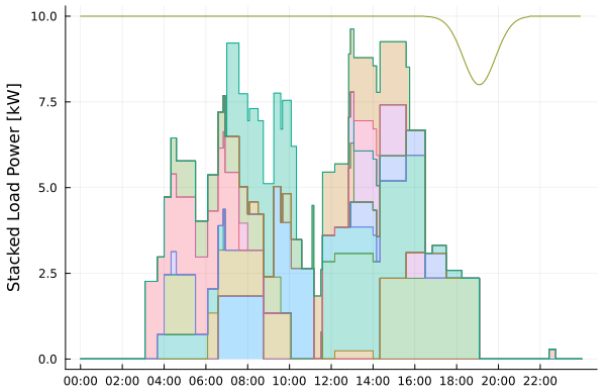

Hierarchical with demand restriction

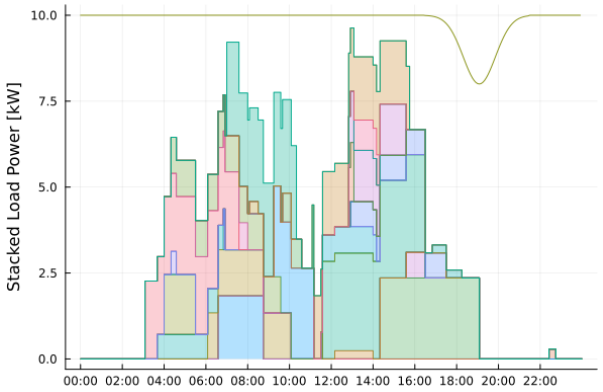

Hierarchical initialized with Geofind output

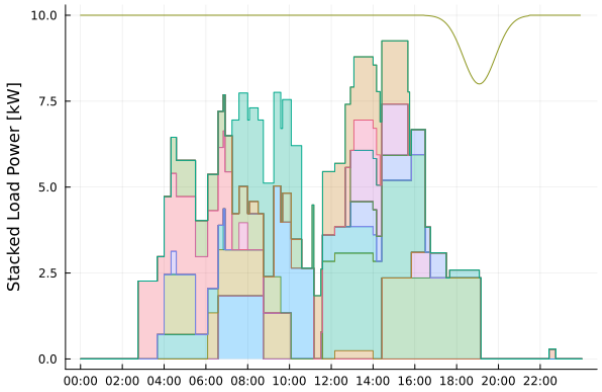

Hybrid Algorithm

Source: Prepared by the author.

Figure 21 – 50 Random Loads Schedule Results.

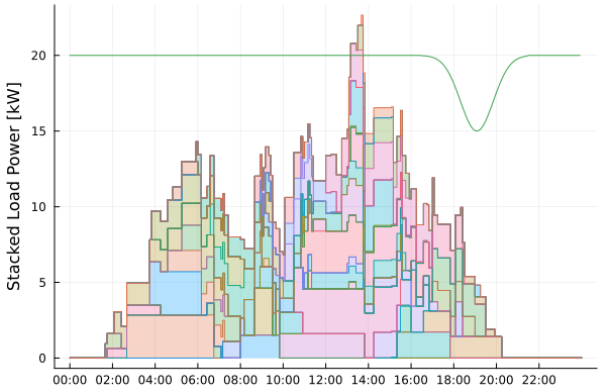

Expected user defined schedule, maximum comfort

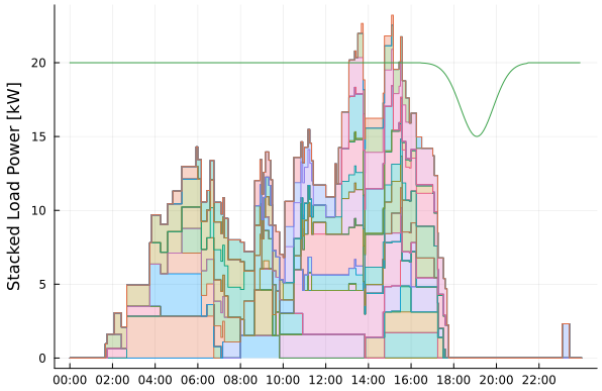

Geofind Algorithm output

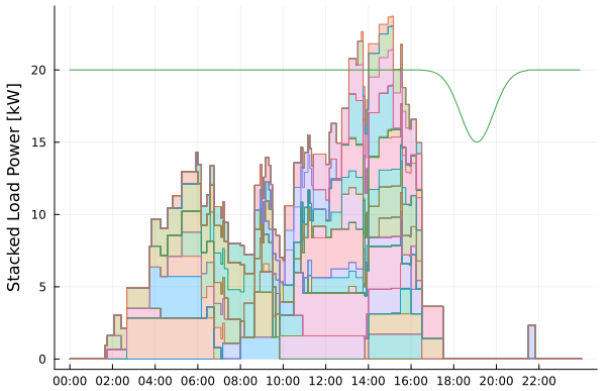

Hierarchical without demand restriction

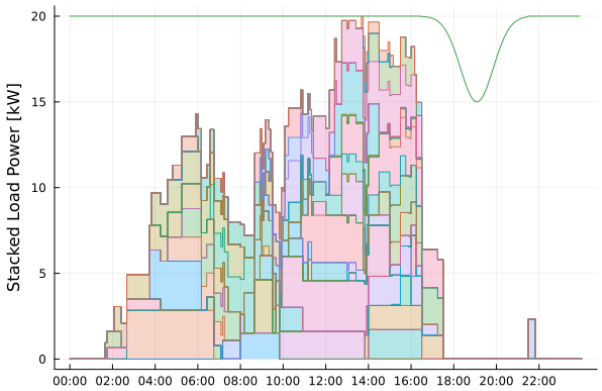

Hierarchical with demand restriction

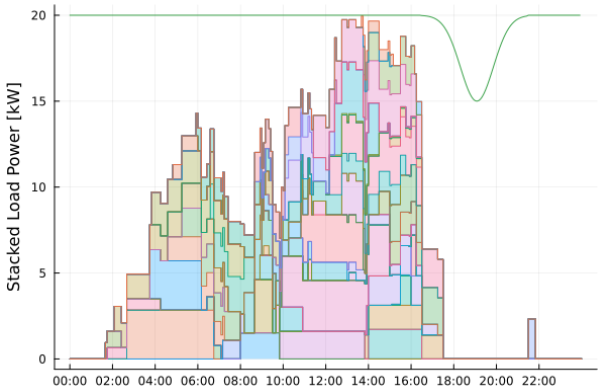

Hierarchical initialized with Geofind output

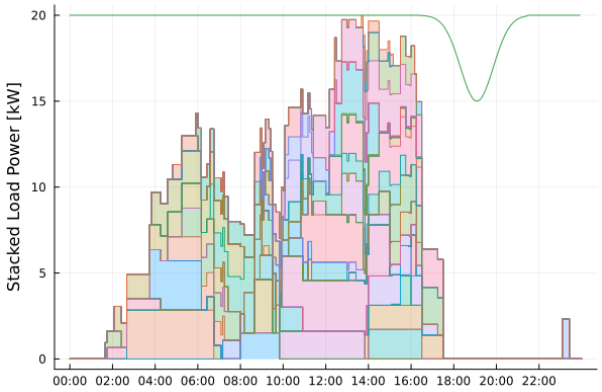

Hybrid Algorithm

Source: Prepared by the author.

Figure 22 – 75 Random Loads Schedule Results.

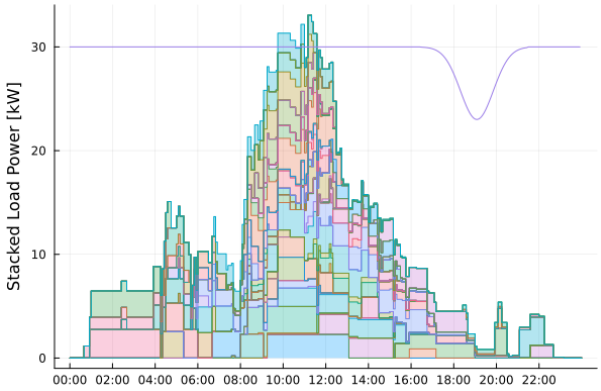

Expected user defined schedule, maximum comfort

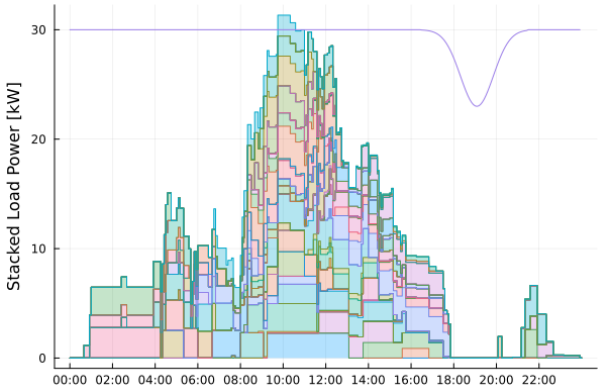

Geofind Algorithm output

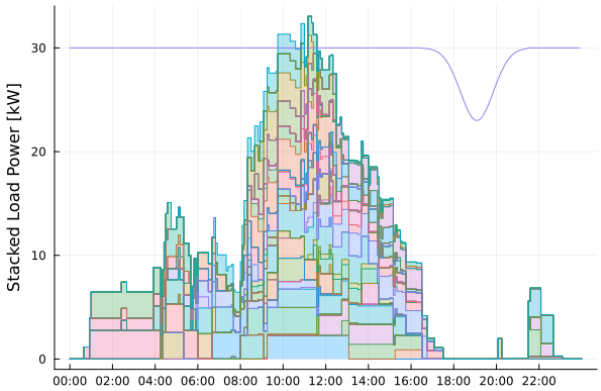

Hierarchical without demand restriction

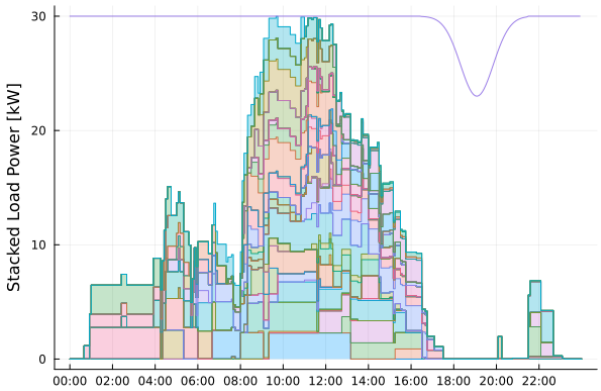

Hierarchical with demand restriction

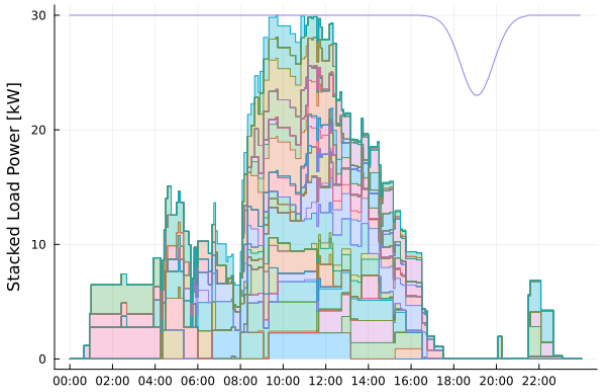

Hierarchical initialized with Geofind output

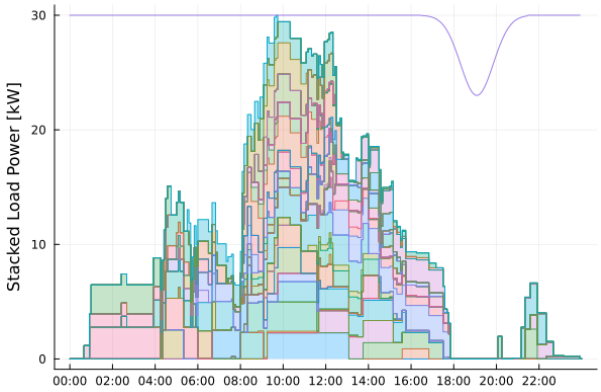

Hybrid Algorithm

Source: Prepared by the author.

Figure 23 – 100 Random Loads Schedule Results.

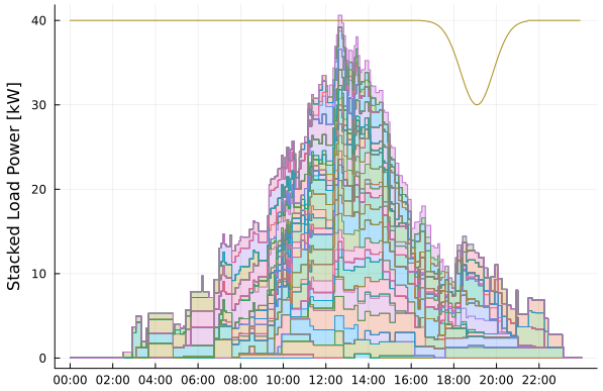

Expected user defined schedule, maximum comfort

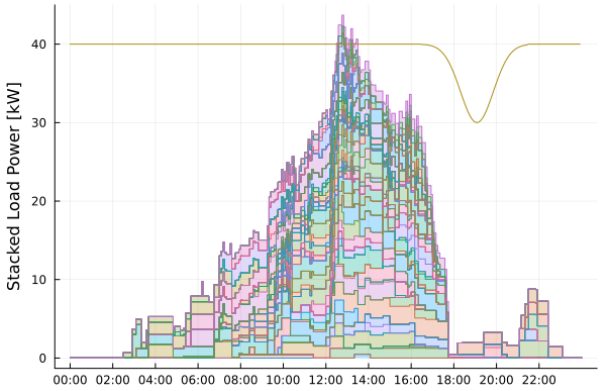

Geofind Algorithm output

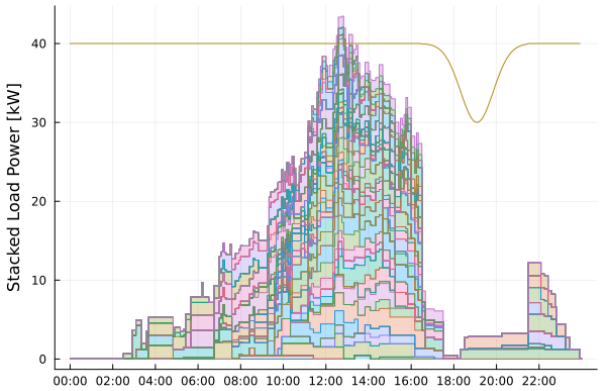

Hierarchical without demand restriction

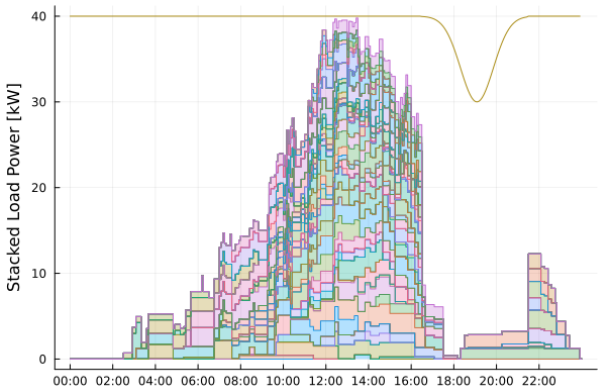

Hierarchical with demand restriction

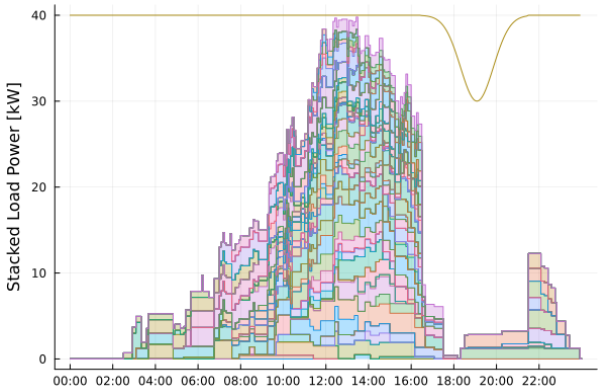

Hierarchical initialized with Geofind output

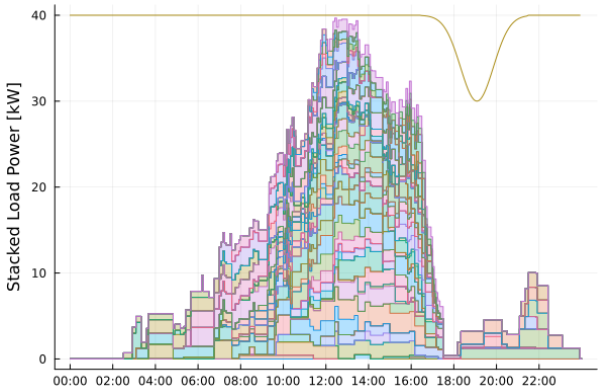

Hybrid Algorithm

Source: Prepared by the author.

Figure 24 – 250 Random Loads Schedule Results.

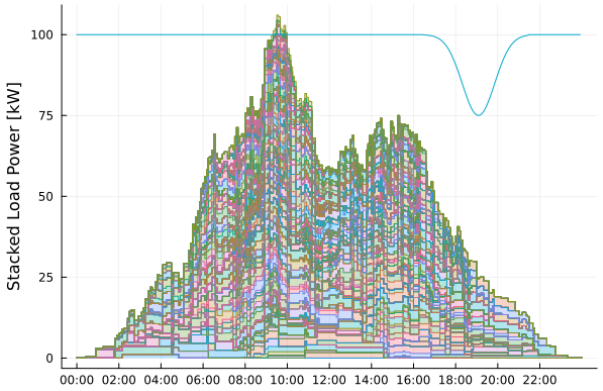

Expected user defined schedule, maximum comfort

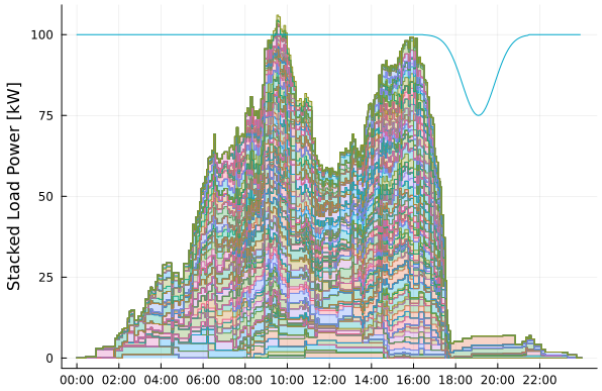

Geofind Algorithm output

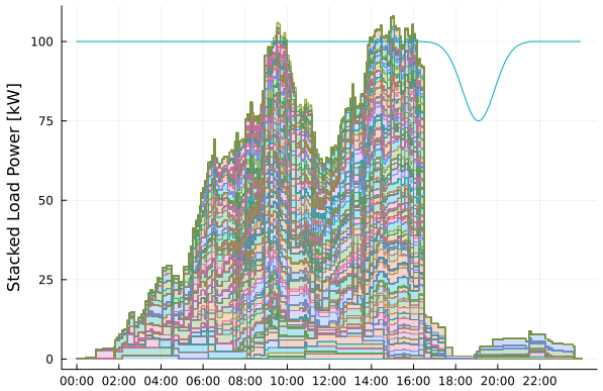

Hierarchical without demand restriction

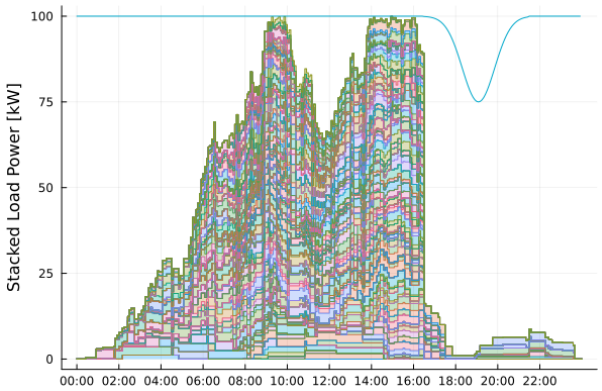

Hierarchical with demand restriction

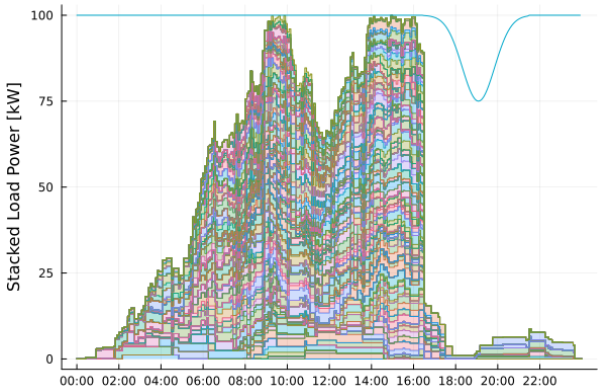

Hierarchical initialized with Geofind output

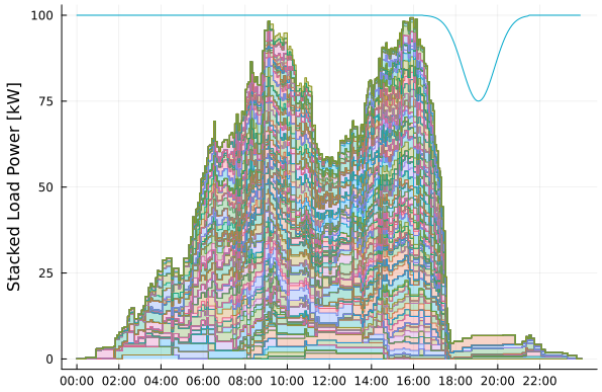

Hybrid Algorithm

Source: Prepared by the author.

Figure 25 – 500 Random Loads Schedule Results.

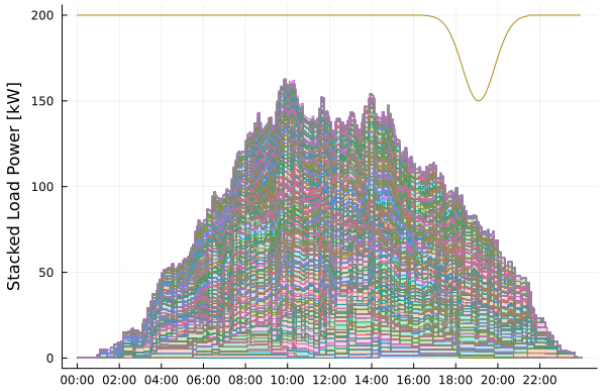

Expected user defined schedule, maximum comfort

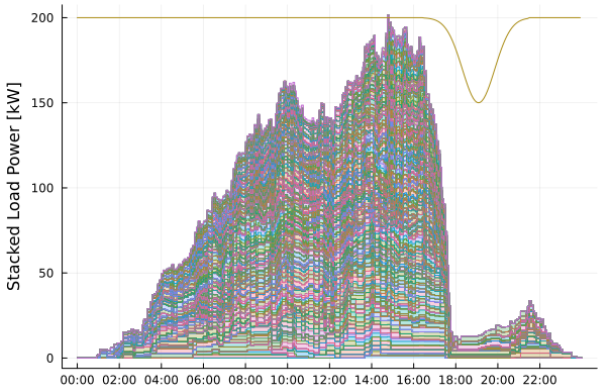

Geofind Algorithm output

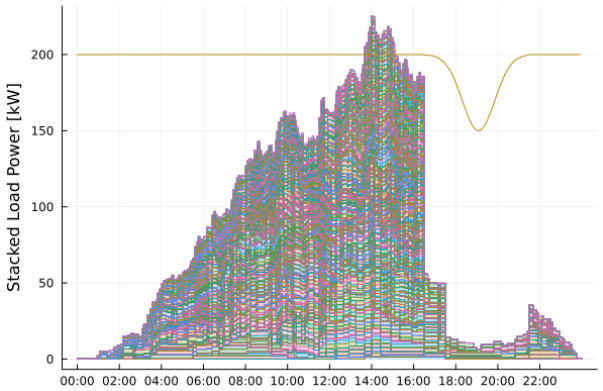

Hierarchical without demand restriction

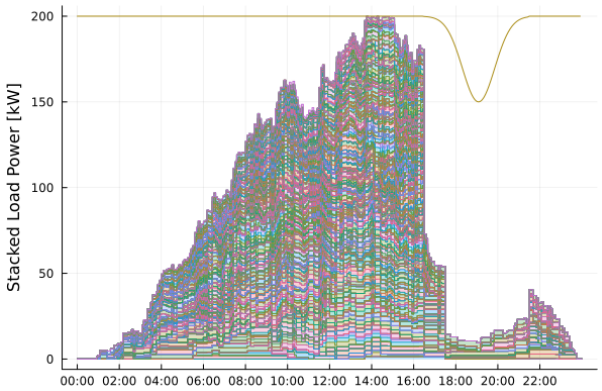

Hierarchical with demand restriction

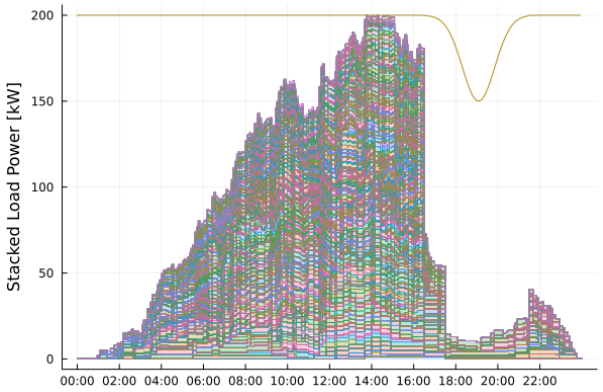

Hierarchical initialized with Geofind output

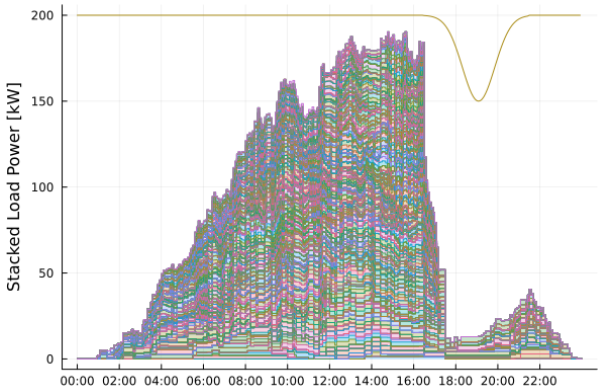

Hybrid Algorithm

Source: Prepared by the author.

Figure 26 – 750 Random Loads Schedule Results.

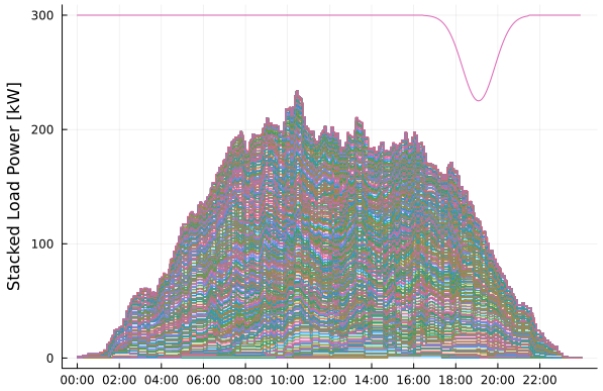

Expected user defined schedule, maximum comfort

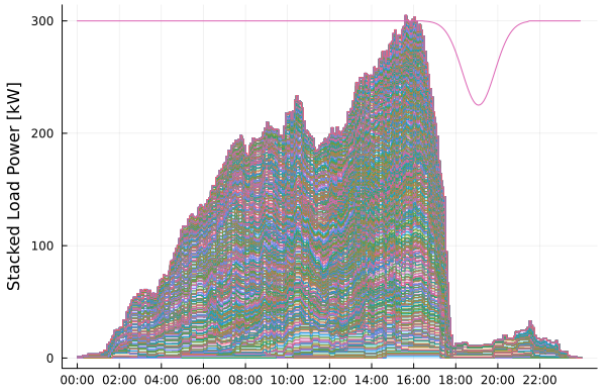

Geofind Algorithm output

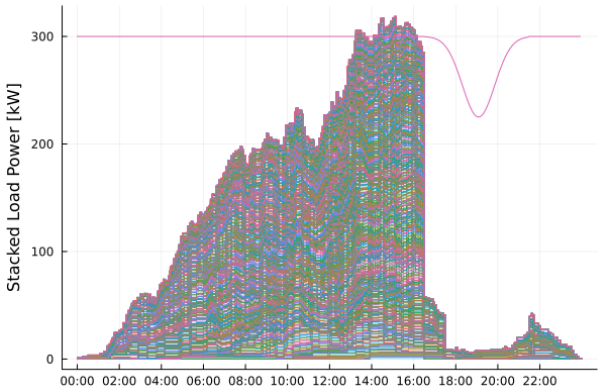

Hierarchical without demand restriction

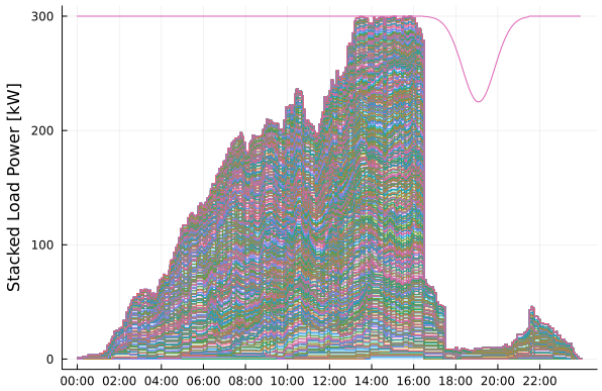

Hierarchical with demand restriction

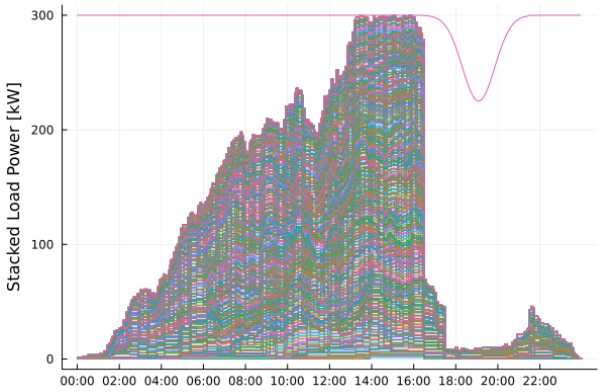

Hierarchical initialized with Geofind output

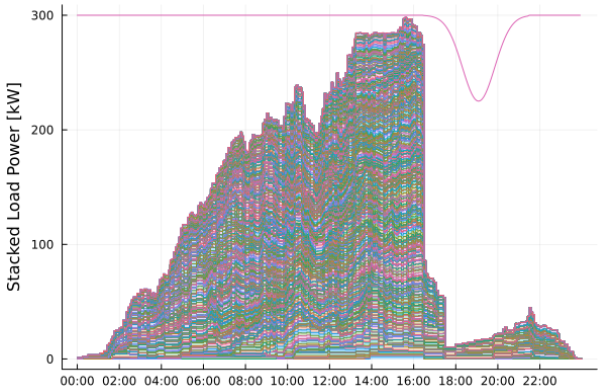

Hybrid Algorithm

Source: Prepared by the author.

APPENDIX D – DETAILED BENCHMARKS OUTPUTS

All benchmarks data generated are available in GitHub link provided at Appendix A inside **data folder** and identified by its alias "RNDxx.BSON". In Figure 27 is illustrated the main attributes of the generated output. Each benchmark trial has fully executed the referenced procedure for *n* samples, and this samples have been repeated in *m* evaluations.

Figure 27 – Graphic Tutorial to Read Benchmark Outputs

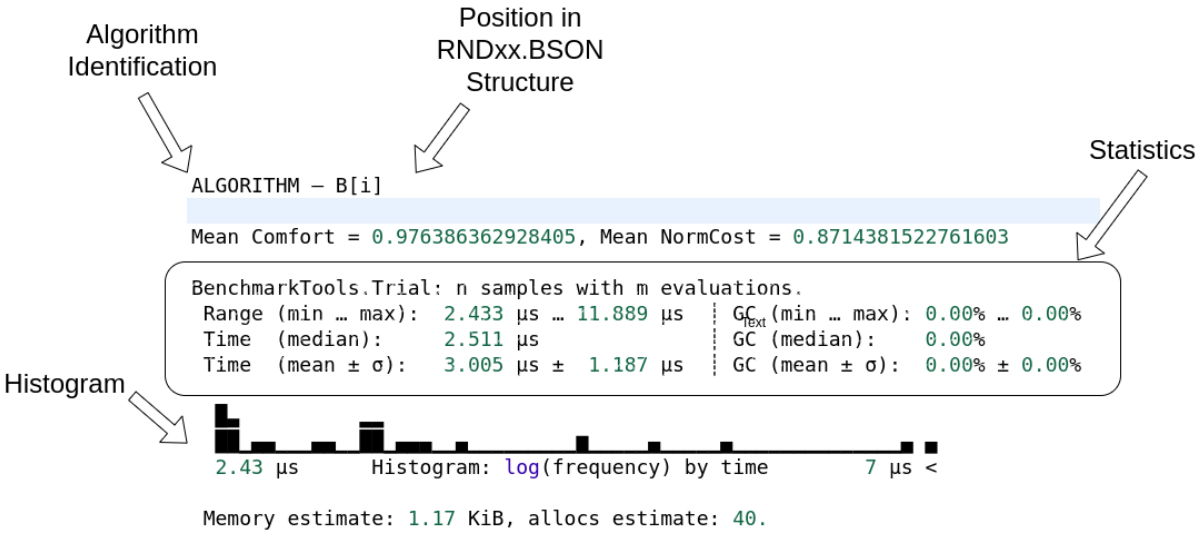

Source: Prepared by the author.

The Code written in Julia language presented in 3 could be used to read the refered "*.BSON" files.

Algorithm 3 – "*.BSON" files load function

```
using BenchmarkTools
using BSON

function Load_Benchmarks(filename::String)
    Temp = BSON.load(filename * ".bson")
    return Vector{BenchmarkTools.Trial}(Temp[:H])
end
```

```
# 10 random LOADS

GEOFINDER – B[1]
Mean Comfort = 0.976386362928405, Mean NormCost = 0.8714381522761603

BenchmarkTools.Trial: 100 samples with 9 evaluations.
 Range (min … max):  2.433 µs … 11.889 µs  ┊ GC (min … max): 0.00% … 0.00%
 Time  (median):     2.511 µs              ┊ GC (median):    0.00%
 Time  (mean ± σ):   3.005 µs ±  1.187 µs  ┊ GC (mean ± σ):  0.00% ± 0.00%

  2.43 µs      Histogram: log(frequency) by time        7 µs <

 Memory estimate: 1.17 KiB, allocs estimate: 40.

MOA NO DEMAND - B[2]
Mean Comfort = 0.9749415934038286, Mean NormCost = 0.8283399571996333

BenchmarkTools.Trial: 100 samples with 1 evaluation.
 Range (min … max):  17.325 ms … 66.797 ms  ┊ GC (min … max): 0.00% … 63.51%
 Time  (median):     20.823 ms              ┊ GC (median):    0.00%
 Time  (mean ± σ):   21.857 ms ±  6.373 ms  ┊ GC (mean ± σ):  3.71% ±  8.84%

  17.3 ms         Histogram: frequency by time        62.1 ms <

 Memory estimate: 5.84 MiB, allocs estimate: 111352.

MOA WITH DEMAND NO INITIALIZATION - B[3]
Mean Comfort = 0.8874726559393806, Mean NormCost = 0.8432466187473191

BenchmarkTools.Trial: 100 samples with 1 evaluation.
 Range (min … max):  1.195 s …   1.753 s  ┊ GC (min … max): 0.00% … 0.00%
 Time  (median):     1.228 s              ┊ GC (median):    0.00%
 Time  (mean ± σ):   1.249 s ± 81.524 ms  ┊ GC (mean ± σ):  0.35% ± 0.85%

  1.2 s          Histogram: frequency by time        1.66 s <

 Memory estimate: 37.84 MiB, allocs estimate: 858383.

MOA WITH DEMAND INITIALIZED WITH GEOFINDER - B[4]
Mean Comfort = 0.8874726559393806, Mean NormCost = 0.8432466187473191

BenchmarkTools.Trial: 100 samples with 1 evaluation.
 Range (min … max):  1.038 s …   1.267 s  ┊ GC (min … max): 0.00% … 0.00%
 Time  (median):     1.055 s              ┊ GC (median):    0.00%
 Time  (mean ± σ):   1.066 s ± 31.774 ms  ┊ GC (mean ± σ):  0.41% ± 0.97%

  1.04 s         Histogram: frequency by time        1.17 s <

 Memory estimate: 37.87 MiB, allocs estimate: 859654.

HYBRID - B[5]
Mean Comfort = 0.8874726559393806, Mean NormCost = 0.8432466187473191
MOA in Hybrid executed for 1 times with 9 loads, limited to 5 iterations

BenchmarkTools.Trial: 100 samples with 1 evaluation.
 Range (min … max):  1.152 s …   1.639 s  ┊ GC (min … max): 0.00% … 2.23%
 Time  (median):     1.187 s              ┊ GC (median):    0.00%
 Time  (mean ± σ):   1.208 s ± 73.616 ms  ┊ GC (mean ± σ):  0.36% ± 0.89%

  1.15 s         Histogram: frequency by time        1.58 s <

 Memory estimate: 36.53 MiB, allocs estimate: 810913.
```

```
# 25 random LOADS

GEOFINDER – B[26]
Mean Comfort = 0.9639094809094808, Mean NormCost = 0.9230197173139565

BenchmarkTools.Trial: 100 samples with 4 evaluations.
 Range (min … max):   7.850 µs … 22.425 µs  ┊ GC (min … max): 0.00% … 0.00%
 Time  (median):      8.488 µs              ┊ GC (median):    0.00%
 Time  (mean ± σ):   10.074 µs ±  3.063 µs  ┊ GC (mean ± σ):  0.00% ± 0.00%

  7.85 µs      Histogram: log(frequency) by time      21.8 µs <

 Memory estimate: 3.66 KiB, allocs estimate: 150.

MOA NO DEMAND - B[27]
Mean Comfort = 0.948171976487766, Mean NormCost = 0.8932962131930267

BenchmarkTools.Trial: 100 samples with 1 evaluation.
 Range (min … max):  52.094 ms … 148.151 ms  ┊ GC (min … max): 0.00% …  0.00%
 Time  (median):     61.573 ms               ┊ GC (median):    0.00%
 Time  (mean ± σ):   65.340 ms ±  15.461 ms  ┊ GC (mean ± σ):  4.79% ± 11.08%

  52.1 ms         Histogram: frequency by time          116 ms <

 Memory estimate: 19.09 MiB, allocs estimate: 347771.

MOA WITH DEMAND NO INITIALIZATION - B[28]
Mean Comfort = 0.9450894177234609, Mean NormCost = 0.8932962131930267

BenchmarkTools.Trial: 78 samples with 1 evaluation.
 Range (min … max):  1.188 s …    1.796 s  ┊ GC (min … max): 0.00% … 0.00%
 Time  (median):     1.250 s               ┊ GC (median):    0.00%
 Time  (mean ± σ):   1.285 s ± 108.193 ms  ┊ GC (mean ± σ):  1.13% ± 1.62%

  1.19 s         Histogram: frequency by time         1.74 s <

 Memory estimate: 92.67 MiB, allocs estimate: 2340138.

MOA WITH DEMAND INITIALIZED WITH GEOFINDER - B[29]
Mean Comfort = 0.9450894177234609, Mean NormCost = 0.8932962131930267

BenchmarkTools.Trial: 80 samples with 1 evaluation.
 Range (min … max):  1.202 s …   1.621 s  ┊ GC (min … max): 0.00% … 0.00%
 Time  (median):     1.243 s              ┊ GC (median):    0.00%
 Time  (mean ± σ):   1.256 s ± 55.580 ms  ┊ GC (mean ± σ):  1.17% ± 1.66%

  1.2 s          Histogram: frequency by time        1.44 s <

 Memory estimate: 92.64 MiB, allocs estimate: 2340086.

HYBRID - B[30]
Mean Comfort = 0.9574150417544913, Mean NormCost = 0.9149488437502726
MOA in Hybrid executed for 1 times with 14 loads, limited to 5 iterations, demand scale = 0.95

BenchmarkTools.Trial: 100 samples with 1 evaluation.
 Range (min … max):  779.227 ms …   1.221 s  ┊ GC (min … max): 0.00% … 5.05%
 Time  (median):     809.448 ms              ┊ GC (median):    0.00%
 Time  (mean ± σ):   821.517 ms ± 47.871 ms  ┊ GC (mean ± σ):  1.07% ± 1.95%

  779 ms          Histogram: frequency by time          886 ms <

 Memory estimate: 60.82 MiB, allocs estimate: 1417806.
```

```
# 50 random LOADS

GEOFINDER — B[6]
Mean Comfort = 0.9424540465743902, Mean NormCost = 0.859369331571671

BenchmarkTools.Trial: 100 samples with 1 evaluation.
 Range (min … max):  12.400 µs … 66.200 µs  ┊ GC (min … max): 0.00% … 0.00%
 Time  (median):     17.500 µs              ┊ GC (median):    0.00%
 Time  (mean ± σ):   20.748 µs ±  8.883 µs  ┊ GC (mean ± σ):  0.00% ± 0.00%

  12.4 µs      Histogram: log(frequency) by time      57.1 µs <

 Memory estimate: 5.45 KiB, allocs estimate: 199.

MOA NO DEMAND - B[7]
Mean Comfort = 0.9422429981279123, Mean NormCost = 0.8332566146021511

BenchmarkTools.Trial: 100 samples with 1 evaluation.
 Range (min … max):   85.064 ms … 192.506 ms  ┊ GC (min … max): 0.00% … 29.27%
 Time  (median):      99.148 ms               ┊ GC (median):    0.00%
 Time  (mean ± σ):   105.358 ms ±  20.351 ms  ┊ GC (mean ± σ):  6.74% ± 11.55%

  85.1 ms          Histogram: frequency by time          153 ms <

 Memory estimate: 40.51 MiB, allocs estimate: 805825.

MOA WITH DEMAND NO INITIALIZATION - B[8]
Mean Comfort = 0.941484632300033, Mean NormCost = 0.8394151118337146

BenchmarkTools.Trial: 100 samples with 1 evaluation.
 Range (min … max):  2.274 s …   2.860 s  ┊ GC (min … max): 0.00% … 0.00%
 Time  (median):     2.354 s              ┊ GC (median):    1.42%
 Time  (mean ± σ):   2.370 s ± 79.184 ms  ┊ GC (mean ± σ):  0.99% ± 0.71%

  2.27 s         Histogram: frequency by time        2.73 s <

 Memory estimate: 180.14 MiB, allocs estimate: 4505808.

MOA WITH DEMAND INITIALIZED WITH GEOFINDER - B[9]
Mean Comfort = 0.941484632300033, Mean NormCost = 0.8394151118337146

BenchmarkTools.Trial: 100 samples with 1 evaluation.
 Range (min … max):  2.274 s …   2.595 s  ┊ GC (min … max): 0.00% … 0.00%
 Time  (median):     2.340 s              ┊ GC (median):    1.49%
 Time  (mean ± σ):   2.343 s ± 49.459 ms  ┊ GC (mean ± σ):  1.01% ± 0.73%

  2.27 s         Histogram: frequency by time        2.54 s <

 Memory estimate: 180.07 MiB, allocs estimate: 4505707.

HYBRID - B[10]
Mean Comfort = 0.9355471323000331, Mean NormCost = 0.8394151118337146
MOA in Hybrid executed for 1 times with 22 loads, limited to 5 iterations

BenchmarkTools.Trial: 100 samples with 1 evaluation.
 Range (min … max):  919.000 ms …   1.075 s  ┊ GC (min … max): 0.00% … 3.54%
 Time  (median):     955.835 ms              ┊ GC (median):    0.00%
 Time  (mean ± σ):   965.704 ms ± 32.149 ms  ┊ GC (mean ± σ):  0.96% ± 1.42%

  919 ms          Histogram: frequency by time          1.07 s <

 Memory estimate: 82.99 MiB, allocs estimate: 1944734.
```

```
# 75 random LOADS

GEOFINDER – B[31]
Mean Comfort = 0.965594157994735, Mean NormCost = 0.8731028016424748

BenchmarkTools.Trial: 100 samples with 1 evaluation.
 Range (min … max):  17.800 µs … 45.300 µs  ┊ GC (min … max): 0.00% … 0.00%
 Time  (median):     18.700 µs              ┊ GC (median):    0.00%
 Time  (mean ± σ):   19.975 µs ±  4.019 µs  ┊ GC (mean ± σ):  0.00% ± 0.00%

  17.8 µs         Histogram: frequency by time        39.5 µs <

 Memory estimate: 7.50 KiB, allocs estimate: 280.

MOA NO DEMAND - B[32]
Mean Comfort = 0.9641357587807503, Mean NormCost = 0.8520352126644017
BenchmarkTools.Trial: 100 samples with 1 evaluation.
 Range (min … max):  146.323 ms … 269.027 ms  ┊ GC (min … max): 0.00% … 21.46%
 Time  (median):     166.986 ms               ┊ GC (median):    0.00%
 Time  (mean ± σ):   178.618 ms ±  30.085 ms  ┊ GC (mean ± σ):  8.15% ± 11.10%

  146 ms           Histogram: frequency by time          248 ms <

 Memory estimate: 72.37 MiB, allocs estimate: 1427439.

MOA WITH DEMAND NO INITIALIZATION - B[33]
Mean Comfort = 0.9623237967523719, Mean NormCost = 0.8522446853593528

BenchmarkTools.Trial: 100 samples with 1 evaluation.
 Range (min … max):  3.822 s …    5.029 s  ┊ GC (min … max): 1.17% … 0.80%
 Time  (median):     3.902 s               ┊ GC (median):    1.20%
 Time  (mean ± σ):   3.933 s ± 142.631 ms  ┊ GC (mean ± σ):  1.17% ± 0.24%

  3.82 s         Histogram: frequency by time         4.36 s <

 Memory estimate: 273.62 MiB, allocs estimate: 6894608.

MOA WITH DEMAND INITIALIZED WITH GEOFINDER - B[34]
Mean Comfort = 0.9623237967523719, Mean NormCost = 0.8522446853593528

BenchmarkTools.Trial: 100 samples with 1 evaluation.
 Range (min … max):  3.611 s …   4.166 s  ┊ GC (min … max): 0.00% … 1.06%
 Time  (median):     3.692 s              ┊ GC (median):    1.13%
 Time  (mean ± σ):   3.715 s ± 89.649 ms  ┊ GC (mean ± σ):  1.10% ± 0.25%

  3.61 s         Histogram: frequency by time        4.11 s <

 Memory estimate: 273.53 MiB, allocs estimate: 6894512.

HYBRID - B[35]
Mean Comfort = 0.9631459800762635, Mean NormCost = 0.8731028016424748
MOA in Hybrid executed for 2 times with 19 loads, limited to 5 iterations, demand scale = 0.95

BenchmarkTools.Trial: 100 samples with 1 evaluation.
 Range (min … max):  1.714 s …    2.452 s  ┊ GC (min … max): 0.00% … 3.48%
 Time  (median):     1.802 s               ┊ GC (median):    1.93%
 Time  (mean ± σ):   1.829 s ± 112.209 ms  ┊ GC (mean ± σ):  1.19% ± 1.10%

  1.71 s         Histogram: frequency by time         2.27 s <

 Memory estimate: 153.42 MiB, allocs estimate: 3424844.
```

```
# 100 random LOADS

GEOFINDER – B[11]
Mean Comfort = 0.9415650261786803, Mean NormCost = 0.910174210245961

BenchmarkTools.Trial: 100 samples with 1 evaluation.
 Range (min … max):  32.000 µs … 68.300 µs  ┊ GC (min … max): 0.00% … 0.00%
 Time  (median):     32.950 µs              ┊ GC (median):    0.00%
 Time  (mean ± σ):   35.647 µs ±  6.777 µs  ┊ GC (mean ± σ):  0.00% ± 0.00%
```

```
  32 µs           Histogram: frequency by time        61.7 µs <

 Memory estimate: 15.59 KiB, allocs estimate: 598.

MOA NO DEMAND - B[12]
Mean Comfort = 0.935025223525277, Mean NormCost = 0.8635966532303432

BenchmarkTools.Trial: 100 samples with 1 evaluation.
 Range (min … max):  206.271 ms … 344.406 ms  ┊ GC (min … max): 0.00% … 13.60%
 Time  (median):     247.769 ms               ┊ GC (median):    0.00%
 Time  (mean ± σ):   252.238 ms ±  32.443 ms  ┊ GC (mean ± σ):  8.60% ±  8.65%
```

```
  206 ms           Histogram: frequency by time          308 ms <

 Memory estimate: 123.39 MiB, allocs estimate: 2347730.

MOA WITH DEMAND NO INITIALIZATION - B[13]
Mean Comfort = 0.934350172260752, Mean NormCost = 0.8635966532303432

BenchmarkTools.Trial: 100 samples with 1 evaluation.
 Range (min … max):  5.777 s …    7.111 s  ┊ GC (min … max): 0.54% … 0.56%
 Time  (median):     5.976 s               ┊ GC (median):    0.79%
 Time  (mean ± σ):   6.055 s ± 241.260 ms  ┊ GC (mean ± σ):  1.10% ± 0.53%
```

```
  5.78 s          Histogram: frequency by time         6.82 s <

 Memory estimate: 421.92 MiB, allocs estimate: 10058408.

MOA WITH DEMAND INITIALIZED WITH GEOFINDER - B[14]
Mean Comfort = 0.934350172260752, Mean NormCost = 0.8635966532303432

BenchmarkTools.Trial: 100 samples with 1 evaluation.
 Range (min … max):  5.781 s …    6.777 s  ┊ GC (min … max): 0.68% … 1.92%
 Time  (median):     5.937 s               ┊ GC (median):    0.78%
 Time  (mean ± σ):   5.968 s ± 167.129 ms  ┊ GC (mean ± σ):  1.09% ± 0.48%
```

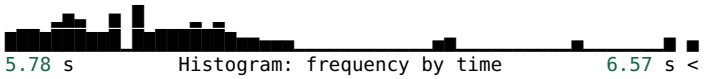

```
  5.78 s          Histogram: frequency by time         6.57 s <

 Memory estimate: 421.79 MiB, allocs estimate: 10058257.

HYBRID - B[15]
Mean Comfort = 0.9452532449688483, Mean NormCost = 0.9072415400919384
MOA in Hybrid executed for 1 times with 41 loads, limited to 5 iterations

BenchmarkTools.Trial: 100 samples with 1 evaluation.
 Range (min … max):  1.871 s …    3.101 s  ┊ GC (min … max): 0.00% … 0.00%
 Time  (median):     1.956 s               ┊ GC (median):    1.75%
 Time  (mean ± σ):   1.975 s ± 149.731 ms  ┊ GC (mean ± σ):  1.08% ± 0.96%
```

```
  1.87 s          Histogram: frequency by time         2.64 s <

 Memory estimate: 161.99 MiB, allocs estimate: 3552429.
```

```
# 250 random LOADS

GEOFINDER – B[36]
Mean Comfort = 0.9686602443650579, Mean NormCost = 0.8814729522448811

BenchmarkTools.Trial: 100 samples with 1 evaluation.
 Range (min … max):   99.000 μs … 128.500 μs  ┊ GC (min … max): 0.00% … 0.00%
 Time  (median):     101.250 μs               ┊ GC (median):    0.00%
 Time  (mean ± σ):   102.471 μs ±   4.588 μs  ┊ GC (mean ± σ):  0.00% ± 0.00%
```

```
  99 μs            Histogram: frequency by time          125 μs <

 Memory estimate: 31.16 KiB, allocs estimate: 1182.

MOA NO DEMAND - B[37]
Mean Comfort = 0.9597947104532378, Mean NormCost = 0.8471496564591503

BenchmarkTools.Trial: 100 samples with 1 evaluation.
 Range (min … max):  870.018 ms …   1.262 s  ┊ GC (min … max):  8.55% … 12.45%
 Time  (median):     955.984 ms              ┊ GC (median):    14.49%
 Time  (mean ± σ):   961.677 ms ± 59.026 ms  ┊ GC (mean ± σ):  13.15% ±  2.82%
```

```
  870 ms          Histogram: frequency by time          1.21 s <

 Memory estimate: 508.57 MiB, allocs estimate: 10688015.

MOA WITH DEMAND NO INITIALIZATION - B[38]
Mean Comfort = 0.9588104658178256, Mean NormCost = 0.8477152327355184

BenchmarkTools.Trial: 50 samples with 1 evaluation.
 Range (min … max):  16.501 s …   17.951 s  ┊ GC (min … max): 1.39% … 1.80%
 Time  (median):     16.864 s               ┊ GC (median):    1.61%
 Time  (mean ± σ):   16.958 s ± 347.121 ms  ┊ GC (mean ± σ):  2.05% ± 1.24%
```

```
  16.5 s          Histogram: frequency by time          18 s <

 Memory estimate: 1.21 GiB, allocs estimate: 29612248.

MOA WITH DEMAND INITIALIZED WITH GEOFINDER - B[39]
Mean Comfort = 0.9588104658178256, Mean NormCost = 0.8477152327355184

BenchmarkTools.Trial: 50 samples with 1 evaluation.
 Range (min … max):  16.534 s …   18.245 s  ┊ GC (min … max): 1.63% … 1.46%
 Time  (median):     16.779 s               ┊ GC (median):    1.61%
 Time  (mean ± σ):   16.919 s ± 412.275 ms  ┊ GC (mean ± σ):  2.01% ± 1.20%
```

```
  16.5 s          Histogram: frequency by time        18.2 s <

 Memory estimate: 1.21 GiB, allocs estimate: 29611768.

HYBRID - B[40]
Mean Comfort = 0.9679278437007202, Mean NormCost = 0.8814729522448811
MOA in Hybrid executed for 1 times with 75 loads, limited to 5 iterations, demand scale = 0.95

BenchmarkTools.Trial: 50 samples with 1 evaluation.
 Range (min … max):  3.973 s …   4.313 s  ┊ GC (min … max): 0.00% … 1.13%
 Time  (median):     4.044 s              ┊ GC (median):    1.20%
 Time  (mean ± σ):   4.061 s ± 63.910 ms  ┊ GC (mean ± σ):  1.19% ± 0.31%
```

```
  3.97 s         Histogram: frequency by time        4.31 s <

 Memory estimate: 303.17 MiB, allocs estimate: 6868449.
```

```
# 500 random LOADS

GEOFINDER – B[16]
Mean Comfort = 0.9477226036278417, Mean NormCost = 0.8976236764940347

BenchmarkTools.Trial: 25 samples with 1 evaluation.
 Range (min … max):  147.600 µs … 374.300 µs  ┊ GC (min … max): 0.00% … 0.00%
 Time  (median):     155.000 µs               ┊ GC (median):    0.00%
 Time  (mean ± σ):   173.276 µs ±  52.319 µs  ┊ GC (mean ± σ):  0.00% ± 0.00%

  148 µs           Histogram: frequency by time          374 µs <

 Memory estimate: 68.56 KiB, allocs estimate: 2632.

MOA NO DEMAND - B[17]
Mean Comfort = 0.9340477659599157, Mean NormCost = 0.854916245697625

BenchmarkTools.Trial: 25 samples with 1 evaluation.
 Range (min … max):  3.073 s …    4.562 s  ┊ GC (min … max): 13.39% … 36.05%
 Time  (median):     3.368 s               ┊ GC (median):    15.09%
 Time  (mean ± σ):   3.509 s ± 422.020 ms  ┊ GC (mean ± σ):  18.76% ±  7.37%

  3.07 s         Histogram: frequency by time         4.56 s <

 Memory estimate: 1.72 GiB, allocs estimate: 37102644.

MOA WITH DEMAND NO INITIALIZATION - B[18]
Mean Comfort = 0.9374017478498075, Mean NormCost = 0.8589854911857181

BenchmarkTools.Trial: 25 samples with 1 evaluation.
 Range (min … max):  36.424 s …   38.919 s  ┊ GC (min … max): 1.93% … 4.04%
 Time  (median):     37.140 s               ┊ GC (median):    2.14%
 Time  (mean ± σ):   37.316 s ± 720.675 ms  ┊ GC (mean ± σ):  2.90% ± 1.04%

  36.4 s           Histogram: frequency by time         38.9 s <

 Memory estimate: 3.13 GiB, allocs estimate: 74251275.

MOA WITH DEMAND INITIALIZED WITH GEOFINDER - B[19]
Mean Comfort = 0.9374017478498075, Mean NormCost = 0.8589854911857181

BenchmarkTools.Trial: 25 samples with 1 evaluation.
 Range (min … max):  36.535 s …   38.210 s  ┊ GC (min … max): 2.00% … 2.09%
 Time  (median):     37.307 s               ┊ GC (median):    2.27%
 Time  (mean ± σ):   37.328 s ± 427.619 ms  ┊ GC (mean ± σ):  2.88% ± 0.90%

  36.5 s           Histogram: frequency by time         38.2 s <

 Memory estimate: 3.13 GiB, allocs estimate: 74250288.

HYBRID - B[20]
Mean Comfort = 0.9440877054912669, Mean NormCost = 0.8858661444044644
MOA in Hybrid executed for 2 times with 123 loads, limited to 5 iterations, demand scale = 0.9

BenchmarkTools.Trial: 25 samples with 1 evaluation.
 Range (min … max):  15.800 s …   17.031 s  ┊ GC (min … max): 1.23% … 1.51%
 Time  (median):     16.068 s               ┊ GC (median):    1.50%
 Time  (mean ± σ):   16.124 s ± 281.248 ms  ┊ GC (mean ± σ):  1.42% ± 0.18%

  15.8 s           Histogram: frequency by time           17 s <

 Memory estimate: 1.22 GiB, allocs estimate: 28035690.
```

```
# 750 random LOADS

GEOFINDER — B[21]
Mean Comfort = 0.9544973455513059, Mean NormCost = 0.885632940326576

BenchmarkTools.Trial: 25 samples with 1 evaluation.
 Range (min … max):  309.100 µs … 377.100 µs  ┊ GC (min … max): 0.00% … 0.00%
 Time  (median):     312.000 µs               ┊ GC (median):    0.00%
 Time  (mean ± σ):   319.320 µs ±  18.712 µs  ┊ GC (mean ± σ):  0.00% ± 0.00%
```

```
  309 µs           Histogram: frequency by time          377 µs <

 Memory estimate: 97.38 KiB, allocs estimate: 3719.

MOA NO DEMAND - B[22]
Mean Comfort = 0.9401988131896606, Mean NormCost = 0.8469380416492673

BenchmarkTools.Trial: 15 samples with 1 evaluation.
 Range (min … max):  6.154 s …    8.206 s  ┊ GC (min … max): 15.17% … 30.54%
 Time  (median):     6.525 s               ┊ GC (median):    15.89%
 Time  (mean ± σ):   6.699 s ± 594.260 ms  ┊ GC (mean ± σ):  18.24% ±  5.11%
```

```
  6.15 s         Histogram: frequency by time         8.21 s <

 Memory estimate: 3.67 GiB, allocs estimate: 80863966.

MOA WITH DEMAND NO INITIALIZATION - B[23]
Mean Comfort = 0.9410324265947129, Mean NormCost = 0.8486072582247249

BenchmarkTools.Trial: 22 samples with 1 evaluation.
 Range (min … max):  91.284 s …   93.604 s  ┊ GC (min … max): 2.32% … 2.33%
 Time  (median):     92.362 s               ┊ GC (median):    2.29%
 Time  (mean ± σ):   92.339 s ± 548.134 ms  ┊ GC (mean ± σ):  2.27% ± 0.18%
```

```
  91.3 s           Histogram: frequency by time         93.6 s <

 Memory estimate: 5.93 GiB, allocs estimate: 146133549.

MOA WITH DEMAND INITIALIZED WITH GEOFINDER - B[24]
Mean Comfort = 0.9410324265947129, Mean NormCost = 0.8486072582247249

BenchmarkTools.Trial: 24 samples with 1 evaluation.
 Range (min … max):  83.063 s … 92.177 s  ┊ GC (min … max): 1.77% … 2.26%
 Time  (median):     84.655 s             ┊ GC (median):    2.48%
 Time  (mean ± σ):   84.897 s ±  1.698 s  ┊ GC (mean ± σ):  2.43% ± 0.24%
```

```
  83.1 s         Histogram: frequency by time        92.2 s <

 Memory estimate: 5.93 GiB, allocs estimate: 146125698.

HYBRID - B[25]
Mean Comfort = 0.9461439865428813, Mean NormCost = 0.8623114111212535
MOA in Hybrid executed for 2 times with 217 loads, limited to 5 iterations, demand scale = 0.95

BenchmarkTools.Trial: 25 samples with 1 evaluation.
 Range (min … max):  37.821 s …   40.890 s  ┊ GC (min … max): 1.32% … 3.17%
 Time  (median):     38.451 s               ┊ GC (median):    1.45%
 Time  (mean ± σ):   38.664 s ± 667.657 ms  ┊ GC (mean ± σ):  1.78% ± 0.83%
```

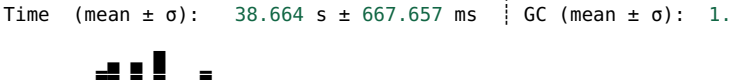

```
  37.8 s           Histogram: frequency by time         40.9 s <

 Memory estimate: 2.67 GiB, allocs estimate: 62802981.
```

APPENDIX E – BINOMIAL TARIFF ANALYSIS

In this appendix will be considered two types of Energy Tariff: A constant one T_C and a binomial composed by a off-peak and an peak posts $C_B = \{T_f, T_p\}$. For all cases here analyzed $T_f < T_C < T_p$. Table 11 lists two hypothetical values for these tariffs that will be used for graphical analysis later in this text.

Table 11 – Comparison between constant tariff and binomial tariffs A and B.

Tariff Post	T_c (R$/kWh)	Tariff A (R$/kWh)	Tariff B (R$/kWh)
Off-peak	1.00	0.50	0.50
Peak	1.00	1.50	2.00

Source: Prepared by the author.

Repeating the procedures in Chapter: Proposed Definitions and Methodology, we can define the cost of a load in Binomial Tariff as Equation (E.1).

$$C_B = k \cdot L.\hat{P} \cdot [(\hat{f}, \hat{p}) \centerdot (T_f, T_p)] \tag{E.1}$$

where:

$$|\hat{f}| + |\hat{p}| = L.W\Delta; \tag{E.2}$$

Equation (E.2) is geometrically a line that intercept the axis $\hat{f}$ and $\hat{p}$ at $L.W\Delta$. For the binomial tariff scenario, the line segment of this Equation for $\hat{f} \geq 0$ and $\hat{p} \geq 0$ also represent the basic load *locus* in binomial tariff space. That stated, we can also define the thresholds for Equation (E.1) resulting in the Inequation (E.5):

$$C_{min} = k \cdot L.\hat{P} \cdot L.W\Delta \cdot T_f \tag{E.3}$$

$$C_{max} = k \cdot L.\hat{P} \cdot L.W\Delta \cdot T_c \tag{E.4}$$

$$C_{min} \leq C_B \leq C_{max} \longleftrightarrow L.W\Delta \cdot T_f \leq [\hat{f} \cdot T_f + \hat{p} \cdot T_p] \leq L.W\Delta \cdot T_c \tag{E.5}$$

As expected, the lower bound can only be reached if the load is fully moved to off-peak post. The analysis of upper bound results in a single point illustrated in Equation (E.6):

$$\left(\hat{p} = L.W\Delta\frac{T_c - T_f}{T_p - T_f};\quad \hat{f} = L.W\Delta\frac{T_p - T_c}{T_p - T_f}\right) \tag{E.6}$$

Using values of Tariff A from Table 11 in Equation (E.6) we find: $\hat{f} = \frac{1}{2}L.W\Delta$ and $\hat{p} = \frac{1}{2}L.W\Delta$. That result can be represented by a line shown in Equation (E.7):

$$\hat{f} = \hat{p} \tag{E.7}$$

The intersection point between the line defined by Equation (E.2) and the line from Equation (E.7) represents a set point at which the cost of a load under Tariff A equals the cost under a Constant Tariff. The line segment originating from this point towards the point $(\hat{f} = L.W, 0)$ denotes the lower-cost region that needs to be identified. Figure 28 illustrates the tariff space for the binomial tariff, with the lower-cost region highlighted in gray for a load with a duration of 3h under Tariff A settings. Any point within this line segment is a valid result for scheduling to optimize cost. To achieve the comfort goal, it is necessary to first locate the load in the Tariff Space. If the load is already in the lower-cost region at the expected instant defined by the user, no further action is necessary. Otherwise, select the inner point of this line segment closest to the point defined in Equation (E.6).

Using values of Tariff B from Table 11 in Equation (E.6) we find: $\hat{f} = \frac{2}{3}L.W\Delta$ and $\hat{p} = \frac{1}{3}L.W\Delta$. That result can be represented by a line shown in Equation (E.8):

$$\hat{f} = 2 \cdot \hat{p} \tag{E.8}$$

Like in first case, the intersection point between the line defined by Equation (E.2) and the line from Equation (E.8) represents a set point at which the cost of a load under Tariff B equals the cost under a Constant Tariff. The line segment originating from this point towards the point $(\hat{f} = L.W, 0)$ denotes the lower-cost region that needs to be identified. In Figure 28 the lower-cost region is highlighted in purple for a load with a duration of 6h under Tariff B settings. Any point within this line segment is a valid result for scheduling to optimize cost. To achieve the comfort goal, it is necessary to first locate the load in the Tariff Space. If the load is already in the lower-cost region no further action is necessary. Otherwise, select the inner point of this line segment closest to the point defined in Equation (E.6).

Figure 28 – Binomial Tariff Basic Analysis

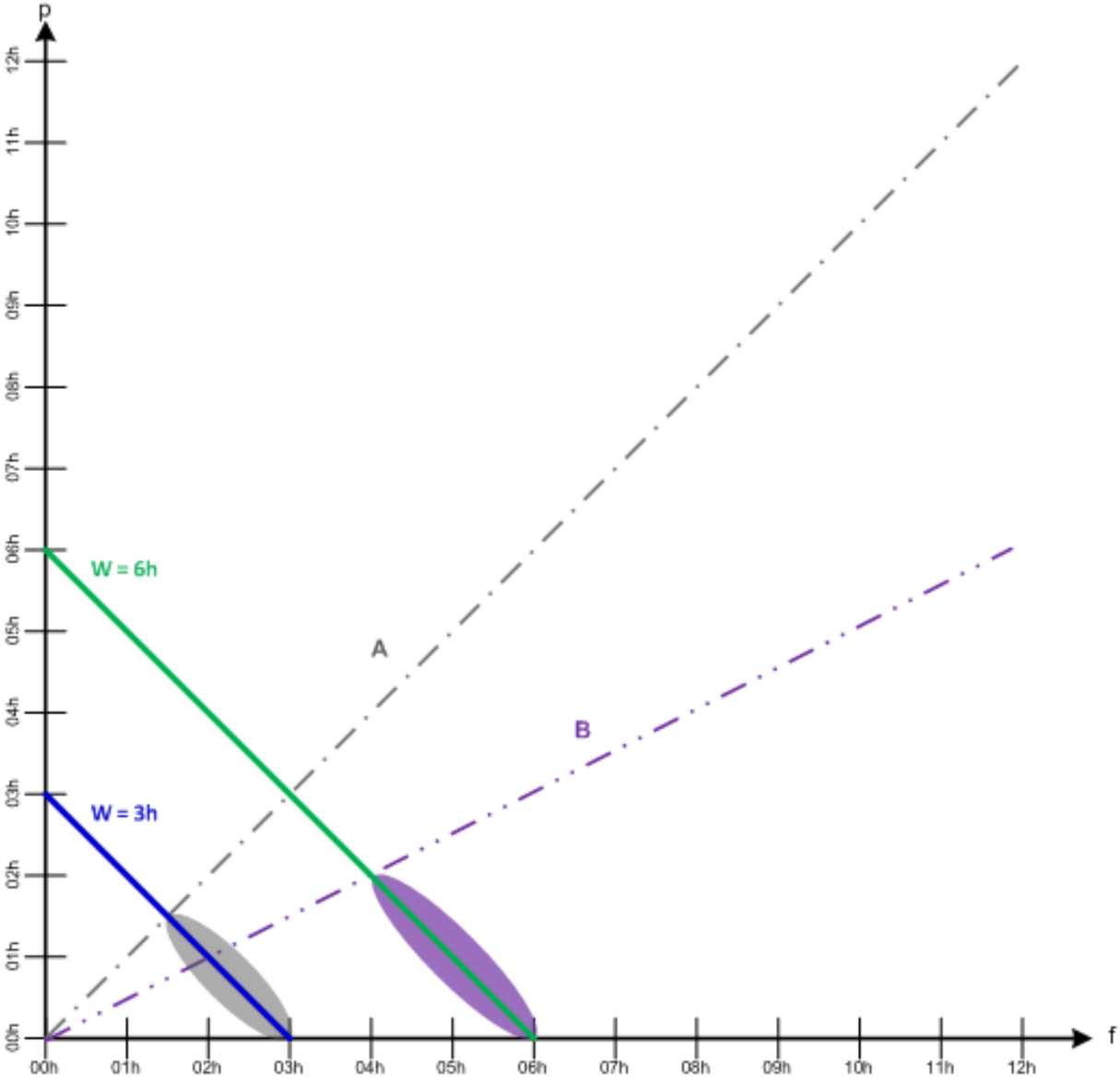

Source: Prepared by the author.

Graphically, it's important to note that the lines resulting from settings in Tariffs A and B could intersect any available load locus with a duration of 12 hours or less. However, this intersection can not occur when the tariff post length is restricted, as in the case of the Brazilian White Tariff. To better understand this restriction, we will analyze a set of ten loads whose properties are listed in Table 12 under different scenarios for peak and off-peak duration.

The following five figures will have common features. The first timeline graphic will display loads from L1 to L5, shown in blue, representing small-length loads. The second timeline graphic will showcase loads from L6 to L10, depicted in green, with durations of 12 hours or more, demonstrating the typical behavior of large-length loads. Loads from L1 to L3 and L6 to L8 share the same *locus* due to their identical durations.

Additionally, the third graphic will illustrate the Tariff Space for the binomial Tariff scheme. In Tariff Space, the gray and purple lines represent the solutions for the upper bound of Inequation (E.5) for Tariffs A and B, respectively. The red asymptotes signify the size restriction for the Tariff Posts, while the yellow area highlights all possible space for a load *locus* exists within the post-size restrictions.

In the upper right corner of the figures, there will be a depiction of the time decomposition into Binomial Tariff Space, considering the starting instant from Table 12 and a sample rate Δt of 30min. Here the reader is invited to observe how the time decomposition values change due to the realocation of tariff posts.

Table 12 – Properties of loads used in tariff post size restriction analysis.

Load	Start instant (L.s)	Length (L.W)
L1	0h	3h
L2	10h30m	3h
L3	21h	3h
L4	0h30m	9h
L5	16h30m	6h
L6	0h	12h
L7	6h	12h
L8	12h	12h
L9	0h	18h
L10	2h	22h

Source: Prepared by the author.

Figure 29 illustrates a homogeneous case in which all tariff posts have the same duration and are allocated contiguously. Observe that this scenario has an interesting symmetry around the *locus* of a 12h duration load. All *locus* equations that result in points outside the yellow area should not be considered, as they express negative time components or loads with more than 24h of duration.

Figure 30 illustrates a heterogeneous case where the peak post has only 6 hours of duration, and the posts are allocated contiguously. Here, observe how the *loci* region changes in response to the restrictions. Additionally, note that the Tariff B scheme has more valid points within the yellow region than Tariff A. This observation suggests that the Tariff Space methodology could be of interest to Energy Distributors for determining the price and positioning of Tariff Posts.

Figure 31 shows a homogeneous symmetric case in which the peak post is positioned between 6h and 18h, creating two off-peak regions of 6h each. In this scenario, it's notable that loads with more than 18h of duration have the same time decomposition value regardless of their

starting instant. Additionally, observe that the *loci* region is now restricted to a small yellow rectangle between the asymptotes and a line segment parallel to the $\hat{f}$ axis. This line segment corresponds to the load locus of loads larger than 18h and smaller than 24h.

Figure 32 shows a heterogeneous symmetric case in which a 6h peak post is positioned between 9h and 15h, creating two off-peak regions of 9h each. In this scenario, it's notable that loads with more than 15h (= 6h + 9h) of duration have the same time decomposition value regardless of their starting instant. Additionally, observe that the *loci* region has changed to adapt to the new restrictions from the asymptotes. Also note that line segment parallel to the $\hat{f}$ axis also belongs to *loci* region. This line segment corresponds to the load *locus* of loads larger than 15h and smaller than 24h.

Our final scenario, seen in Figure 33, depicts a heterogeneous asymmetric case where a 6-hour peak post is allocated between 12h and 18h. Similar to the previous scenarios, some long-duration loads (exceeding 18h = 12h + 6h) will exhibit a fixed-time decomposition into Tariff Space, resulting again in a *loci* region comprised of a rectangle and a line segment.

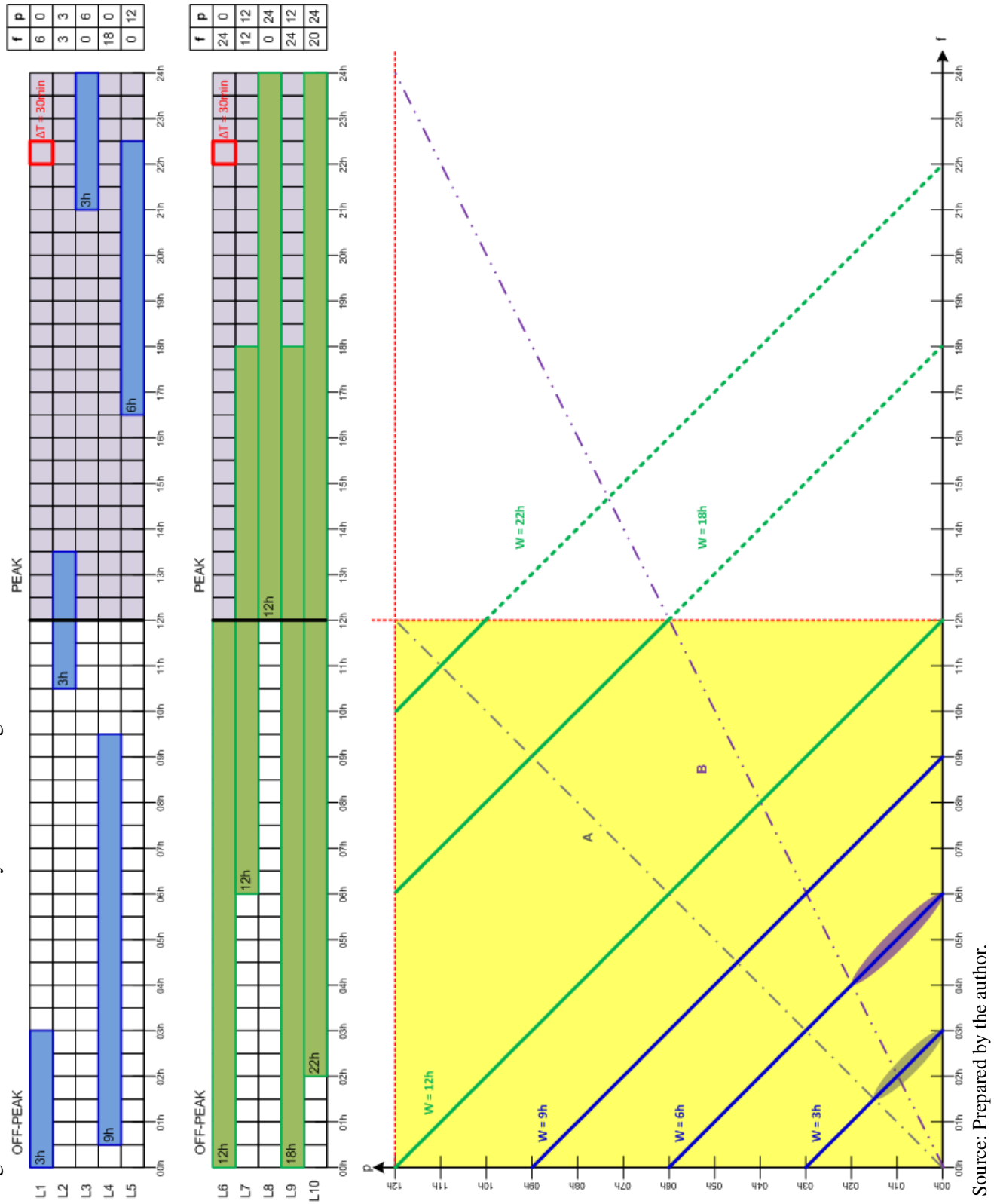

Source: Prepared by the author.

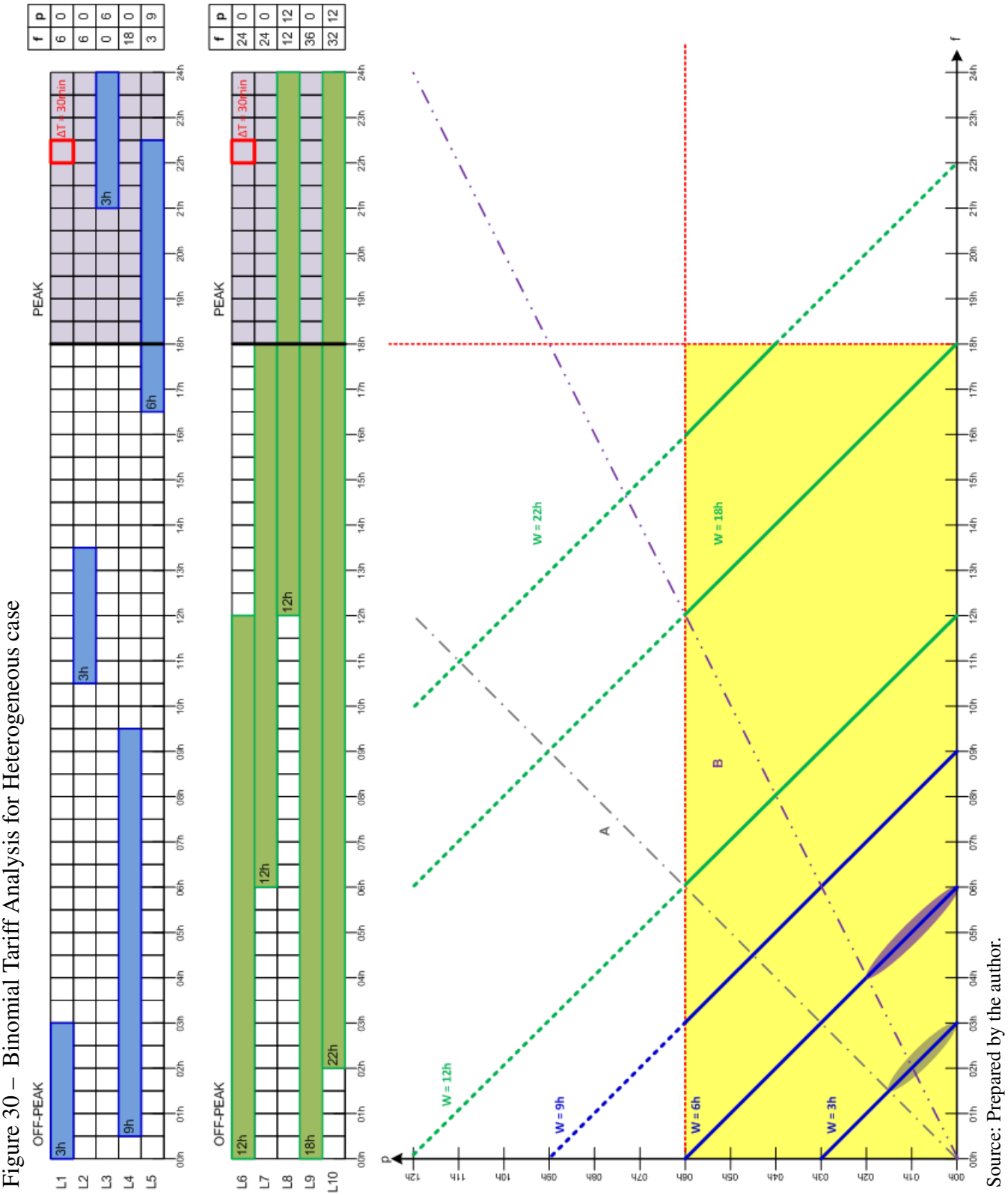

Source: Prepared by the author.

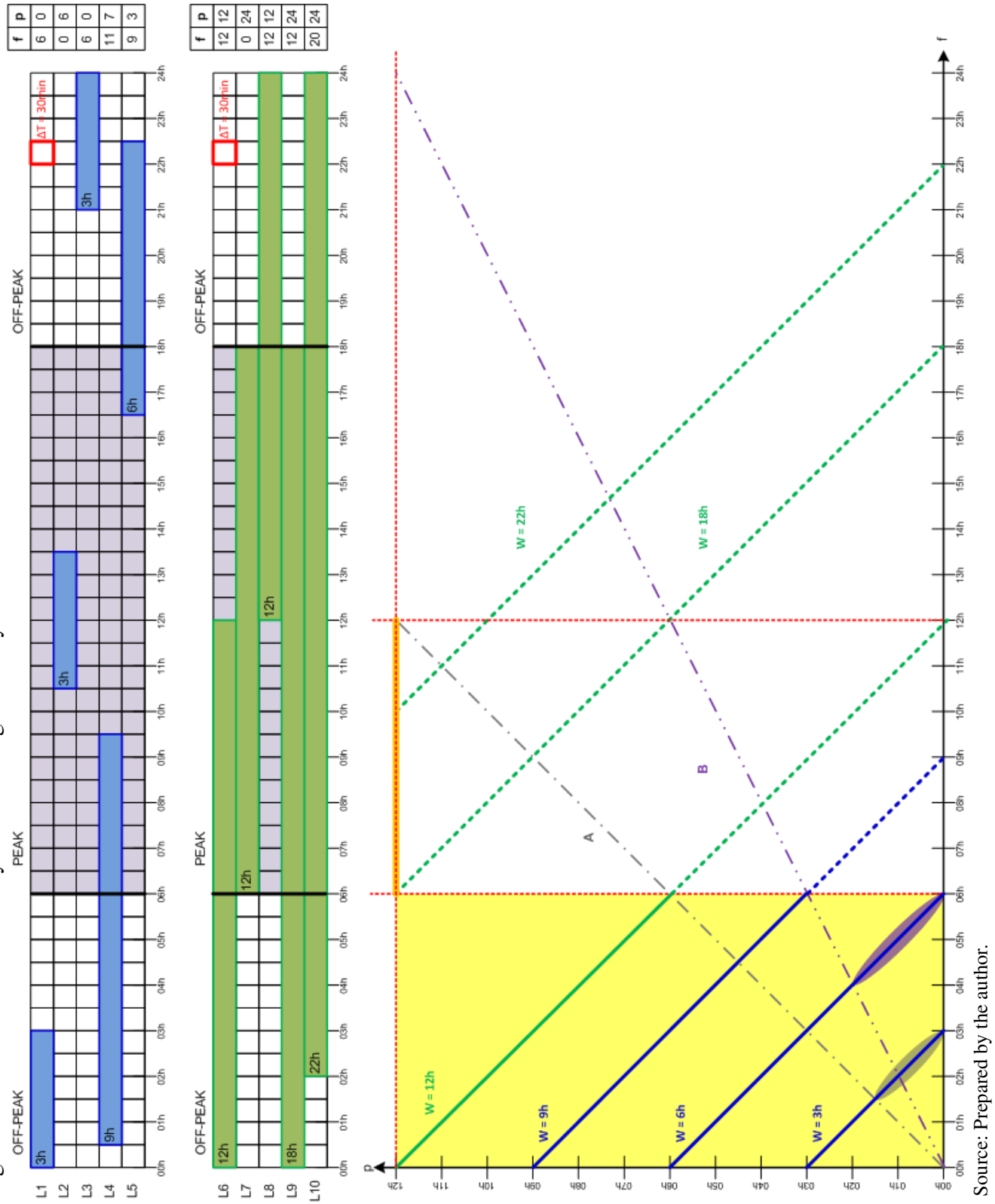

Source: Prepared by the author.

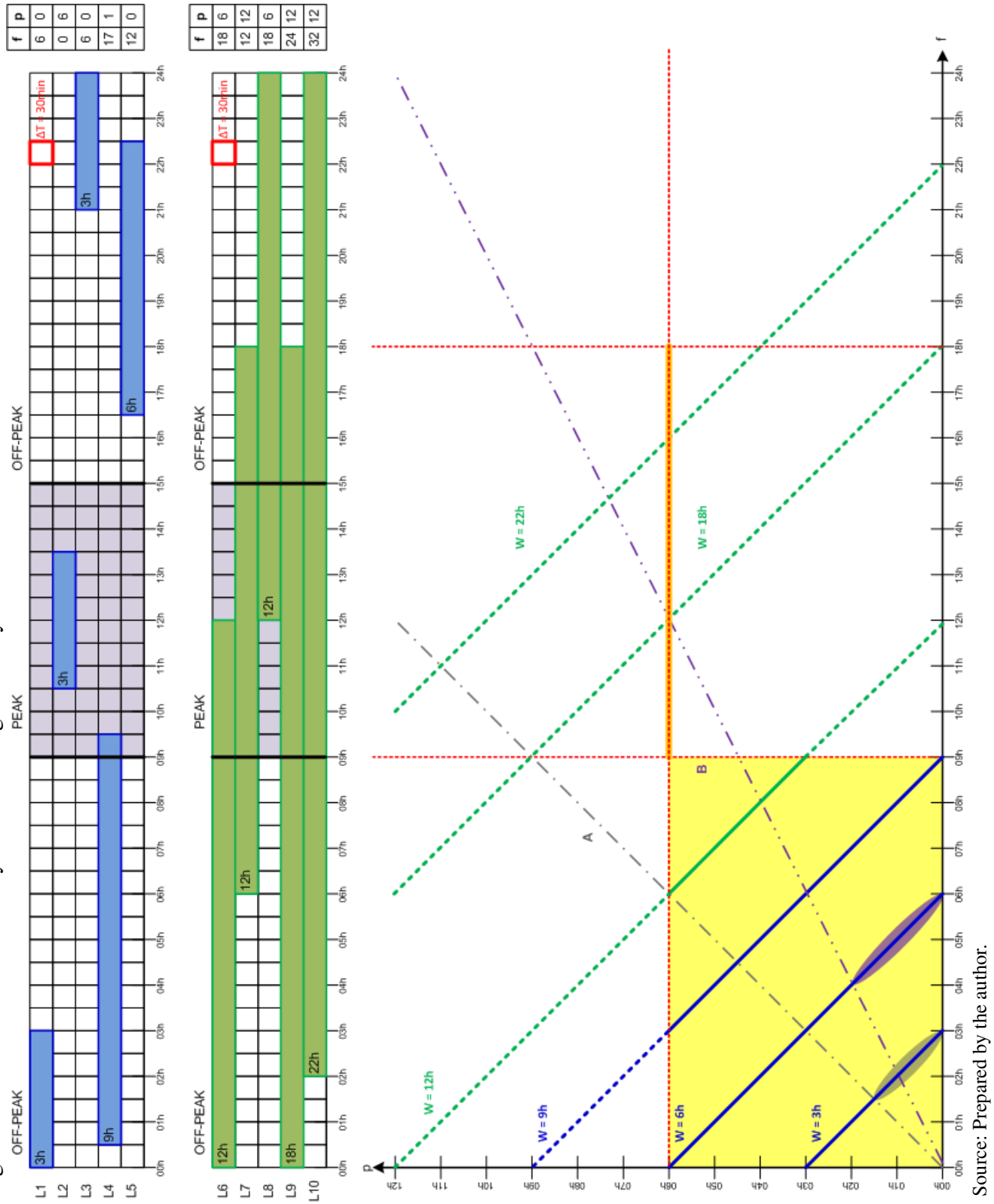

Source: Prepared by the author.

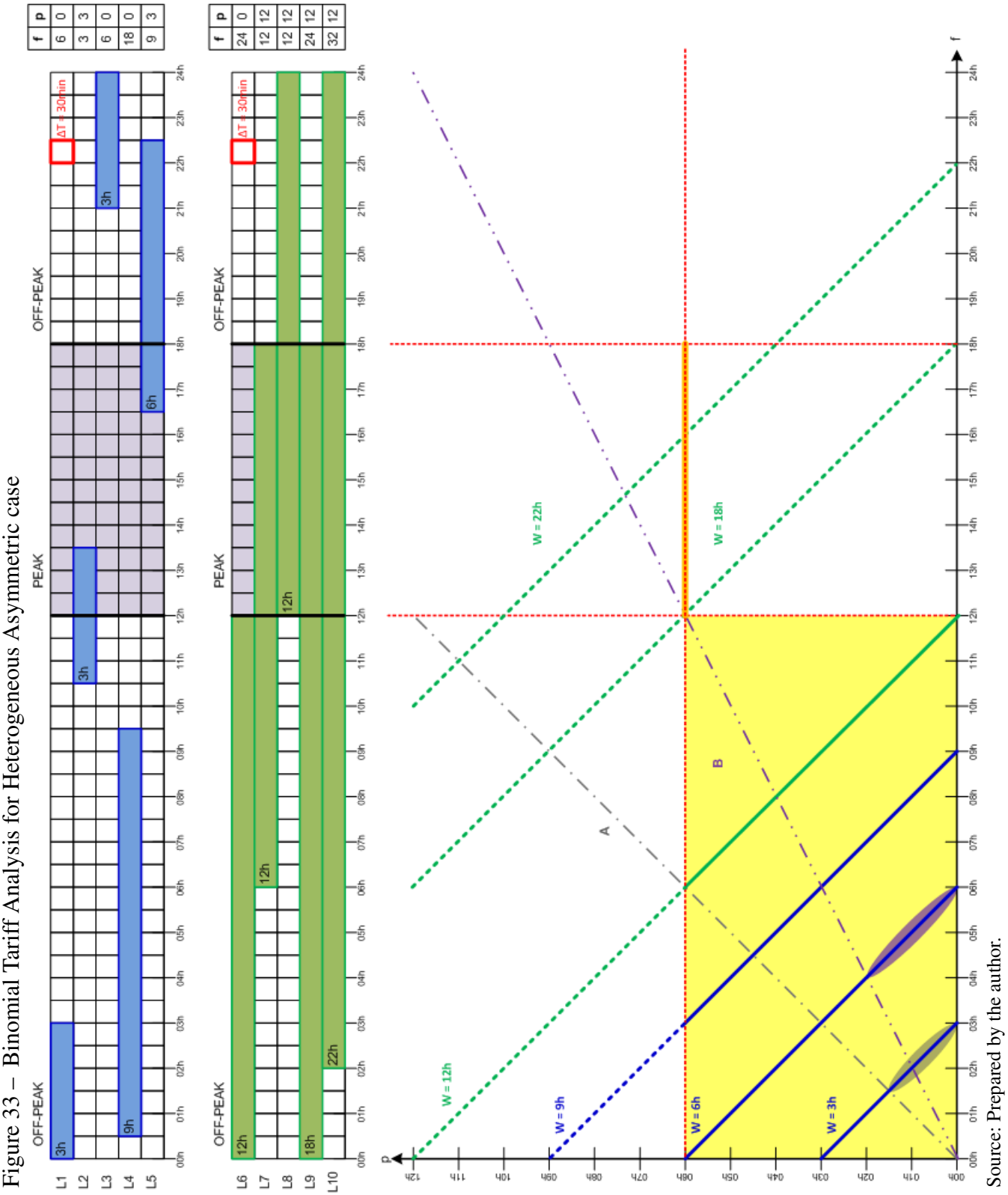

Figure 33 – Binomial Tariff Analysis for Heterogeneous Asymmetric case

Source: Prepared by the author.